~~Future prediction of Siberian wildfire and aerosol emissions via the improved fire module of the spatially explicit individual-based dynamic global vegetation model~~Future projections of Siberian wildfire and aerosol emissions by process-based ecosystem model

Reza Kusuma Nurrohman[1,2], Tomomichi Kato[3], Hideki Ninomiya[4], Lea Végh[3,5], Nicolas Delbart[6], Tatsuya Miyauchi[3], Hisashi Sato[7], Tomohiro Shiraishi[8] and Ryuichi Hirata[5]

[1]Graduate School of Agriculture, Hokkaido University, Sapporo, Hokkaido 060-8589, Japan
[2]Department of Agricultural Engineering, University of Mataram, Mataram, Nusa Tenggara Barat 83126, Indonesia
[3]Research Faculty of Agriculture, Hokkaido University, Sapporo, Hokkaido 060-8589, Japan
[4]Graduate School of Global Food Resources, Hokkaido University, Sapporo, Hokkaido 060-8589, Hokkaido, Japan
[5]National Institute for Environmental Studies, Tsukuba, Ibaraki, Japan
[6]Laboratoire Interdisciplinaire des Energies de Demain, UMR 8236 CNRS – Université de Paris, 75013 Paris, France
[7]Japan Agency for Marine-Earth Science and Technology (JAMSTEC), 3173-25 Showamachi, Kanazawa-ku, Yokohama-City, Kanagawa 236-0001, Japan
[8]Nippon Bunri University, Oita, Oita, 870-0397, Japan

Correspondence to: Tomomichi Kato (tkato@agr.hokudai.ac.jp)

Abstract. Fires are among the most influential disturbances affecting ecosystem structure and biogeochemical cycles in Siberia. Therefore, accurate ~~precise~~ fire modeling via dynamic global vegetation models is important for predicting greenhouse gas emissions and other burning biomass emissions to understand changes in biogeochemical cycles. In this study, we integrated the widely used SPread and InTensity of FIRE (SPITFIRE) fire module into the spatially explicit individual-based dynamic global vegetation model (SEIB-DGVM) to improve the accuracy of fire predictions and then simulated future fire regimes to better understand their impacts. The model is able to reproduce historical data well compared to the benchmark datasets, based on the spatial validation, has the following results: AGB (R^2=0.43, RMSE=21.9 Mg ha^{-1}), burned fraction (R^2=0.75, RMSE=0.01), burned area (R^2=0.609, RMSE=690 ha), dry matter emission (R^2=0.63, RMSE=0.01 Kg DM m^{-2}), GFED4s CO_2 emission (R^2=0.608, RMSE=52.4 Tg), GBEI CO_2 emission (R^2=0.67, RMSE=69.5 Tg). Spatially, the model is able to produce data with the same distribution pattern with a value of 61.8%. Numerically and on a long-term average, the model is able to produce values with very high accuracy of around 99% compared with the benchmark datasets.

Under the Representative Concentration Pathways 8.5 climate scenario, we estimated that the CO_2, CO, $PM_{2.5}$, total particulate matter (TPM), and total particulate carbon (TPC) emissions in Siberia will continue to increase annually until 2100 by 0.0264 ± 0.01 % $year^{-1}$ or individually by 214.4 ± 79.4, 17.16 ± 6.35, 2.8 ± 1.03, 2.1 ± 0.78, and 1.47 ± 0.54 Gg species $year^{-1}$, respectively. ~~an average of 214.4, 17.16, 2.8, 2.1, and 1.47 Gg species $year^{-1}$, respectively.~~ Under the same scenario and period, 185 trees ha^{-1} $year^{-1}$ are estimated to be killed by wildfires, resulting in a 319.3 g C m^{-2} $year^{-1}$ loss of net primary production (NPP). These findings show that Siberia faces an increasing frequency of extreme fire events due to changing climate

conditions. Our study offers insights into future fire regimes and provides helpful information for development strategies for enhancing regional resilience and for mitigating the broader environmental consequences of heightened fire activity in Siberia.

Formatted: Font: (Default) Times New Roman, Not Bold, Complex Script Font: Times New Roman, 12 pt

1 Introduction

Fires are among the most significant disturbances affecting biogeochemical cycles, atmospheric chemistry, the carbon cycle, and ecosystem structure and function worldwide (Pickett et al., 1999). Wildfires are also the dominant climate-driven disturbance agent in boreal forests (Goldammer and Furyaev, 1996; Shorohova et al., 2011; De Groot et al., 2013), shaping major forest cover in Russia (Krylov et al., 2014) and rapidly increasing burned area and emission intensity in Canada and Alaska (Zheng et al., 2021). Fires influence vegetation dynamics by allowing plants to adapt to fire regimes, influencing vegetation productivity, litter, and fuel load (Cochrane, 2003; Bergeron et al., 2004; Whelan, 2009). The intensity and frequency of large-scale boreal forest fires are expected to increase in the future due to increased global temperatures, drier conditions, and longer fire seasons, which will cause more emissions from biomass burning (Flannigan et al., 2009; Gauthier et al., 2015) ~~(Flannigan et al., 2009)~~ and human activity (Schmoldt et al., 1999; Hantson et al., 2016) ~~(Schmoldt et al., 1999)~~. Globally, from 2000 to 2019, satellites detected a decrease in the burned area of grassland, while there was a slight increase in the area of forest fires in Russia (Zheng et al., 2021). Europe, France, Spain, Portugal, and Greece are already experiencing larger and more devastating fires (Carnicer et al., 2022). Not only large fires but also small fires have a significant impact: Areas burned by small fires contributed 35% to the total burnt area, from 345 Mha $year^{-1}$ to 464 Mha $year^{-1}$, and related carbon emissions increased from 1.9 Pg C $year^{-1}$ to 2.5 Pg C $year^{-1}$ from 2001-2010 (Randerson et al., 2012). This finding is in line with current studies reporting that the global mean CO_2 emission intensity has increased by 0.9 ± 0.9% (NS) $year^{-1}$ from 2000 to 2019 (Zheng et al., 2021) and that the Fire Weather Index (FWI) reached levels above 30, corresponding to high, very high, and extreme levels of fire frequency, causing CO_2 emissions to increase as well in Europe since 1980 (Carnicer et al., 2022).

Forest fires are important ecological factors that influence both the establishment and succession of vegetation (Abaimov and Sofronov, 1996). Climate-driven large fires are responsible for rapid changes in vegetation (Cleve and Viereck, 1981), soil properties (Pastor and Post, 1986; Pellegrini et al., 2021), biogeochemical cycling, microclimate, forest ecosystems (Crutzen and Goldammer, 1993), productivity, stability, and many other ecological properties (Melillo et al., 1993). Forest fires also indirectly affect vegetation dynamics by increasing CO_2 levels in the atmosphere (Seiler and Crutzen, 1980; Nguyen and Wooster, 2020), as CO_2 is one of the primary products of biomass combustion and is emitted in all phases of fire (ignition, flaming, glowing, pyrolysis, and extinction) (Andreae and Merlet, 2001), with the flaming phase leading to emissions (Lobert et al., 1991; Ward and Hardy, 1991). Thus, it is challenging to estimate CO_2 emissions because they are generated in large quantities during biomass combustion and because of the different emission timelines produced during each combustion stage. Prolonged exposure to high CO_2 concentrations has negative impacts on health (Jacobson et al., 2019) and agriculture (Kimball and Idso, 1983), alters the global carbon cycle (Van Der Werf et al., 2006, 2010, 2017; Neto et al., 2009; Kaiser et al., 2012;

Lin et al., 2013), and has a feedback effect between climate and the biosphere (Bowman et al., 2009). Therefore, accurate modeling of future wildfires and their emissions is required to understand the associated risks.

Boreal vegetation store between 17% of the world's carbon, yet encompasses almost 30% of all terrestrial carbon stocks (Kasischke, 2000; Gauthier et al., 2015), and two-thirds are located in Siberia, Russia ~~Current estimates suggest that 10–17% of global carbon is stored in the vegetation and soils of boreal forests, two-thirds of which are located in Siberia, Russia~~(Shvidenko and Nilsson, 2003) ~~(Tchebakova et al., 1994; Shvidenko and Nilsson, 2003)~~. In Siberia, burned biomass emissions approached 0.4 Gt C $year^{-1}$ in 2021, three times the average value between 1997 and 2020 according to GFED4s (Friedlingstein et al., 2020; Kharuk et al., 2022) also stated that the decadal frequency of wildfires tripled between 2001–2010 and 2011–2020. Catastrophic boreal forest fires are expected to continue to increase in the future due to increased global temperature, drier conditions, and longer fire seasons, and these fires will increase the severity and emissions produced from biomass burning (Flannigan et al., 2009). Burning vegetation is a major source of black carbon (BC), carbon monoxide (CO) (Forster, P. et al., 2018), and particulate matter (PM) (Reddington et al., 2016). According to records from the Copernicus Atmosphere Monitoring Service (CAMS), Russia experienced a drastic increase to 8 megatons (Mt) in $PM_{2.5}$ emissions in 2021, which is 78% higher than the average level between 2004 and 2021 (4.5 Mt) (Romanov et al., 2022). Furthermore, increased emissions negatively affect the climate (Randerson et al., 2006; Westerling et al., 2006; Bowman et al., 2009) and weather systems by modulating solar radiation and cloud properties (Schultz et al., 2008).

Understanding how long-term climate change, fire regimes, and forest vegetation interact under multiple climate scenarios is critical for forecasting forest succession trends (Clark and Richard, 1996). Modeling of fire regimes using dynamic global vegetation models (DGVMs) is a key approach to analyzing these factors. However, including interactive fire disturbances in vegetation models is critical for accurately simulating vegetation dynamics (Thonicke et al., 2001). A well-structured process-based fire module can accurately assess fire activity, consumed biomass due to fire, and biomass burning emissions. The assessment of each fire-related variable is interconnected with another variable, so the module must be well constructed because the amount of consumed biomass during forest fires can vary significantly. Several factors affect burned biomass, such as spatial and temporal variations in burned area based on ignition factors, the quantity and quality of the fuels available, and vegetation or plant functional type (PFT); additionally, every PFT reacts differently to fire disturbance (Cramer et al., 2001; Ito, 2011). Since the first global fire models were integrated into dynamic global vegetation models (DGVMs) two decades ago, the variety and complexity of fire models have expanded (Hantson et al., 2016). The Fire Modeling Intercomparison Project (FireMIP) compared eleven current fire models by structure and simulation protocols, using a benchmarking system to evaluate the models (Rabin et al., 2017). The results indicate that models that explicitly distinguish ignition factors, such as lightning and human-caused “ignition events”, as well as physical properties and processes that determine fire spread and intensity by plant functional type (PFT), performed better. One such fire module is SPITFIRE (an upgrade of GlobFIRM) (Thonicke et al., 2010), which has been used in several DGVMs: LPJ-GUESS-SPITFIRE, ORCHIDEE-SPITFIRE, JSBACH-SPITFIRE, and LPJ-LMfire. In this study, we integrated the SPITFIRE fire module into the spatially explicit individual-based dynamic global vegetation model (SEIB-DGVM) to predict fire, vegetation, and burned

biomass emission variables in Siberia in the future. We selected the SEIB-DGVM because of its high-quality biogeochemical model coupled with a three-dimensional representation of forest structure where individual trees compete for light and space (Sato et al., 2007). The SEIB-DGVM processes physical, physiological, and vegetation dynamics and was previously used for reconstructing the geographical distributions of fundamental plant productivity properties (Sato et al., 2020), evaluating the geographic and environmental heterogeneity of larch forests with a special focus on topography (Sato and Kobayashi, 2018), and assessing the impacts of global warming on Siberian larch forests and their interactions with vegetation dynamics and thermohydrology (Sato et al., 2016). The SEIB-DGVM accurately simulates forest ecology after typhoon disturbances (Wu et al., 2019), nonstructural carbohydrate dynamics (Ninomiya et al., 2023), and masting in a temperate forest (Végh and Kato, 2024).

The original fire module of the SEIB-DGVM is Glob-FIRM (Thonicke et al., 2001), which has several limitations; for example, human-changed fire regimes and other land use impacts are not considered (Thonicke et al., 2001). In addition, GlobFIRM derives the burnt fractional area of a grid cell from the simulated length of the fire season and from the minimum annual fuel load; this method does not specify ignition sources and assumes a constant fire-induced mortality rate for each plant functional type (PFT) (Thonicke et al., 2010). To improve the fire simulations with the SEIB-DGVM, we replaced its fire module with the SPITFIRE model (Thonicke et al., 2010) by adding complete ignition equations (human and lightning effects, etc.). The module included a calculation mechanism for trace gas and aerosol emissions (Andreae and Merlet, 2001) and was adjusted to produce monthly outputs for all variables in the SEIB-DGVM. These improvements allowed us to simulate fire activity and aboveground biomass dynamics and spatiotemporally assess the projected burned biomass and its emissions for the 21st century in Siberia under representative concentration pathways (RCPs).

2 Methods

2.1 Study sites

Boreal forests represent the largest forest biome and one-third of global forest cover (De Groot et al., 2013) and play an important role in the atmosphere–land interactions of the global climate system (Randerson et al., 2006; Bonan, 2008). Geographically, boreal forests are found in Canada, Alaska, and Siberia, of which Siberia has the largest forested area. Siberia is largely covered by deciduous needleleaf conifers (Figure 1), which consist mostly of the larch species *Larix sibirica*, *L. decidua*, and *L. dahurica* (Abaimov et al., 1998), which are categorized as pyrophytic species, meaning that they require periodic fires to persist on the landscape (Kharuk et al., 2011). The Siberian land cover has changed very little over the last century (Ivanov et al., 2022), and the boreal forest covers approximately >15 million km^2, and contain a large amount of carbon that is comparable to the combined carbon storage in tropical and temperate forests (Dixon et al., 1994; Kasischke, 2000).

The main external factors affecting Siberian boreal forests are fires and climate change (Goldammer and Furyaev, 1996; Shorohova et al., 2009). Climate change increased the frequency of forest fires, which in turn amplified the impacts of climate change locally. ~~Global warming caused more pronounced summer warming in Siberia, with an increase in temperature between~~

~~0.5 and 2.0 °C (Chapin et al., 2005). Winter and spring temperatures also increase, affecting the duration and speed of snowmelt, which results in drier ground cover, an increased frequency of wildfires, longer fire seasons, and increased ignition sources (Kharuk et al., 2022).~~ In the Arctic, a rapid warming trend has been observed, and the increase in temperature over the last 20 years of the 20th century was 2 to 3 times higher than the global average, while in the first 20 years of the 21st century, it exceeded four times (Chylek et al., 2022). This enormous increase in temperature in Siberia, affecting the duration and speed of snowmelt and accelerates thawing of carbon-rich permafrost (Natali et al., 2019; Schuur et al., 2015; Nitzbon et al., 2020), which results in drier ground cover, an increased frequency of wildfires, longer fire seasons, and increased ignition sources (Kharuk et al., 2022). These changes may result in a new climate state in which heatwaves as well as the associated the occurrence of wildfires may become routine and more severe (Hantemirov et al., 2022; Landrum and Holland, 2020). Produced emissions from thawing permafrost and from wildfire are likely to feed into the global carbon cycle's feedback on climate change (Schuur et al., 2015), and triggering further warming trends globally (Schimel et al., 2001; Kharuk et al., 2011; Krylov et al., 2014).~~These changes may result in the area becoming a source of greenhouse gas emissions (IPCC, 2007) and in triggering further warming trends globally (Schimel et al., 2001; Kharuk et al., 2011; Krylov et al., 2014).~~

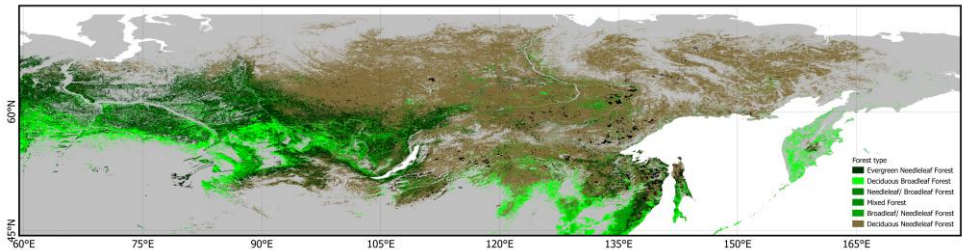

Figure 1. Study site (black rectangle: 60º-180ºE and 45º-80ºN). Green and brown color indicate the forest types in Siberia are provided from Global Land Cover dataset (GLC 2000): Northern Eurasia (Bartalev et al., 2003). Grey color indicate other vegetation types in the Siberian area provided by Database of Global Administrative Areas (GADM).

Formatted: Complex Script Font: 12 pt

Formatted: Normal

2.2 Improved fire module principles

We improved the SEIB-DGVM fire module by replacing the Glob-FIRM (Thonicke et al., 2001) with the SPITFIRE model (Thonicke et al., 2010). First, we added two new input variables for fire ignition: population and lightning data. Second, we incorporated the complete SPITFIRE equation (Thonicke et al., 2010), which included new variables, PFT parameters, and local parameters, and improved the output to be able to be produced on a monthly scale (Figure 2). The variable integration between the default and improved fire models requires several parameter-specific PFTs (Table 1).

The default SEIB-DGVM model uses annual time steps for vegetation dynamics and disturbance, which we improved to monthly time step outputs. The fraction of individual trees killed by a fire depends on PFT fire resistance (M3, Table 1). All grass leaf biomass, all dead and living tree leaf biomass, half of the dead tree trunk biomass, and half of the litter pool are released into the atmosphere as CO_2 during a fire, while the dead tree's residual biomass is converted into litter. In reaction to fire, all deciduous PFTs convert their phenology phase to dormancy, and if the stock resource of grass PFTs (gmassstock) does not meet the minimal value (50 g DM m^{-2}) following fire, the deficit is supplemented from litter (Sato et al., 2007). Furthermore, related to the fire-vegetation relationships, for herbaceous PFTs, both below-ground and storage biomass are preserved after a wildfire and used for the recovery of above-ground biomass. During this recovery period, herbaceous PFTs work on producing above-ground biomass while reducing their storage biomass, thus increasing the allocation ratio to above-

ground biomass in the post-fire phase. For woody PFTs, fire only gives the option for individual trees to either die or survive. The surviving trees only lose their foliage biomass. As the foliage is lost, fine root biomass becomes unnecessary, leading to its rapid loss due to its fast turnover rate. In the spring following a fire, surviving trees convert storage resources into foliage and fine root biomass. The new net primary production (NPP) from the newly formed foliage first prioritizes the recovery of leaves and fine roots. Therefore, fires increase the allocation ratio to the foliage and fine roots in surviving woody plants.

The basic equation of fire disturbance is the area burned, which we adjusted with the SPITFIRE equation (Thonicke et al., 2010) by including the fire probability and area of the grid cell:

$$A_b = P_b \times A \quad (1)$$

where A_b is the area burned in a grid cell per month (ha month^{-1}), P_b is the product of the probability of fire per month at any point inside the grid cell (month^{-1}) and A is the area of the grid cell (ha). P_b is the fire probability and is the product of the fuel load (litter + aboveground biomass) and its moisture factor. We used the same P_b mechanism as that of the default fire module, where if the fuel load satisfies the minimum fuel threshold (200 gC m^{-2}), random fires can occur at any point location inside the grid cell. In this improvement, P_b was modified by considering the ignition event $E(n_{ig})$ (ha^{-1}) by anthropogenic (human population density) and natural (lightning strikes) ignition possibilities, the fire danger index (FDI), and the mean fire area $\bar{a}f$ (ha). ~~af (ha).~~ Thus, Equation 2 can be represented as follows:

$$A_b = E(n_{ig}) \times FDI \times \underline{a}f \times A \quad (2)$$

Technically, the SEIB-DGVM simulation of each grid cell ~~grid~~ is carried out independently among the surrounding grid cell~~grids~~, so the fire cannot spread to other ~~grids~~ grid cell without those ~~grids~~ grid cell meeting the ignition requirements (fuel load and fuel moisture).

After all variables in the SPITFIRE fire module were integrated, we added the trace gas and aerosol emission calculation process to the model. Trace gas and aerosol emissions estimation is referred to the Fire Modeling Intercomparison Project (FireMIP) protocols (Li *et al.*, 2019), the comprehensive study comparison of nine dynamic global vegetation models (DGVMs) and produced important estimation for long-term and large-scale fire emissions. By using FireMIP protocol reference, SEIB-DGVM SPITFIRE improved to output PFT-level fire emissions.

Trace gas and aerosol emissions are the result of the total amount of burned biomass, the sum of dead and live fuel consumption as the result of surface fire and crown scorch. Trace gas emissions are estimated based on fire carbon emissions, vegetation characteristics from DGVMs, and fire emissions factors. Fire emissions of trace gas and aerosol for each species i and PFT j, $E_{i,j}$ (g species m^{-2}) are estimated based on Andreae and Merlet, (2001):

$$E_{i,j} = EF_{i,j} \times \frac{CE_j}{C} \quad (3)$$

$EF_{i,j}$ (g species (kg dry matter (DM))$^{-1}$) is PFT specific emission factor, CE_j is the combusted biomass of PFT_j due to the fire (g C m^{-2}), and C is the unit conversion factor from carbon to dry matter, $C = 0.5 \times 10^3 gC(kg\ DM)^{-1}$. The Emission factors

(EF) used in this study are based on Andreae and Merlet, (2001), and the updated pyrogenic emissions species by various types of biomass burning (Andreae, 2019) (Table S2 in the Supplement).

DGVMs generally simulate vegetation as a combination of PFTs in a given grid location to represent plant function at a global scale, instead of land cover types (Li *et al.*, 2019). In this, we classified the PFTs with the LCTs to integrate the emission factors of each LCTs for trace gas and aerosol emissions estimation process. TrBE and TrBR are classified as Tropical Forest; TeNE, TeBE, and TeBS are classified as Temperate Forest; BoNE, BoNS, and BoBs are classified as Boreal Forest, and the last is Teh and TrH are classified as Grassland/ Savana, SEIB-DGVM didn't classify crop PFTs so cropland LCTs will not be used.

Further changes in the input and output of the new SEIB-DGVM SPITFIRE model are shown in Appendix A.1, while Appendix A.2 summarizes the improvement processes represented in this study, which can be classified into two groups: disturbance and biogeochemical dynamics. Appendix A.3 lists the symbols used in the model's equations.

After all the SPITFIRE variables were installed, we also conducted a verification process for all the variables. The verification process included assessing the new input data (lightning and population data), as well as all new variables, by testing their outputs and units. The module verification process is highly important for ensuring that the module produces the correct outputs but not for the wrong reasons (Rabin et al., 2017). Detailed information about the integration of the SPITFIRE module in the SEIB-DGVM, which includes the improvement and adjustment of all the variables and the main important variables, such as ignition events $E(n_{ig})$, fire danger index (FDI), mean fire area $\bar{a}f$ ~~af~~, fuel moisture content, rate of spread, fire fraction and intensity, fire damage to plants, and trace gas and aerosol emissions, is provided in the Supplemental File (2.2.1-2.2.7~~8~~).

Formatted: Font: (Default) Times New Roman, Complex Script Font: Times New Roman, 12 pt

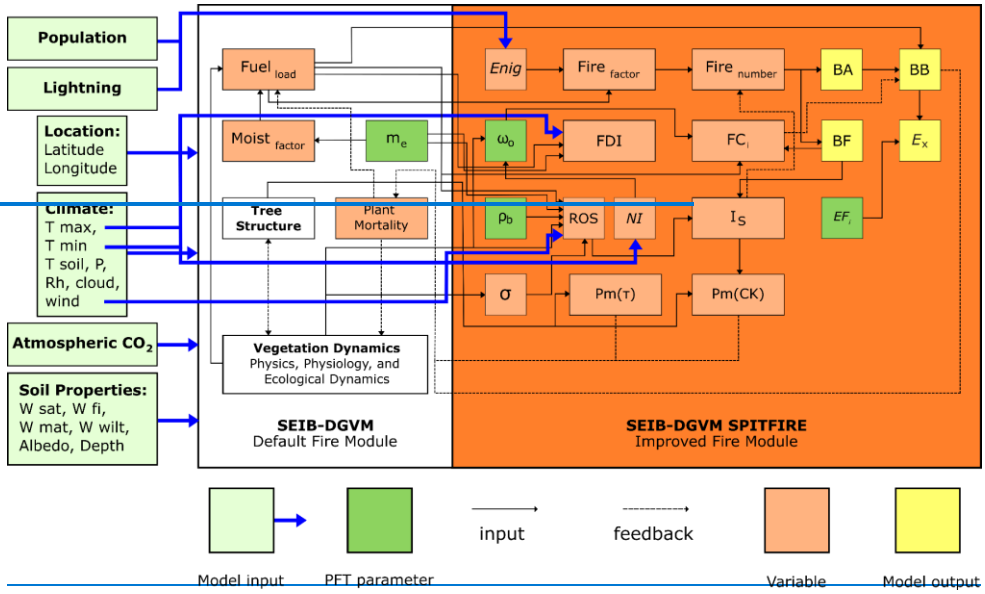
Population
Lightning
Location:
Latitude
Longitude
Climate:
T max,
T min
T soil, P,
Rh, cloud,
wind
Atmospheric CO2
Soil Properties:
W sat, W fi,
W mat, W wilt,
Albedo, Depth
Fuel load
Moist factor
me
Tree Structure
Plant Mortality
Vegetation Dynamics
Physics, Physiology, and Ecological Dynamics
SEIB-DGVM
Default Fire Module
Enig
Fire factor
Fire number
BA
BB
ωo
FDI
FCi
BF
Ex
ρb
ROS
NI
IS
EFi
σ
Pm(T)
Pm(CK)
SEIB-DGVM SPITFIRE
Improved Fire Module
input
feedback
Model input
PFT parameter
Variable
Model output

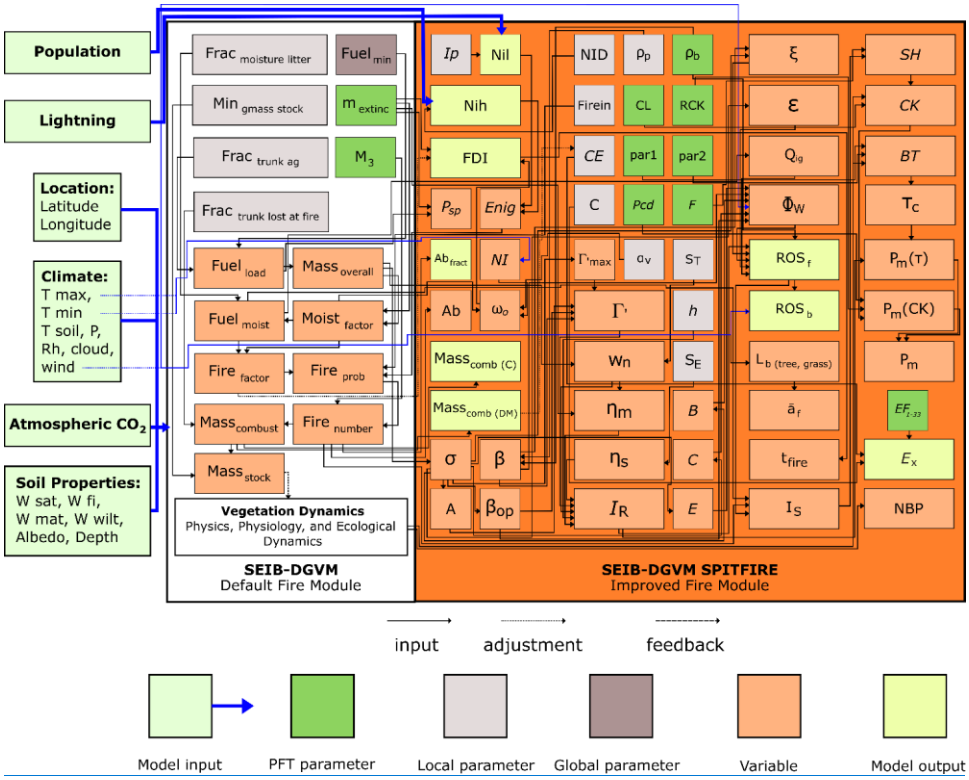

Figure 2. SEIB-DGVM SPITFIRE ~~simplified~~ systems diagram. ~~Only major variables are displayed, d~~Describing the improvements (SPITFIRE), the interaction between the previous fire module (Glob-FIRM). All original SPITFIRE variables were integrated: ignition factor (lightning and population), PFT parameters, and other fire-related variables. In addition to the default annual output, the improved module had monthly outputs of all variables depending on the user needs. For the meaning of abbreviations, refer to the Appendix A.3.

Table 1. SEIB-DGVM SPITFIRE Plant Functional Type (PFT)-specific model parameter values and their attribution to land cover types (LCTs). This table was modified from Thonicke et al. (2010).

PFTs	**Land Cover Types (LCTs)**	**Fuel bulk density (kg m^{-3})**		**Scorch height parameter**		**Crown length parameter**	**Bark thickness parameters**			**Crown damage parameter**		**Fire resistance**
		Pb	Reference	*F*	Reference	*CL*	par1	par2	Reference	*R(CK)*	*p*	*M3*
BoNE		25	(Miller and Urban, 1999; Hély et al., 2000)	0.11	(Hély et al., 2003)	1/3	0.0292	0.2632	(Reinhardt et al., 1997)	1	3	0.12
BoNS	Boreal Forest	22	(Keane et al., 1990)	0.094	(Dickinson and Johnson, 2001)	1/3	0.0347	0.1086	(Reinhardt et al., 1997)	1	3	0.12
BoBS		22	(Keane et al., 1990)	0.094	(Dickinson and Johnson, 2001)	1/3	0.0347	0.1086	(Reinhardt et al., 1997)	1	3	0.12

PFTs attributed to land cover types (LCTs) are needed to classify the fire emission factor (*EF*) (Table S2 in the Supplement) to estimate trace gas and aerosol emissions (Andreae and Merlet, 2001).

2.3 Model calibration

We calibrate the improved model by using all of the benchmark datasets (Table 3). The calibration process is done sequentially for all of the major variables, from burned fraction, burned area, dry matter, aboveground biomass, burned biomass emissions, and the forest ecology variables (Figure 3). The process is sequential because one variable is used for the calculation of another variable (such as burned fraction and burned area affecting aboveground biomass, forest structure, dry matter, and emissions). One calibration process is performed with multiple iterations until the output variable has similar numerical values and spatial distribution to the benchmark data, and the process is repeated for other variables once the previous variable has been calibrated.

2.43 Model application

The original SEIB-DGVM utilizes three computational time steps: a daily time step for all physical and physiological processes except for soil decomposition and tree growth, a monthly time step for soil decomposition and tree growth, and an annual time step for vegetation dynamics and fire disturbance (Sato et al., 2007). In this study, we improved the fire module to calculate natural and anthropogenic fire ignition factors (based on lightning flashes and population density) and adjusted it to produce monthly outputs using temporal resolution statistical downscaling methods with user-defined weighted monthly parameters (Table 2).

The model was run in three phases: 1) a 1000-year spin-up phase to bring the soil and vegetation carbon pools into equilibrium with the climate using daily baseline CRU TS3.22 climate data, 2) a 156-year historical phase also using daily baseline CRU TS3.22 climate data and spin-up simulation results as inputs, and 3) a 95-year future phase using daily MirocAR5 base V2 RCP8.5, RCP6.0, RCP4.5, and RCP2.6 climate data and historical simulation results as inputs[2] (Figure 3).~~inputs.~~ The MirocAR5 Base V2 dataset is generated from CRU TS3.22 climate data, so the use of these two datasets consecutively in spin-up, historical, and future simulations ensures the harmony of the input climate data.

In the previous SEIB-DGVM study, a 2000-year spin-up was needed to obtain the convergence amount of soil organic matter (Sato et al., 2010). However, we have conducted preliminary simulations with the same study area by setting the spin-up years to 1000 years and 2000 years. We confirmed that the outputs of the 1000-year and 2000-year spin-up simulations were very similar; thus, the 1000-year spin-up was enough to reach carbon stock equilibrium. This parameter setting is also in line with the simulation settings in other SEIB-DGVM studies: Sato et al. (2007) performed a 1000-year spin-up and combined it with all of the simulation phases to extract general trends of postfire succession. Another study by Arakida et al. (2021) also confirmed that a spin-up period of 100 years was enough for the saturation of the LAI, aboveground biomass, and GPP at all of the study sites in Siberia.

~~One full-stage simulation consisted of spin-up, historical, and future simulations, and one full-stage simulation was repeated 5 times to calculate the average data values from the random runs. The annual average ignition factor variables (population density and lightning flash rate) are used constantly throughout all phases to compare the improved fire regime module product~~

Formatted: Font: (Default) Times New Roman, Complex Script Font: Times New Roman, 12 pt, Not Highlight

~~with the default, previous fire module, and we run both models with the same protocols (Figure S3 in the Supplement). To determine the impact of fire and climate on forest structure and their interactions, we also ran the simulations with a fire-off setting under 5 climate scenarios (baseline, RCP8.5, RCP6.0, RCP4.5, and RCP2.6) using the same configuration as the fire-on simulation (Figure 3).~~SEIB-DGVM code modification are described in the section 2.2., and annual average ignition factor variables (population density and lightning flash rate) are used constantly throughout all phases to compare the improved fire regime module product with the default, previous fire module, and we run both models with the same protocols (Figure S3 in the Supplement)*. Simulations were run in three phases (spin-up, historical and future) and the simulation was run with the fire mode on and fire mode off to compare and assess the vegetation products during fire, and also each phase was replicated 5 times to minimize bias due to random variables in the tree morality[1]. Verification stage is to ensure the new input data can be read, produced, and processed properly[3], then we calibrate all of the major emission individually and sequentially with the benchmark dataset, because each variable affect other variables and to make sure the final output was comparable with the benchmark datasets[4]. After verifying that the new module was incorporated seamlessly, we validated the model outputs (fire, vegetation and emissions variables) by using GFED4, GFED4s, ESA Biomass CCI and GBEI benchmark datasets[5]. To determine the impact of fire and climate on forest structure and their interactions, we ran the simulations with 5 climate scenarios (baseline, RCP8.5, RCP6.0, RCP4.5, and RCP2.6) using the same configuration as the fire-on simulation (Figure 3).

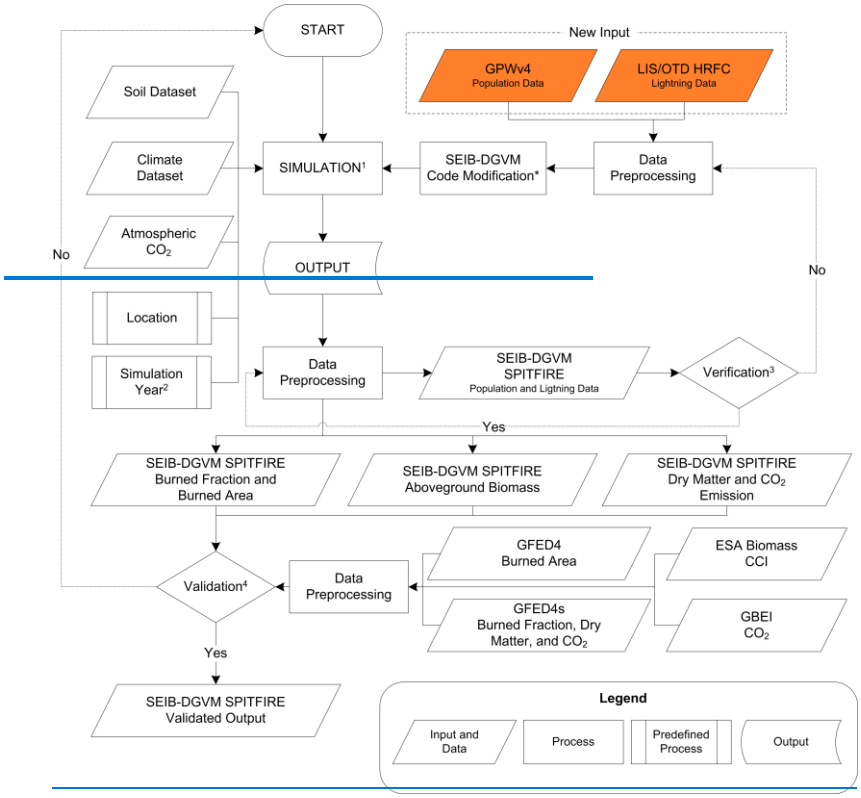
START
New Input
GPWv4
Population Data
LIS/OTD HRFC
Lightning Data
Soil Dataset
Climate Dataset
SIMULATION¹
SEIB-DGVM Code Modification*
Data Preprocessing
Atmospheric CO_2
No
OUTPUT
No
Location
Simulation Year²
Data Preprocessing
SEIB-DGVM SPITFIRE
Population and Ligtning Data
Verification³
Yes
SEIB-DGVM SPITFIRE Burned Fraction and Burned Area
SEIB-DGVM SPITFIRE Aboveground Biomass
SEIB-DGVM SPITFIRE Dry Matter and CO_2 Emission
GFED4 Burned Area
ESA Biomass CCI
Validation⁴
Data Preprocessing
GFED4s Burned Fraction, Dry Matter, and CO_2
GBEI CO_2
Yes
SEIB-DGVM SPITFIRE Validated Output
Legend
Input and Data
Process
Predefined Process
Output

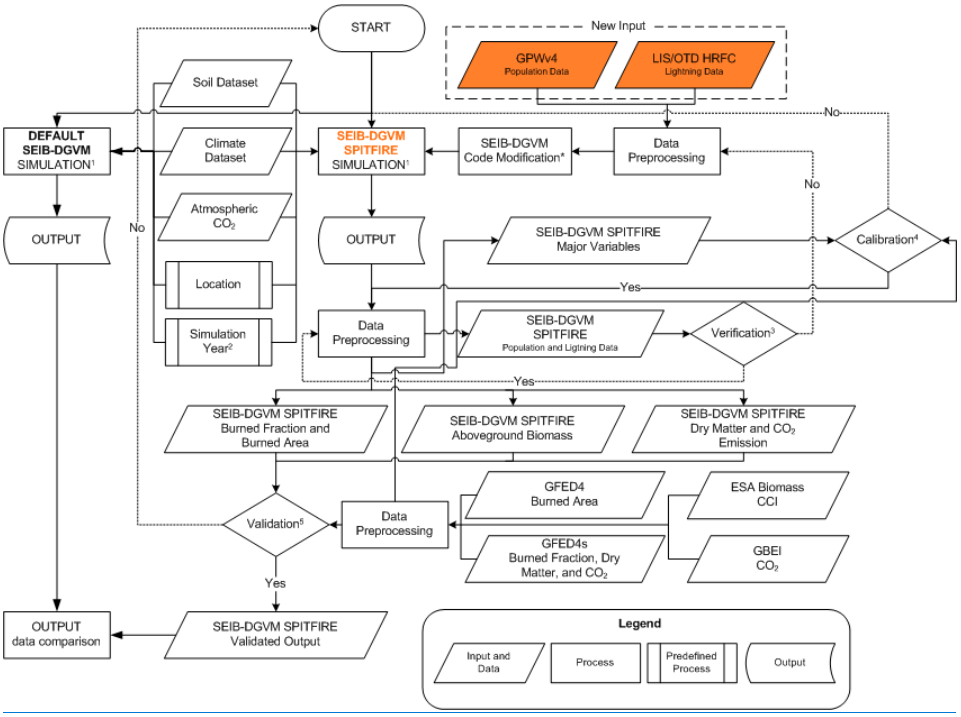

Figure 3. Workflow of improving the SEIB-DGVM fire module. After verifying that the new module was incorporated seamlessly, we validated the model outputs by using GFED4, GFED4s, ESA Biomass CCI and GBEI benchmark datasets. *Modified the code to adjust for two new inputs (Population and Lightning), implemented all variables in the SPITFIRE model, created new output variables and added monthly output options. [1]Simulations were run in three phases (spinup, historical and future) and the simulation was run with the fire mode on and off to compare and assess the vegetation products during fire, and also each phase was replicated 5 times to minimize bias due to random variables in the tree morality. [2]Simulation year is different for each phase (spinup, historical and future): 1000, 156, and 95 years, respectively. [3]First stage verification to ensure new input data can be read and produced properly. [4]The second validation is the model output (fire products, vegetation, and emissions) with some satellite data.

Table 2. SEIB-DGVM SPITFIRE input data descriptions

Model Input	Product	Variable	Spatial Resolution	Temporal Resolution	Temporal Coverage	Reference
Climatic data	CRU TS3.22 High-Resolution Gridded Data of Month-by-month Variation in Climate	Cloud cover, diurnal temperature range, frost day frequency, PET, precipitation, daily mean temperature, monthly average daily maximum and minimum temperature, vapor pressure, and wet day frequency	0.5 degree	monthly	1901–2013	(NCAS, 2014)
	~~MirocAR5 base daily V3 (RCP80, RCP60, RCP45, and RCP26)~~Miroc AR5 base daily V3 (RCP8.5, RCP6.0, RCP4.5, and RCP2.6)	Air temperature, soil temperature, fraction of cloud cover, precipitation, humidity, and wind velocity	0.5 degree	daily	~~251 years~~1850-2100	
CO_2	-	Global atmospheric Carbon dioxide concentrations (CO_2)	-	-	1850-2100~~251 years~~	-

Model Input	Product	Variable	Spatial Resolution	Temporal Resolution	Temporal Coverage	Reference
Soil properties	Global Soil Wetness Project 2	Soil moisture at saturation point, field capacity, matrix potential, wilting point, and albedo	1 degree (360 x 180)	time-fixed	time-fixed	www.iges.org/gswp
Ignition factors	LIS/OTD High-Resolution Full Climatology (HRFC) V2.3.2015	Lightning flash rate	2.5 arc-minute	Annual	2000-2020	(CIESIN, 2018)
	Gridded Population of the World (GPWv4)	Population density	0.5 degree (720 x 360)	Annual	2015	(Cecil and Daniel, 2001)

2.45 Model benchmarks

A common method for validating the outputs of dynamic global vegetation models (DGVMs) is to use satellite-based product datasets. For instance, direct observations of global fire occurrence by satellite-borne sensors can detect active fires, fire radiative power, and burned areas, and these observations have been available since the 1990s (Mouillot et al., 2014). The Fire Modeling Intercomparison Project (FireMIP) also used the satellite-based product database as a benchmark to evaluate the model simulation (Rabin et al., 2017; Li et al., 2019).

In the last few decades, several global biomass burning emission datasets based on burning area and fire radiative energy detection have been developed and used for many purposes, such as global climate and vegetation modeling, together with environmental, health, and security assessments (Ichoku et al., 2008; Mouillot et al., 2014). Although fire-related observation datasets are available and globally accessible, they have relatively large uncertainties and are poorly constrained, especially in models at the global and regional levels (Liousse et al., 2010; Petrenko et al., 2012, 2017; Bond et al., 2013; Zhang et al., 2014; Pan et al., 2015; Pereira et al., 2016).

Pan et al. (2020) reported that this uncertainty could be caused by various measurement and/or analysis processes, including the detection of fire or burned areas, retrieval of fire radiative power, emission factor information, biome type, burning stage, and fuel consumption estimation. The emission factor (EF) is considered an important factor for obtaining specific gaseous or particulate species of smoke emitted from burned dry matter in all major burned biomass (BB) emission datasets. Some EFs originate from laboratory experiments where fuel samples are burned in combustion chambers (Christian et al., 2003; Freeborn et al., 2008), whereas others originate from large-scale, open biomass burning and wildfire experiments. The combustion properties might differ greatly between these two categories; e.g., because of personnel security and other logistical considerations, some EF measurement locations are often not close enough to the biomass-burning source (Aurell et al., 2019). Another factor is the biome type, which affects the scaling factor of the emission coefficient for the FRP-based BB datasets (GFAS, FEER, and QFED). The emission factors of all BB datasets were assigned based on the type of biome, and most of the examined BB datasets had different definitions of major biome types, so uncertainty might be present at certain levels (Pan et al., 2020).

We validated the improved SEIB-DGVM fire module products by using the burned area (GFED4) and burned fraction (GFED4s) datasets, corresponding to the model's output. These datasets have higher resolutions than other burned area-based datasets, and all of the uncertainty probabilities regarding the selected database described by Pan et al. (2020) were adjusted with our model configurations. We used the emission factor (EF) from Andreae and Merlet (2001) with the latest update from Andreae (2019) and integrated the Plant Functional Types (PFTs) model with the land cover types (LCTs) used in the EF (Table 1 and Table S2 in the Supplement).

Furthermore, fire models should be evaluated together with their associated vegetation models because the former might produce burned areas perfectly but incorrectly simulate aboveground biomass (AGB) patterns. Fire products depend on AGB availability, and fire also affects AGB availability and succession after forest fires. Thus, to ensure that the model conducted

correct assessments, we evaluated the aboveground biomass variable using the ESA Biomass Climate Change Initiative dataset (Table 3). The AGB data from the ESA Biomass Climate Change Initiative (CCI) v.3 (2010,2017, and 2018) include high-quality data with a large resolution of 100 m × 100 m obtained from multiple remote sensing observations collected around the year 2010 (Santoro et al., 2021), making them suitable for validating our improved model product.

Overall, we validated the model spatially and numerically at Siberian level and in smaller regions, to determine the performance of the model in many points of view (spatial, numeric, wide and small region). We classified Siberia into three regions: west region (60º-90ºE and 45º-80ºN), central region (90º-120ºE and 45º-80ºN), and east region (120º-180ºE and 45º-80ºN) (Figure S12).

Table 3. Description of the observational datasets used for model evaluation

Type	Variable	Unit	Source	Spatial resolution	Temporal resolution	Temporal coverage	Reference
Fire	Burned area	Hectares	Global Fire Emissions Database, Version 4.0 (GFED4)	0.25 degree	Monthly, Annual	1996-2016	(Giglio et al., 2013)
	Burned fraction	-	Global Fire Emissions Database, Version 4.1 (GFED4s)	0.25 degree	Monthly, Annual	1997-2016	(Giglio et al., 2013)
	Dry matter	kg DM^{-1} m^{-2}					
	CO_2 emissions	g CO_2 $year^{-1}$					
	CO_2 emissions	g CO_2 $year^{-1}$	Global Biomass Burning Emissions Inventory (GBEI)	1-degree	Annual	2001-2020	Shiraishi et al., (2021)
Vegetation	Above-ground biomass	Mg $hectares^{-1}$	ESA Biomass Climate Change Initiative (Biomass CCI): Global datasets of forest above-ground biomass for the years 2010, 2017 and 2018, v3	100 m	Annual	2010, 2017-2018	(Santoro and Cartus, 2021)

3 Results

3.17 Improved mModel vValidation

3.17.1 Fire products

~~We compared the distribution patterns of burn fraction variables in the SEIB-DGVM SPITFIRE and GFED4s data, and most patterns differed only in eastern Siberia (Figure 7). The annual average spatial distribution of the burned fraction and burned area (1996-2016) was 78.9% (Figure S12.b and Figure S13.b), the GFED4s burned fraction was 89% (Figure S12.a), and the GFED4 burned area was 87% (Figure S13.a) from the total research grid area. The fire products (burned fraction and burned area) in the improved model have the same spatial distribution because they are calculated based on one core variable (Eq. 1). However, the spatial distributions of GFED4s (burned fraction) and GFED4 (burned area) differ for two reasons: first, because GFED4 does not consider small fires (Giglio et al., 2013) while GFED4s does, and second, because GFED4s use the modified burned fraction equation, which is able to calculate the exact fire fraction and fuel load (not uniformized) in a grid cell (Van Der Werf et al., 2017).~~We compared the annual average distribution patterns of burned fraction variable (1997-2016) in the SEIB-DGVM SPITFIRE and GFED4s data, and most patterns differed only in eastern Siberia (Figure 4, Figure S10). Compared to the burned fraction variable, burned area GFED4 has a smaller distribution pattern because it does not consider small fires (Figure S9.a). Comparison analysis of burned fraction variables between SEIB-DGVM SPITFIRE and GFED4s showed a linear relationship with a correlation coefficient of R=0.87 (R^2=0.75) (Figure S11.a). Similar to the comparison with GFED4s, the comparison of SEIB-DGVM SPITFIRE output of burned area variables with GFED4 data (1996-2016) shows a linear relationship with a correlation coefficient of R=0.78 (R^2=0.61) (Figure S11.b). Furthermore, in the three regions (west, central and east), the partial comparison of the burned fraction variable with GFED4s showed values of R^2=0.68, R^2=0.51, and R^2=0.58 (Figure S13), while for the burned area variable showed values of R^2=0.51, R^2=0.54, and R^2=0.506 (Figure S14), respectively. The burned fraction correlated better because both the GFED4s and the model's fire module considered small fires; many scattered fire data with values less than 0.1 and approximately 0.1 were found in both the model's output and the GFED4s data.

The fire products (burned fraction and burned area) in the improved model have the same spatial distribution because they are calculated based on one core variable (Eq. 1). However, the spatial distributions of GFED4s (burned fraction) and GFED4 (burned area) differ for two reasons: first, because GFED4 does not consider small fires (Giglio et al., 2013) while GFED4s does, and second, because GFED4s use the modified burned fraction equation, which is able to calculate the exact fire fraction and fuel load (not uniformized) in a grid cell (Van Der Werf et al., 2017).

Although the spatial distributions and patterns of the fire products (burned fraction and burned area) in the model and benchmark datasets (GFED4s and GFED4) ~~burned areas in the model and GFED4~~ data slightly differed, the model was able to produce annual mean value data that were similar to ~~the GFED data~~ both benchmark datasets. The mean average burned

fraction during 1997-2016 was 0.0137 in the simulations, ~~while that of the GFED4s was 0.0137~~ compared to the GFED4s, which recorded the same value of 0.0137 with an RMSE value of 7.2 x 10^{-4}. Furthermore, the mean average burned area of the model in 1996-2016 was 1428.5 ha $grid^{-1}$ $year^{-1}$, ~~while the GFED4 burned area data had a value of 1425.1 ha $grid^{-1}$ $year^{-1}$.~~ compared to the GFED4 burned area data, which closely recorded value of 1425.1 ha $grid^{-1}$ $year^{-1}$ by an RMSE value of 70.2 ha $grid^{-1}$ $year^{-1}$. In summary, the model was able to produce mean average data that precisely resembled observational data.

~~We also compared the spatial distributions of the annual averages (1996–2016) of the burned fraction and burned area variables from the model under the CRU TS3.22 climate dataset and benchmark datasets (GFED4 and GFED4s). The burn fraction data were in agreement with 75% of the total data, and the burned area data were in agreement with 61% of the total data (Figure S14). The burned fraction correlated better because both the GFED4s and the model's fire module considered small fires; many scattered fire data with values less than 0.1 and approximately 0.1 were found in both the model's output and the GFED4s data.~~

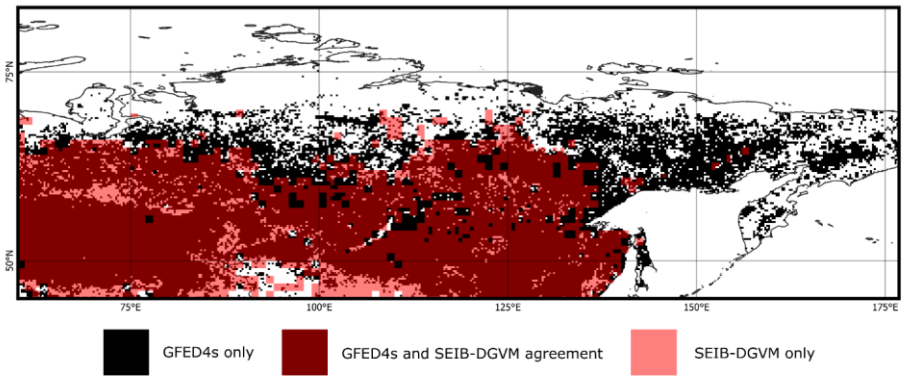

Figure 4~~7~~. ~~Spatial distribution comparison between SEIB-DGVM SPITFIRE and GFED4s burned fraction product (1997-2016)~~ Spatial distribution comparison of annual averaged burned fraction variable (1997-2016) of SEIB-DGVM SPITFIRE and GFED4s

Formatted: Justified, Space Before: 0 pt, After: 0 pt

3.17.2 Aboveground biomass

The improved model simulated similar aboveground biomass values to those of the benchmark data. In 2010, 2017, and 2018, the simulations predicted 63.714 ± 64.89 Mg DM ha^{-1} $year^{-1}$, 64.141 ± 65.54 Mg DM ha^{-1} $year^{-1}$, and 64.313 ± 65.61 Mg DM ha^{-1} $year^{-1}$, respectively, while the ESA Biomass CCI data showed 64.027 ± 56.95 Mg DM ha^{-1} $year^{-1}$, 64.548 ± 54.69 Mg DM ha^{-1} $year^{-1}$, and 65.05 ± 55.78 Mg DM ha^{-1} $year^{-1}$, respectively, for the same years. ~~In 2010, 2017, and 2018, the simulations predicted 63.714 Mg DM ha^{-1} $year^{-1}$, 64.141 Mg DM ha^{-1} $year^{-1}$, and 64.313 Mg DM ha^{-1} $year^{-1}$, respectively, while the ESA Biomass CCI data showed 64.027 Mg DM ha^{-1} $year^{-1}$, 64.548 Mg DM ha^{-1} $year^{-1}$, and 65.05 Mg DM ha^{-1} $year^{-1}$, respectively, for the same years.~~ The annual average AGB of the model in these years also showed the same increasing trend as that of the benchmark data, and the spatial distributions of the AGB model under CRU TS3.22 climate data and ESA Biomass CCI also agreed, with values of 83%, 84%, and 84%, respectively (Figure S15 and Figure S16 in the Supplement). Furthermore, when viewed on a smaller regional scale, the model is able to project better values in the eastern, western and central regions, with average values of R^2=0.74, R^2=0.73, and R^2=0.68, respectively (Figure S17). Although there was an annual average increase in the number of forest fires, there was a high variability trend in the model AGB values, indicating succession after forest fires (Figure 9.d). ~~indicating succession after forest fires (Figure S10.b).~~

3.17.3 Annual and seasonal fluctuations in burned dry matter

~~The model's dry matter data have a spatial distribution pattern similar to that of the model's fire products (burned fraction and burned biomass), as calculated from the available fire and fuel load data (fire product derivatives). The annual average dry matter variability from the 1997–2016 model (under the baseline climate product [CRU TS.3.22]) and the GFED4s data agreed with 63%, similar to the agreement of the fire products (Figure S19).~~

~~We also compared seasonal dry matter data to ensure that the monthly outputs of the SEIB-DGVM-SPITFIRE model agree with the observations, as this difference influences seasonal aerosol emissions. Between 1997 and 2016, the GFED4s data exhibited high fluctuations/dynamics depending on the month and year, while the SEIB-DGVM-SPITFIRE was not able to reproduce these dynamics or accurately predict the occurrence of extreme events (Figure S17a). For example, intense forest fires were recorded in 2003, 2012, and 2016. The monthly burned dry matter data for these years peaked in 2003 in May and in 2012 and 2016 in July (Figure S17.b–d). Severe wildfires in 2023 were due to low precipitation, as total rainfall reached only 36.0 mm in the Buryatia Republic and 45.7 mm in the Chita Oblast (IFFN, 2003). However, in the same period, the average total rainfall in the Buryatia Republic was approximately 332.23 mm, and that in the Chita Oblast was approximately 119.45 mm.~~

~~Furthermore, the monthly average burned dry matter in 2003, 2012 and 2016 was also lower in the model data than in the GFED4s data; the burned dry matter values of the improved model were 58.64 ± 5.86 kg DM m^{-2}, 59.41 ± 5.9 kg DM m^{-2}, and 59.98 ± 5.99 kg DM m^{-2}, while the benchmark data showed values of 122.36 kg DM m^{-2}, 101.7 kg DM m^{-2}, and 69.95 kg DM m^{-2}, respectively. However, considering the whole period of 1997–2016, not only years with extreme fire events, the model~~

~~was able to reproduce similar average values for multiple years and time-series data. When comparing the monthly averages during 1997-2016, the model data yield a value of 58.94 ± 5.89 kg DM m^{-2}, while the GFED4s data yield 59.12 kg DM m^{-2}. The model is not yet able to reproduce the exact value at a specific time of year or month because the model is run in a long-term phase and is not yet able to predict sudden natural and anthropogenic conditions (factors). Overall, the spatial distribution comparison of the monthly dry matter variables from GFED4s and SEIB-DGVM SPITFIRE for 20 years (1997-2016) revealed a correlation of 99% (Figure 8); therefore, the model was able to approximate the monthly averages.~~The model's dry matter data have a spatial distribution pattern similar to that of the model's fire products (burned fraction and burned biomass), as calculated from the available fire and fuel load data (fire product derivatives). The annual average dry matter variability from the 1997–2016 model (under the baseline climate product [CRU TS.3.22]) and the GFED4s data agreed with 63%, similar to the agreement of the fire products (Figure S20). Spatial comparisons at the regional scale in the western, central and eastern regions of Siberia show lower values than the Siberian region as a whole, which has an agreement of 54%. 51%, and 58% (Figure S21).

We also compared seasonal dry matter data to ensure that the monthly outputs of the SEIB-DGVM SPITFIRE model agree with the observations, as this difference influences seasonal aerosol emissions. Between 1997 and 2016, the GFED4s data exhibited high fluctuations/dynamics depending on the month and year, while the SEIB-DGVM SPITFIRE was not able to reproduce these dynamics or accurately predict the occurrence of extreme events (Figure S18a). For example, intense forest fires were recorded in 2003, 2012, and 2016. The monthly burned dry matter data for these years peaked in 2003 in May and in 2012 and 2016 in July (Figure S18.b-d). Severe wildfires in 2003 were due to low precipitation, as total precipitation reached only 36.0 mm in the Buryatia Republic and 45.7 mm in the Chita Oblast between August 2002 and May 2003 (IFFN, 2003). While the 41-year average precipitation between August and May (1981-2022), in the Buryatia Republic was approximately 332.23 mm, and in the Chita Oblast was approximately 119.45 mm. Thus, the low precipitation in 2003 was an anomaly outside of the annual average range.

Furthermore, the monthly average burned dry matter in 2003, 2012 and 2016 was also lower in the model data than in the GFED4s data; the burned dry matter values of the improved model were 58.64 ± 5.86 kg DM m^{-2}, 59.41 ± 5.9 kg DM m^{-2}, and 59.98 ± 5.99 kg DM m^{-2}, while the benchmark data showed values of 122.36 kg DM m^{-2}, 101.7 kg DM m^{-2}, and 69.95 kg DM m^{-2}, respectively. However, considering the whole period of 1997-2016, not only years with extreme fire events, but the model was also able to reproduce similar average values for multiple years and time-series data. When comparing the monthly averages during 1997-2016, the model data yield a value of 58.94 ± 5.89 kg DM m^{-2}, while the GFED4s data yield 59.12 kg DM m^{-2}. The model is not yet able to reproduce the exact value at a specific time of year or month because the model is run in a long-term phase and is not yet able to predict sudden natural and anthropogenic conditions (factors). Overall, the spatial distribution comparison of the monthly dry matter variables from GFED4s and SEIB-DGVM SPITFIRE for 20 years (1997-2016) revealed a correlation of 99% (Figure 5); therefore, the model was able to approximate the monthly averages.

3.17.4 Aboveground biomass Carbon dioxide (CO_2) and $PM_{2.5}$ emissions

We evaluated CO_2 emissions as representative of all emissions because CO_2 is the most emitted agent during biomass combustion (Ritchie et al., 2020). In addition, emissions were estimated from the same burned dry matter variable, which differed only in the emission factor value of each emission. Therefore, the CO_2 emission evaluation results are representative of all the other burned biomass emissions.

The annual average CO_2 emissions were highest in the GFED4s, followed by those in the SEIB-DGVM SPITFIRE model product and then those in the GBEI product, with values of $105.64 \pm 50.69 \times 10^{13}$ g CO_2, $76.41 \pm 0.87 \times 10^{13}$ g CO_2, and $62.4 \pm 26.09 \times 10^{13}$ g CO_2, respectively (Table S3). The GFED4s and GBEI data have higher standard deviation values than does the SEIB-DGVM SPITFIRE data and appear to have a large difference. However, when comparing the annual average CO_2 emissions from SEIB-DGVM SPITFIRE, GFED4s, and GBEI, we found that they were similar: 141.1 Gg CO_2 $year^{-1}$, 157.2 Gg CO_2 $year^{-1}$, and 148.7 Gg CO_2 $year^{-1}$, respectively.

Our study area covers the Boreal Asia (BOAS) area and a small part of Central Asia (CEAS), differing from the GFED4 basis region classification; therefore, we extracted these areas from the GFED4s data for comparison (Figure S20). A comparison of the GFED4s CO_2 data between the BOAS area and the Siberian area showed that the two datasets had a similarity of 98% (Figure S24), confirming the accuracy of the GFED4s validation data.

As all emission products are derived from fire products (dry matter variables), emission factors displayed spatial and value dynamics similar to those of the fire products (Figure S18, Figure S25, and Figure S26). When comparing the annual average dry matter emission data and CO_2 emissions generated by the model, the results correlated perfectly (100%, Figure S27), indicating that the model runs well according to Equation (29) and that CO_2 and other emissions have the same distribution patterns as the dry matter variables. However, they differ in their values because each emission species has a different emission factor. Overall, the annual average CO_2 emission model data were 63% (Figure 9.a) and 67% (Figure 9.b) correlated with the GFED4s and GBEI data, respectively.

We also compared the modeled $PM_{2.5}$ emissions and their distribution patterns with the Copernicus Atmosphere Monitoring Service (CAMS) (Romanov et al., 2022) data in seven Russian territories during 2004-2021. The improved model data and CAMS data both exhibited an increasing trend (Figure 10.a and Figure 2 in Romanov et al. (2022)) and a correlation of 85.8% (Figure 10.b).Emissions from biomass burning contribute significantly to the global budget for residual gases and aerosols that affect the climate. It's estimated that biomass burning contributed up to 50% of global CO and NO_x emissions in the troposphere (Galanter et al., 2000), and the most emitted gas during biomass burning is CO_2 (Ritchie et al., 2020). Since CO_2 emissions are the primary emissions that contribute to climate change, it is critical to assess and monitor them continuously.

In this study, out of 33 projected emissions (Table 4 and Table S6), we validated the CO_2 variable that able to represent all projected emissions because all estimated emissions are derived from the same burned dry matter variable, which differs only in the emission factor value of each gaseous emission. The highest annual average value of CO_2 emissions from 1997 to 2020 is from GFED4 data, followed by SEIB-DGVM SPITFIRE and then the GBEI product, with values of $105.64 \pm 50.69 \times 10^{13}$

g CO_2, 76.41 ± 0.87 × 10^{13} g CO_2, and 62.4 ± 26.09 × 10^{13} g CO_2, respectively (Table S3). The GFED4s and GBEI data have higher standard deviation values than does the SEIB-DGVM SPITFIRE data and appear to have a large difference.

Spatially, the annual average CO_2 emission model data were 63% (Figure 6.a) and 67% (Figure 6.b) correlated with the GFED4s and GBEI data, respectively. Furthermore, CO_2 emissions of the model compared to the GFED4s in the three regions (west, central, and east) showed lower agreement than Siberia as a whole, at 55%, 50.6%, and 52%, respectively (Figure S29). Whereas, the comparison to GBEI data at the three regions, showed agreements of 57.5%, 55%, and 58%, respectively (Figure S30). However, when comparing the mean of averaged CO_2 emissions all the years from 1997 to 2020 of SEIB-DGVM SPITFIRE, GFED4s, and GBEI, we found that they were similar: 141.1 ± 11.5 Gg CO_2 $year^{-1}$, 157.2 ± 14.8 Gg CO_2 $year^{-1}$, and 148.7 ± 7.12 Gg CO_2 $year^{-1}$, respectively.

Our study area covers the Boreal Asia (BOAS) area and a small part of Central Asia (CEAS), differing from the GFED4 basis region classification; therefore, we extracted these areas from the GFED4s data for comparison (Figure S22). A comparison of the GFED4s CO_2 data between the BOAS area and the Siberian area showed that the two datasets had a similarity of 98% (Figure S26), confirming the accuracy of the GFED4s validation data.

As all emission products are derived from fire products (dry matter variables), emission factors displayed spatial and value dynamics similar to those of the fire products (Figure S19, Figure S27, and Figure S40). When comparing the annual average dry matter emission data and CO_2 emissions generated by the model, the results correlated perfectly (100%, Figure S31), indicating that the model runs well according to Equation (3) and the projected CO_2 and other emissions have the same distribution patterns as the dry matter variable, because all of the emissions calculation are based on the dry emission variable. However, they differ in their values because each emission species has a different emission factor.

We also compared the modelled $PM_{2.5}$ emissions and their distribution patterns with the Copernicus Atmosphere Monitoring Service (CAMS) (Romanov et al., 2022) data in seven Russian territories (Amur Region, Buryatia Republic, Irkutsk Region, Khabarovsk Territory, Krasnoyarsk Territory, Transbaikal Territory, Yakutia (Sakha Republic)) during 2004-2021. The improved model data and CAMS data both exhibited an increasing trend (Figure 7.a and Figure 2 in Romanov et al. (2022)) and a correlation of 85.8% (Figure 7.b).

~~We also compared the modeled $PM_{2.5}$ emissions and their distribution patterns with the Copernicus Atmosphere Monitoring Service (CAMS) (Romanov et al., 2022) data in seven Russian territories during 2004-2021. The improved model data and CAMS data both exhibited an increasing trend (Figure 7.a and Figure 2 in Romanov et al. (2022)) and a correlation of 85.8% (Figure 7.b).~~

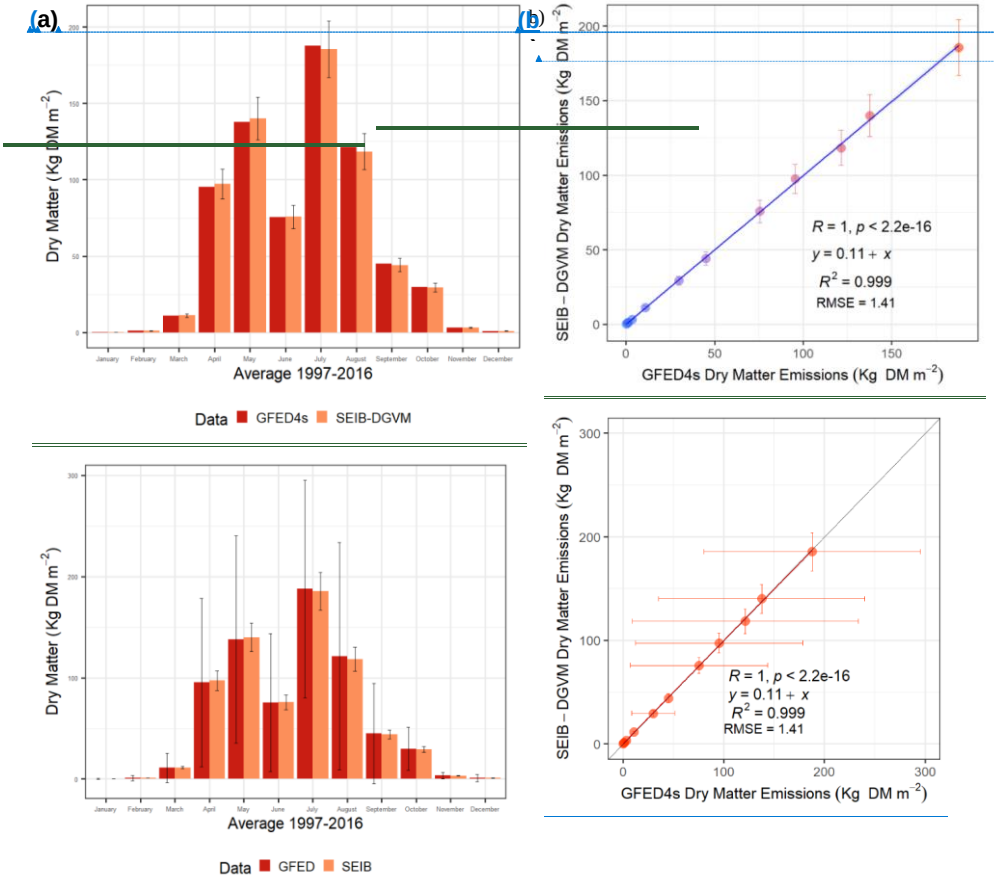

Figure 85. (a) Monthly temporal variability averaged dry matter emission of GFED4s and SEIB-DGVM from 1997 to 2016. **(b)** Comparison of monthly averaged dry matter emissions of GFED4s and SEIB-DGVM from 1997 to 2016. Standard deviation obtained from each monthly data from 1997 to 2016.

Formatted: Font: 12 pt, Bold, Complex Script Font: Bold

Formatted: Font: Arial, 12 pt, Bold, Complex Script Font: Bold

Formatted: Font: Arial, Bold, Complex Script Font: Bold

Formatted: Font: 12 pt, Bold, Complex Script Font: Bold

Formatted: Font: Arial, Bold, Complex Script Font: Bold

Formatted: Font: Bold, Complex Script Font: Bold

Formatted: Font: Bold, Complex Script Font: Bold

Formatted: Justified

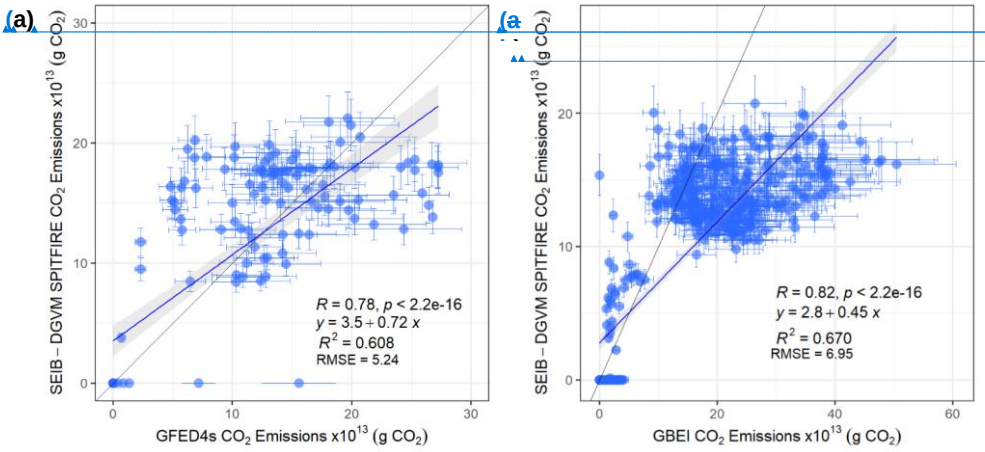

Figure 6. Latitude average spatial comparison of simulated CO_2 emissions of SEIB-DGVM SPITFIRE with GFED4s from 1997 to 2016 **(a)** and GBEI from 2001 to 2020 **(b)** dataset. Standard deviation obtained from the annual CO_2 emission data of each dataset.

~~Monthly Average Dry Matter Emission data comparison of GFED4s and SEIB-DGVM SPITFIRE (1997-2016): a) Monthly average seasonality b) Monthly average comparison~~

Formatted: Font: 12 pt, Bold, Complex Script Font: Bold

Formatted: Font: Arial, 12 pt, Bold, Complex Script Font: Bold

Formatted: Font: Arial, Bold, Complex Script Font: Bold

Formatted: Font: 12 pt, Bold, Complex Script Font: Bold

Formatted: Font: Arial, 12 pt, Bold, Complex Script Font: Bold

Formatted: Font: Arial, Bold, Complex Script Font: Bold

Formatted: Subscript

Formatted: Font: Bold, Complex Script Font: Bold

Formatted: Font: Bold, Complex Script Font: Bold

Formatted: Subscript

Formatted: Justified

Formatted: Justified, Space Before: 0 pt, After: 0 pt, Line spacing: Multiple 1.07 li

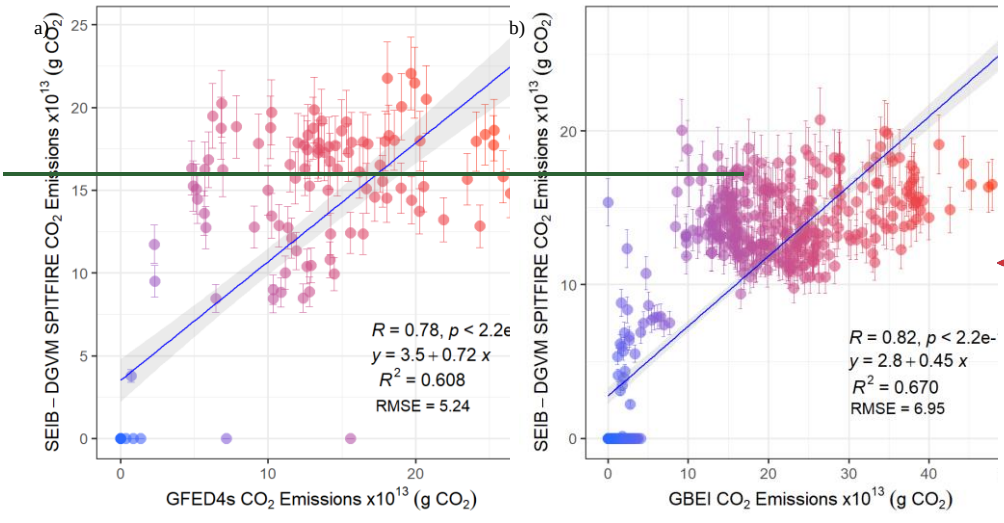

~~**Figure 9.** CO_2 emissions spatial average comparison of SEIB-DGVM-SPITFIRE module product under baseline climate product (CRU TS.3.22) with: a) GFED4s data (1997-2016), b) with GBEI data (2001-2020)~~

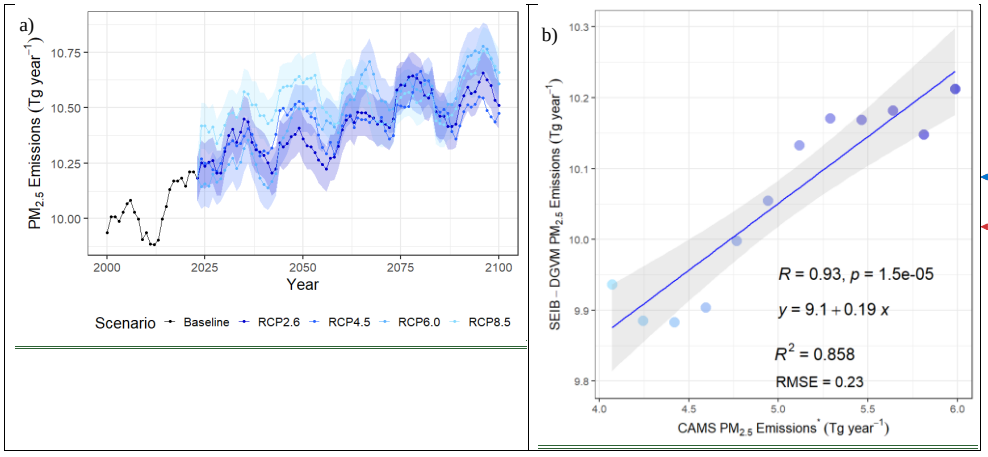

Formatted: Indent: Before: 0", Line spacing: Multiple 1.07 li

Formatted: Line spacing: Multiple 1.07 li, Don't keep with next

Formatted Table

Formatted: Justified, Space Before: 0 pt, After: 0 pt, Line spacing: Multiple 1.07 li

Formatted: Indent: Before: 0", Line spacing: Multiple 1.07 li

Formatted: Line spacing: Multiple 1.07 li, Don't keep with next

Formatted Table

~~**Figure 10.** a) Projected $PM_{2.5}$ emissions under several climate scenarios (2003-2100), b) Comparison of $PM_{2.5}$ emissions from the SEIB-DGVM-SPITFIRE model with *trendline data from the Copernicus Atmosphere Monitoring Service in Russia~~

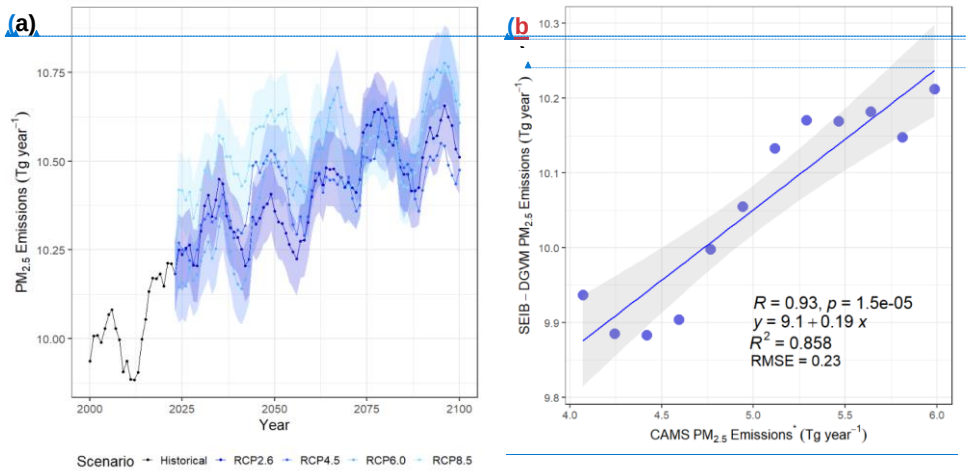

Figure 710. (a) ~~P~~Temporal variation of projected $PM_{2.5}$ emissions under several climate scenarios from ~~(2003~~2000 to ~~-~~2100. Standard deviation obtained from the annual $PM_{2.5}$ emission value of each climate scenarios (RCP8.5, RCP6.0, RCP4.5, and RCP2.6).~~)~~ **(b)** Comparison of $PM_{2.5}$ emissions from the SEIB-DGVM SPITFIRE model with the *trendline processed data from the Copernicus Atmosphere Monitoring Service in seven regions in Russia from 2004 to 2021 (Romanov et al., 2022).~~Russia~~

Formatted: Justified

Formatted: Justified, Space Before: 0 pt, After: 0 pt, Line spacing: Multiple 1.07 li

Formatted Table

Formatted: Font: 12 pt, Bold, Complex Script Font: Bold

Formatted: Font: Arial, 12 pt, Bold, Complex Script Font: Bold

Formatted: Font: Arial, Bold, Complex Script Font: Bold

Formatted: Font: 12 pt, Bold, Complex Script Font: Bold

Formatted: Font: Arial, Bold, Complex Script Font: Bold

Formatted: Font: Bold, Complex Script Font: Bold

Formatted: Justified

Formatted: Font: Bold, Complex Script Font: Bold

Formatted: Normal

3.21 Burned fraction

Improved model (SEIB-DGVM SPITFIRE) is able to produce burned fraction variables better than the default model (SEIB-DGVM GlobFIRM). Based on the spatial comparison of the 1997-2016 average burned fraction variables GFED4s, SEIB-DGVM SPITFIRE, and Default SEIB-DGVM, it is known that SEIB-DGVM SPITFIRE is able to produce data with a similarity of 75% with GFED4s data, while the default model is at 68% (Figure S5).

The burned fraction variable in the improved model exhibited a spatial distribution pattern different from that in the default model (Figure S4.b). According to the improved model, the burned fraction data were distributed in the western, central, and southern areas (Figure S4.e hb). We compared the burned fraction variable with the lightning flash rate and population density data to confirm that the produced variable considered the new ignition factor. The burned fraction showed a 46% correlation with the lightning flash rate and a 6% correlation with population density between 2006 and 2100 (Figure S 78.ab and bd). In general, the burned fraction under all the RCP scenarios exhibited an increasing trend from 2006 to 2100, with the highest value occurring under the RCP8.5 scenario. Under the RCP8.5 scenario, the lowest value was 0.01371, and the highest value was 0.01425, with an average value of 0.01398 (Figure S54.db).

In contrast to the results produced from the improved model, the burned fraction data from the default model were spread throughout most of the area (Figure S4.a d). From 2006 to 2100 under all RCP scenarios, the burned fraction in the default model also exhibited an increasing trend. Under the RCP8.5 scenario, the lowest value is 0.002996, and the highest value is 0.003124, with an average value of 0.00306 (Figure S45.ca), which is well below the outputs of the improved model.

3.23 Burned area

The burned area of the improved model showed a similar spatial distribution pattern under all the RCP scenarios (Figure S6.a). The distribution pattern of the burned area variable was also similar to that of the burned fraction variable, as the burned area and burned fraction calculation processes are both based on fire probability (Eq. 1). Overall, under all the scenarios, the burned area exhibited the same increasing trend, with the RCP4.5 scenario reaching the highest value. Under the RCP4.5 scenario from 2006 to 2100, the burned area has an average value of 1457.6 hHa grid^{-1} year^{-1} and is projected to increase with values of 80.4 to 83.7 x 105 hectares (Figure S6.b7). Since the default model does not compute burned area, this variable could not be compared between the improved model and the default model.

3.34 Burned biomass

The improved model confirmed uniform spatial distribution patterns for the fire variables: burned fraction (Figure S4.b), burned area (Figure S6.a), and burned biomass (Figure 8.b). All of the improved module fire variables confirmed to be mutually integrated because the calculation process comes from the first fire variable (burned fraction). Compared to the improved model, the spatial distribution pattern of the burned biomass variable from the default model was wider and spread across the

entire Siberia region (Figure 8.a). The spatial distribution pattern of burned fraction (S4.a-d) and burned biomass (Figure 8.a) in the default model is different and exhibited a box-like pattern in the center of the map. Moreover, the internal relationship between burned fraction and burned biomass variables in the default model (SEIB-DGVM GlobFIRM) did not show the correct relationship (R^2<0.01), where the higher the burned fraction, the higher the burned biomass (Figure S8.a). While the internal relationship between burned fraction and burned biomass variables in the improved model (SEIB-DGVM SPITFIRE) showed a positive linear correlation (R^2=0.85) (Figure S8.d).

Under all the RCP scenarios from 2006 to 2100, the burned biomass variable from the default model exhibited a decreasing trend (Figure 8.c). Under the RCP8.5 scenario, from 2006 to 2100, the value decreased from 5.09 to 5.05 kg DM m^{-2}, with an overall mean value of 5.07 kg DM m^{-2}. Meanwhile, the burned fraction product from default model shows an increasing trend (Figure S4.c), this indicates a misalignment in the default model between the burned fraction and burned area variables. On the other hand, the burned fraction (Figure S4.d), burned area (Figure S6.b), and burned biomass (Figure 8.d) variables in the improved model all have an increasing trend, indicating harmony between the three variables. Burned biomass variable under the RCP8.5 scenario from 2006 to 2100, the lowest and highest values were 8.0 and 8.71 kg DM m^{-2}, respectively, with an overall mean value of 8.52 kg DM m^{-2}. The twenty-year variations and their trends of dry matter emissions up to 2100 are 8.37 ± 0.07 (3.3%), 8.46 ± 0.04 (0.7%), 8.53 ± 0.06 (1.3%), 8.52 ± 0.05 (-0.68%), 8.57 ± 0.08 (1.07%) (Figure S32).~~The improved model confirmed uniform spatial distribution patterns for the fire variables: burned fraction, burned area, and burned biomass (Figure 4.e-h). There was an increasing trend in the burned biomass variable under all RCP scenarios from 2006 to 2100. Under the RCP8.5 scenario from 2006 to 2100, the lowest and highest values were 8.0 and 8.71 kg DM m^{-2}, respectively, with an overall mean value of 8.52 kg DM m^{-2}.~~

~~Compared to that of the improved model, the spatial distribution pattern of the burned biomass variable from the default model was wider and spread across the entire Siberia region (Figure 4.a-d). The spatial distribution pattern of fire variables (burned fraction and burned biomass) in the default model exhibited a box-like pattern in the center of the map (Figure 4.a-d and Figure S4.a-d). Under all the RCP scenarios from 2006 to 2100, the burned biomass variable exhibited a decreasing trend. Under the RCP8.5 scenario, from 2006 to 2100, the value decreased from 5.09 to 5.05 kg DM m^{-2}, with an overall mean value of 5.07 kg DM m^{-2}.~~

Formatted: Superscript

Formatted: Superscript

Formatted: Not Highlight

Formatted: Not Highlight

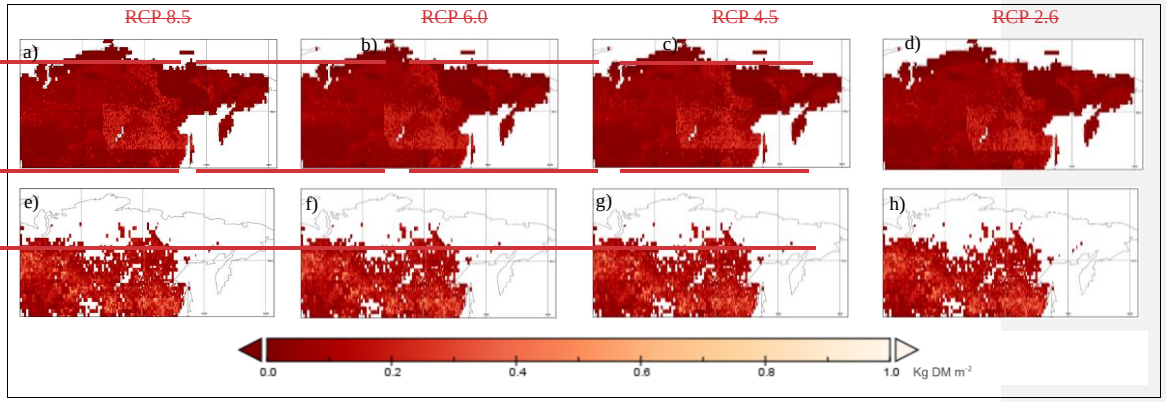

600

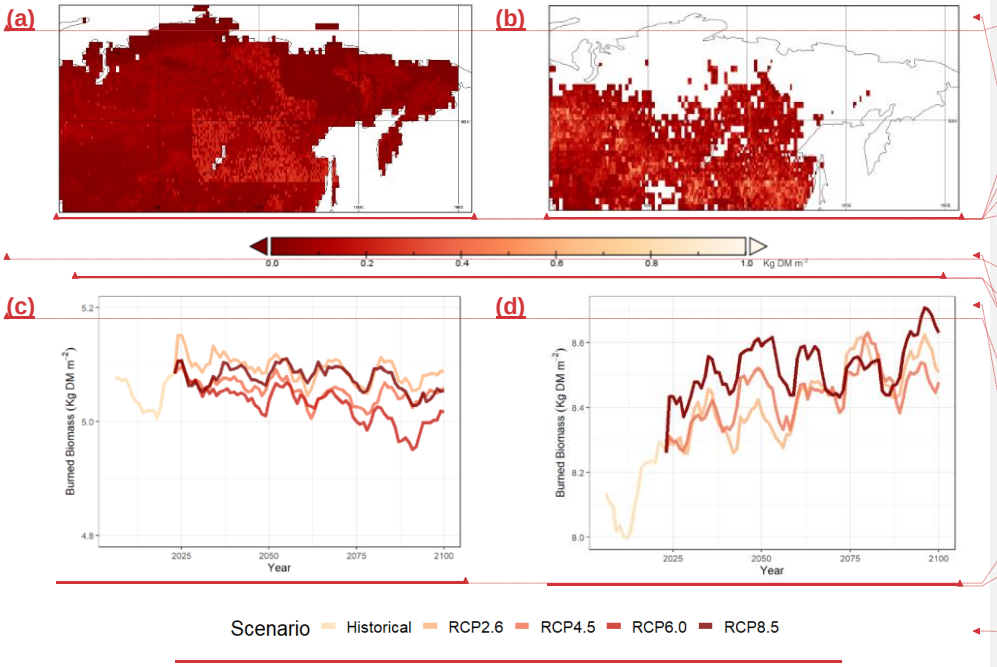

Formatted: Font: (Default) Arial, 12 pt, Complex Script Font: Arial, 12 pt

Formatted: Font: (Default) Arial, 12 pt, Complex Script Font: Arial

Formatted: Font: (Default) Arial, 12 pt, Complex Script Font: Arial, 12 pt

Formatted: Font: (Default) Arial, 12 pt, Complex Script Font: Arial

Formatted: Font: (Default) Arial, 12 pt, Complex Script Font: Arial, 12 pt

Formatted Table

Formatted: Font: (Default) Arial, 12 pt, Complex Script Font: Arial, 12 pt

Formatted: Font: (Default) Arial, 12 pt, Complex Script Font: Arial

Formatted: Font: (Default) Arial, 12 pt, Complex Script Font: Arial, 12 pt

Formatted: Centered

Formatted: Font: (Default) Arial, 12 pt, Complex Script Font: Arial, 12 pt

Formatted: Font: (Default) Arial, 12 pt, Complex Script Font: Arial, 12 pt

Formatted: Font: (Default) Arial, 12 pt, Complex Script Font: Arial, 12 pt

Formatted Table

Formatted: Centered

Figure 84. **(a)** ~~Annual average burned biomass maps (2006-2100) comparison under different RCP scenarios: a-d) SEIB-DGVM Default Fire Module, e-h) SEIB-DGVM SPITFIRE Module~~ Spatial distribution of annual averaged burned biomass of SEIB-DGVM GlobFIRM from 2006 to 2100. **(b)** Spatial distribution of annual averaged burned biomass of SEIB-DGVM SPITFIRE from 2006 to 2100. **(c)** Temporal variation of burned biomass of SEIB-DGVM GlobFIRM from 2006 to 2100. **(d)** Temporal variation of burned biomass of SEIB-DGVM SPITFIRE from 2006 to 2100.

3.54 Aboveground biomass

The aboveground biomass calculations in the default model and improved model used the same estimation process ~~estimation parameters~~ because the trunk biomass in the SEIB-DGVM included coarse root biomass; therefore, only approximately 2/3 of the trunk biomass was classified as aboveground biomass (Sato et al., 2007). However, during the calibration of the aboveground biomass variable with the ESA Biomass CCI benchmark dataset, we adjusted the calculation impact of fire and its distribution pattern (based on natural and anthropogenic ignition factors) on the availability of aboveground biomass.

According to the default model, the AGB distribution pattern appears to be the same as that of the fire variable, a box-like pattern still occurs on the map (Figure 9.a), and annual average aboveground biomass under the RCP 8.5 scenario show an increasing trend (Figure 9.c). The AGB trend also differed between the RCP scenarios. Specifically, under the RCP8.5 and RCP2.6 scenarios, the AGB exhibited little change, while under the RCP6.0 and RCP4.5 scenarios, the AGB exhibited a downward trend (Figure 9.c). Under the RCP6.0 scenario, from 2006 to 2100, the AGB decreased from 69.5 to 68.9 Mg DM ha^{-1}, and the average value was 63.9 Mg DM ha^{-1}.

~~According to the default model, the AGB distribution pattern appears to be the same as that of the fire variable, and a box-like pattern still occurs on the map (Figure 5.a-d). The AGB trend also differed between the RCP scenarios. Specifically, under the RCP8.5 and RCP2.6 scenarios, the AGB exhibited little change, while under the RCP6.0 and RCP4.5 scenarios, the AGB exhibited a downward trend (Figure S10.a). Under the RCP6.0 scenario, from 2006 to 2100, the AGB decreased from 69.5 to 68.9 Mg DM ha^{-1}, and the average value was 63.9 Mg DM ha^{-1}.~~

Compared to the default model, the improved AGB model has differences in distribution patterns (Figure 9.b) and trends in annual average dynamics (Figure 9.d). The distribution pattern of AGB in the improved model is different, in the central Siberian region, in some locations that have high AGB has been reduced due to the impact of forest fires, so that the box-like pattern is no longer visible (Figure 9.b). The annual average dynamics of aboveground biomass in the improved model also shows a downward trend due to the variable trend of fire (forest fires) which is projected to continue to increase (Figure S4.d).

The AGB values under all RCP scenarios exhibited a decreasing trend from 2006 to 2100. The AGB under the RCP8.5 scenario from 2023 to 2100 decreased from 69.15 to 68.5 Mg DM ha^{-1} (Figure 9.d), and the mean was 62.75 Mg DM ha^{-1}. The twenty-year variations and their trends of aboveground biomass up to 2100 are 69.09 ± 0.168 (0.13%), 69.04 ± 0.151 (-0.54%), 68.88 ± 0.128 (-0.07%), 68.37 ± 0.226 (-0.76%), 68.36 ± 0.189 (0.63%) (Figure S33).

~~Although the improved model adjusted for the impact and interaction between fire and vegetation variables, the spatial distribution patterns of the AGB variables in the improved and default models still looked similar because of the common roots (Figure 5). The AGB in the improved model exhibited a different distribution pattern than did the distribution pattern of the fire variables; for example, in southwestern Siberia, there was an area with a high fire frequency, while it had a low AGB value (Figure 5.e-h). The AGB values under all RCP scenarios exhibited a decreasing trend from 2006 to 2100. The AGB under the RCP8.5 scenario from 2023 to 2100 decreased from 69.15 to 68.5 Mg DM ha^{-1} (Figure S10.b), and the mean was 62.75 Mg DM ha^{-1}.~~

Formatted: Not Highlight

Formatted: Not Highlight

Formatted: Not Highlight

Formatted: Not Highlight

Formatted: Not Highlight

Formatted: Not Highlight

~~According to the default model, the AGB distribution pattern appears to be the same as that of the fire variable, and a box-like pattern still occurs on the map (Figure 5.a-d). The AGB trend also differed between the RCP scenarios. Specifically, under the RCP8.5 and RCP2.6 scenarios, the AGB exhibited little change, while under the RCP6.0 and RCP4.5 scenarios, the AGB exhibited a downward trend (Figure S10.a). Under the RCP6.0 scenario, from 2006 to 2100, the AGB decreased from 69.5 to 68.9 Mg DM ha^{-1}, and the average value was 63.9 Mg DM ha^{-1}.~~

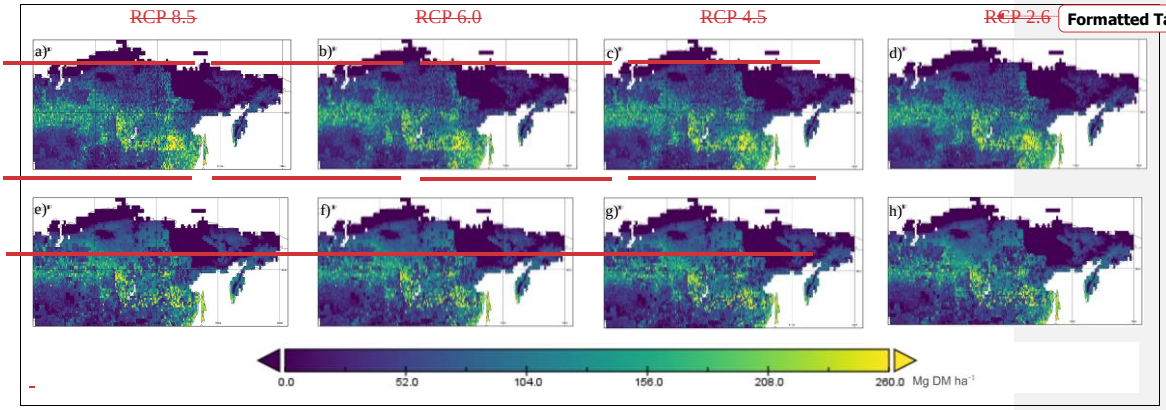

Formatted Table

Figure 5. Annual average aboveground biomass maps (2006-2100) comparison under different RCP scenarios: a-d) SEIB-DGVM Default Fire Module, e-h)

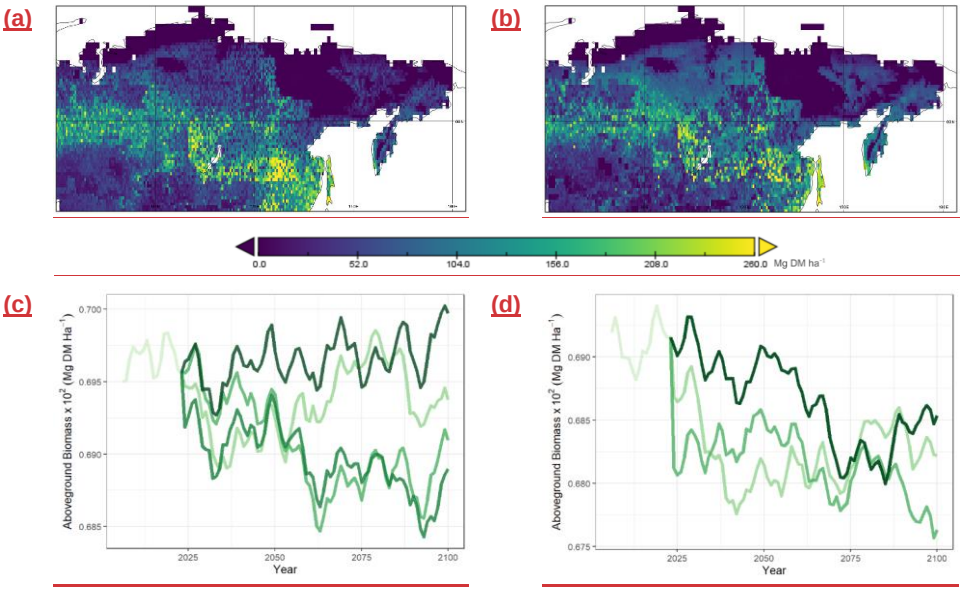

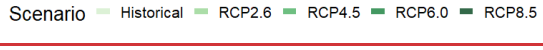

Figure 9. (a) Spatial distribution of annual averaged aboveground biomass of SEIB-DGVM GlobFIRM from 2006 to 2100. **(b)** Spatial distribution of annual averaged aboveground biomass of SEIB-DGVM SPITFIRE from 2006 to 2100. **(c)** Temporal variation of aboveground biomass of SEIB-DGVM GlobFIRM from 2006 to 2100. **(d)** Temporal variation of aboveground biomass of SEIB-DGVM SPITFIRE from 2006 to 2100.

3.65 Forest ecological variables under fire-on and fire-off simulation

We conducted complete ~~full~~ simulations under fire-on and fire-off modes to compare and assess vegetation dynamics during forest fires. Assessing vegetation dynamics can be done by understanding the carbon pools in the certain region or globally, where carbon pools are easier to measure than carbon fluxes. In this study, the net primary production (NPP) is used as a reference variable because is an important metric of the global carbon cycle (Running, 2022) and measures the rate of global plant growth. ~~The net primary production (NPP) is used as a reference variable because it is the most measurable element of the carbon cycle and measures the rate of global plant growth.~~ Based on the comparison of results between the fire-on and fire-off simulations, the NPP variable under all of the RCP scenarios shows a downward trend with some small fluctuations. Under the RCP8.5 scenario, an average NPP loss of 319.3 ± 28.2 g C m^{-2} $year^{-1}$ occurred during 1997–2100 (Figure S25.a). In addition to the NPP variable, the improved model (SEIB-DGVM SPITFIRE) can also simulate Net Biome Production (NBP). Under the same RCP8.5 scenario, the annual average NBP from 2000-2100 shows a positive value of 80.7 Tg C $year^{-1}$ (Figure S25.b), with a continuous decreasing trend.~~, an average loss of 319.3 g C m^{-2} $year^{-1}$ occurred during 1997–2100 (Figure S23.a).~~

In relation to wildfires, assessing pre- and postfire tree density variables is critical for measuring the impact of fires. Under the RCP8.5 scenario, in the fire-on simulation from 1997 to 2100, it is projected that the tree density in Siberia was 2,208 tree ha^{-1}. However, under the same RCP and time range in the fire-off simulation, the tree density was 2,391 tree ha^{-1}. We also compared the tree density between the fire-on and fire-off simulations under all the RCP scenarios and found that the tree density increased in the fire-off simulations compared to that in the fire-on simulations. Under the RCP8.5 scenario, on average, 185 trees ha^{-1} $year^{-1}$ died due to the fire (Figure S253.~~cb~~).

We also conducted a more detailed assessment of several forest structure variables, such as tree DBH, crown area, and tree height, from 2006 to 2100 under all the RCP scenarios. Under the RCP8.5 scenario, in the fire-on simulation, the results showed that tree DBH values varied from 0 to 0.96 m (average 0.6 m), tree height from 0 to 25.8 m (average 17 m), and crown area from 0 to 6.6 m^2 (average 4 m^2). The average tree structure in the fire-off simulation was greater than that in the fire-on simulation, with average tree DBH, tree height, and crown area of 0.67 m, 17.2 m, and 4.6 m^2, respectively. The correlations between the tree structure variables under fire-on and fire-off simulation conditions were similar and highly correlated; the overall average correlation among the tree DBH, tree height, and crown area variables was 98% (Figure 10~~6~~). Specifically, according to region classification, highest to the lowest value of tree height, tree DBH, and crown area value is in the central region, then west region, and east region. On average for 2081-2100 under RCP8.5 in each region, the tree height, tree DBH, and crown area variables show values of 21.5 ± 0.03 m, 0.79 ± 0.001 m, 5.2 ± 0.008 m^2 (central region), 19.5 ± 0.08 m, 0.73 ± 0.003 m, 4.17 ± 0.03 m^2 (west region), and 18.6 ± 0.021 m, 0.65 ± 0.0009 m, 4.45 ± 0.009 m^2 (east region) (Figure S37, Figure S38, and Figure S39). Furthermore, we found an interesting pattern, the simulated tree height, tree DBH, and crown area variables in the west region and central region have a decreasing trend, while in the eastern region the tree height, tree DBH and crown area variables are projected to increase from 2000 to 2100 (Figure S37, Figure S38, and Figure S39). In

Formatted: Not Highlight
Formatted: Not Highlight
Formatted: Not Highlight
Formatted: Not Highlight
Formatted: Not Highlight
Formatted: Superscript
Formatted: Superscript
Formatted: Superscript

addition, the relationship between the three variables (tree height, tree DBH, and crown area) in the west region and central region shows a linear trend where the higher the tree height, the greater the tree DBH and the wider the crown area (Figure 11. a and b). The east region shows an interesting pattern, different from other regions, where the relationship between the three variables is naturally random (Figure 11.c).

~~Fire-on~~

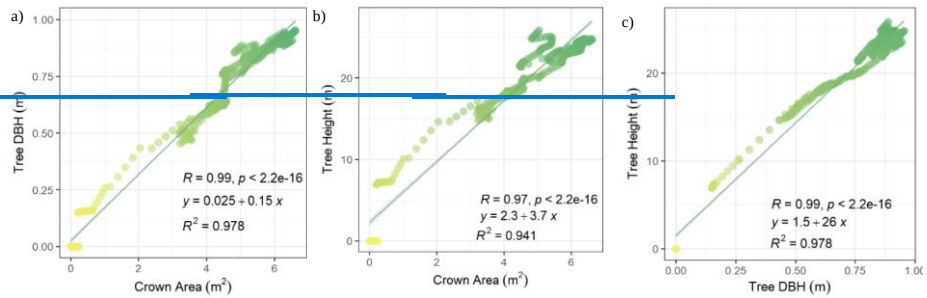

~~Fire-off~~

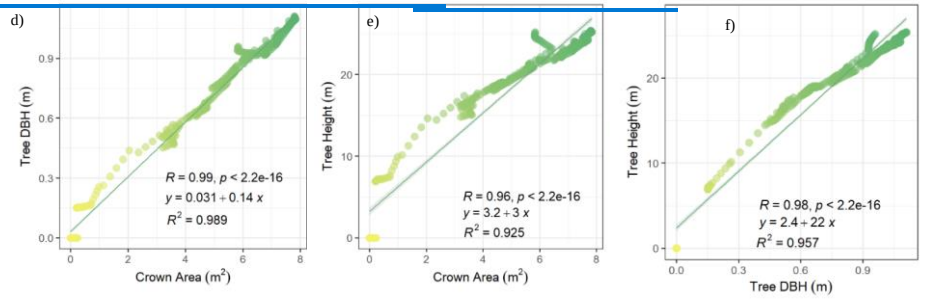

(a) (b) (c)

Fire-on

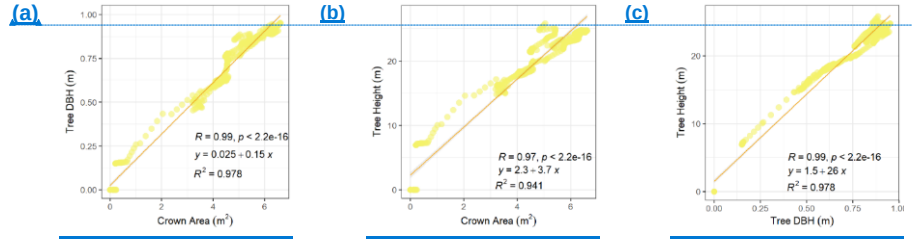

Formatted: Font: (Default) Arial, Complex Script Font: Arial

Formatted: Font: (Default) Arial, 10 pt, Complex Script Font: Arial

Formatted: Centered

Formatted Table

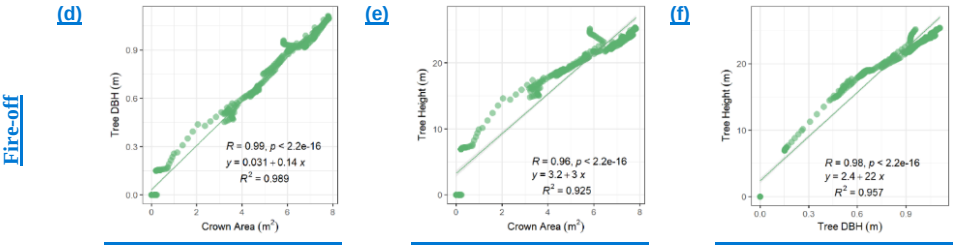

Formatted: Centered

700 **Figure 106.** Annual average comparison of tree DBH, tree height and crown area variables in (a-c) fire-on ~~(a-c)~~ and (d-f) fire-off ~~(d-f) s~~simulations (1996-2100). Each point represents one grid latitude average of each variable. ~~The colors of the plots show the score of the Principle Component 1 (PC1) in the principle component analysis.~~

Formatted: Font: Bold, Complex Script Font: Bold

Formatted: Font: Bold, Complex Script Font: Bold

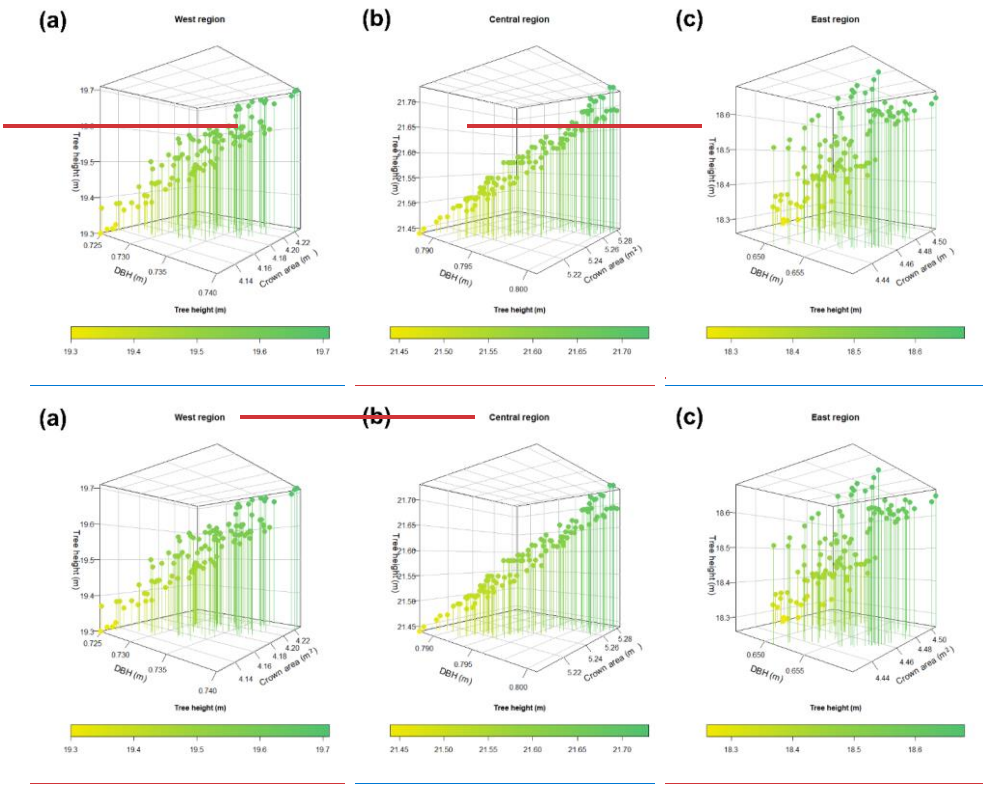

705

Figure 11. Relationships between simulated tree height, tree DBH, and crown area under fire-on simulation and RCP8.5 scenario from 2000 to 2100 in: **(a)** West region, **(b)** Central region, and **(c)** East region of Siberia.

Formatted Table

Formatted: Font: Bold, Complex Script Font: Bold

Formatted: Font: Bold, Complex Script Font: Bold

Formatted: Font: Bold, Complex Script Font: Bold

3.76 Fire and AGB variable comparisons

We performed internal comparisons of fire and AGB variables within the improved model to ensure that the model worked properly and that the variable calculation processes were interrelated. Eastern Siberia had low fire patterns (Figure S23~~Figure S21~~), and when compared with the AGB, this area also had very low AGB. We extracted the AGB data in the marked area with coordinates of 130-142°E and 65-80°N and discovered that the average simulated aboveground biomass in the area was 65.59 g C m^{-2} from 1997 to 2023, compared to 416.4 g C m^{-2} in the one-grid high-AGB areas. Furthermore, we assessed the FDI variable in these low AGB areas and found that the mentioned region had a value of 0, indicating that it had a very low fire potential (Figure S24.a ~~Figure S22.a~~).

We also compared the fire variables (burned fraction, burned biomass) and AGB variables between the improved model and the default model. According to the improved model, the correlation between the burned fraction and burned biomass was 0.92, the burned fraction was negatively correlated with the AGB (-0.88), and there was also a negative correlation between the burned biomass and the AGB (-0.84; Figure S8.d-f ~~S11.d-f~~). According to the default model, the correlation coefficient between the burned fraction and burned biomass was 0.009, that between the burned fraction and AGB was -0.76, and that between the burned biomass and AGB was 0.24 (Figure S8.a-c).~~Figure S11.a-c).~~

~~**3.7 Improved Model Validation**~~

~~**3.7.1 Fire products**~~

~~We compared the distribution patterns of burn fraction variables in the SEIB-DGVM-SPITFIRE and GFED4s data, and most patterns differed only in eastern Siberia (Figure 7). The annual average spatial distribution of the burned fraction and burned area (1996-2016) was 78.9% (Figure S12.b and Figure S13.b), the GFED4s burned fraction was 89% (Figure S12.a), and the GFED4 burned area was 87% (Figure S13.a) from the total research grid area. The fire products (burned fraction and burned area) in the improved model have the same spatial distribution because they are calculated based on one core variable (Eq. 1). However, the spatial distributions of GFED4s (burned fraction) and GFED4 (burned area) differ for two reasons: first, because GFED4 does not consider small fires (Giglio et al., 2013) while GFED4s does, and second, because GFED4s use the modified burned fraction equation, which is able to calculate the exact fire fraction and fuel load (not uniformized) in a grid cell (Van Der Werf et al., 2017).~~

~~Although the spatial distributions and patterns of the burned areas in the model and GFED4 data slightly differed, the model was able to produce annual mean value data that were similar to the GFED data. The mean average burned fraction during 1997-2016 was 0.0137 in the simulations, while that of the GFED4s was 0.0137. Furthermore, the mean average burned area of the model in 1996-2016 was 1428.5 ha $grid^{-1}$ $year^{-1}$, while the GFED4 burned area data had a value of 1425.1 ha $grid^{-1}$ $year^{-1}$. In summary, the model was able to produce mean average data that precisely resembled observational data.~~

~~We also compared the spatial distributions of the annual averages (1996-2016) of the burned fraction and burned area variables from the model under the CRU TS3.22 climate dataset and benchmark datasets (GFED4 and GFED4s). The burn fraction data were in agreement with 75% of the total data, and the burned area data were in agreement with 61% of the total data (Figure S14). The burned fraction correlated better because both the GFED4s and the model's fire module considered small fires; many scattered fire data with values less than 0.1 and approximately 0.1 were found in both the model's output and the GFED4s data.~~

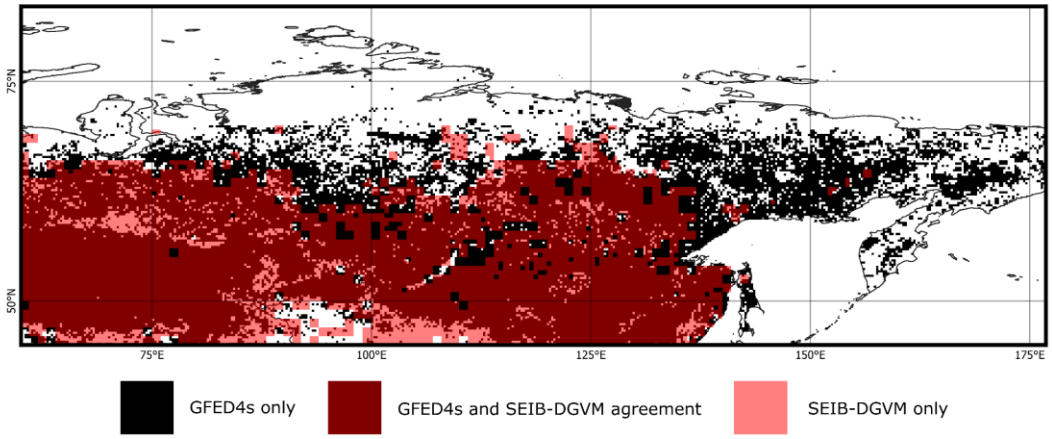

Figure 7. Spatial distribution comparison between SEIB-DGVM SPITFIRE and GFED4s burned fraction product (1997-2016)

3.7.2 Aboveground biomass

The improved model simulated similar aboveground biomass values to those of the benchmark data. In 2010, 2017, and 2018, the simulations predicted 63.714 Mg DM $ha^{-1}year^{-1}$, 64.141 Mg DM $ha^{-1}year^{-1}$, and 64.313 Mg DM $ha^{-1}year^{-1}$, respectively, while the ESA Biomass CCI data showed 64.027 Mg DM $ha^{-1}year^{-1}$, 64.548 Mg DM $ha^{-1}year^{-1}$, and 65.05 Mg DM $ha^{-1}year^{-1}$, respectively, for the same years. The annual average AGB of the model in these years also showed the same increasing trend as that of the benchmark data, and the spatial distributions of the AGB model under CRU TS3.22 climate data and ESA Biomass CCI also agreed, with values of 83%, 84%, and 84%, respectively (Figure S15 and Figure S16 in the Supplement). Although there was an annual average increase in the number of forest fires, there was a high variability trend in the model AGB values, indicating succession after forest fires (Figure S10.b).

3.7.3 Annual and seasonal fluctuations in burned dry matter

The model's dry matter data have a spatial distribution pattern similar to that of the model's fire products (burned fraction and burned biomass), as calculated from the available fire and fuel load data (fire product derivatives). The annual average dry matter variability from the 1997–2016 model (under the baseline climate product [CRU TS.3.22]) and the GFED4s data agreed with 63%, similar to the agreement of the fire products (Figure S19).

We also compared seasonal dry matter data to ensure that the monthly outputs of the SEIB-DGVM-SPITFIRE model agree with the observations, as this difference influences seasonal aerosol emissions. Between 1997 and 2016, the GFED4s data exhibited high fluctuations/dynamics depending on the month and year, while the SEIB-DGVM-SPITFIRE was not able to reproduce these dynamics or accurately predict the occurrence of extreme events (Figure S17a). For example, intense forest fires were recorded in 2003, 2012, and 2016. The monthly burned dry matter data for these years peaked in 2003 in May and in 2012 and 2016 in July (Figure S17.b-d). Severe wildfires in 2023 were due to low precipitation, as total rainfall reached only 36.0 mm in the Buryatia Republic and 45.7 mm in the Chita Oblast (IFFN, 2003). However, in the same period, the average total rainfall in the Buryatia Republic was approximately 332.23 mm, and that in the Chita Oblast was approximately 119.45 mm.

Furthermore, the monthly average burned dry matter in 2003, 2012 and 2016 was also lower in the model data than in the GFED4s data; the burned dry matter values of the improved model were 58.64 ± 5.86 kg DM m^{-2}, 59.41 ± 5.9 kg DM m^{-2}, and 59.98 ± 5.99 kg DM m^{-2}, while the benchmark data showed values of 122.36 kg DM m^{-2}, 101.7 kg DM m^{-2}, and 69.95 kg DM m^{-2}, respectively. However, considering the whole period of 1997-2016, not only years with extreme fire events, the model was able to reproduce similar average values for multiple years and time-series data. When comparing the monthly averages during 1997–2016, the model data yield a value of 58.94 ± 5.89 kg DM m^{-2}, while the GFED4s data yield 59.12 kg DM m^{-2}. The model is not yet able to reproduce the exact value at a specific time of year or month because the model is run in a long-term phase and is not yet able to predict sudden natural and anthropogenic conditions (factors). Overall, the spatial distribution

comparison of the monthly dry matter variables from GFED4s and SEIB-DGVM SPITFIRE for 20 years (1997-2016) revealed a correlation of 99% (Figure 8); therefore, the model was able to approximate the monthly averages.

3.7.4 Aboveground biomass Carbon dioxide (CO_2) and $PM_{2.5}$ emissions

We evaluated CO_2 emissions as representative of all emissions because CO_2 is the most emitted agent during biomass combustion (Ritchie et al., 2020). In addition, emissions were estimated from the same burned dry matter variable, which differed only in the emission factor value of each emission. Therefore, the CO_2 emission evaluation results are representative of all the other burned biomass emissions.

The annual average CO_2 emissions were highest in the GFED4s, followed by those in the SEIB-DGVM SPITFIRE model product and then those in the GBEI product, with values of $105.64 \pm 50.69 \times 10^{13}$ g CO_2, $76.41 \pm 0.87 \times 10^{13}$ g CO_2, and $62.4 \pm 26.09 \times 10^{13}$ g CO_2, respectively (Table S3). The GFED4s and GBEI data have higher standard deviation values than does the SEIB-DGVM SPITFIRE data and appear to have a large difference. However, when comparing the annual average CO_2 emissions from SEIB-DGVM SPITFIRE, GFED4s, and GBEI, we found that they were similar: 141.1 Gg CO_2 $year^{-1}$, 157.2 Gg CO_2 $year^{-1}$, and 148.7 Gg CO_2 $year^{-1}$, respectively.

Our study area covers the Boreal Asia (BOAS) area and a small part of Central Asia (CEAS), differing from the GFED4 basis region classification; therefore, we extracted these areas from the GFED4s data for comparison (Figure S20). A comparison of the GFED4s CO_2 data between the BOAS area and the Siberian area showed that the two datasets had a similarity of 98% (Figure S24), confirming the accuracy of the GFED4s validation data.

As all emission products are derived from fire products (dry matter variables), emission factors displayed spatial and value dynamics similar to those of the fire products (Figure S18, Figure S25, and Figure S26). When comparing the annual average dry matter emission data and CO_2 emissions generated by the model, the results correlated perfectly (100%, Figure S27), indicating that the model runs well according to Equation (29) and that CO_2 and other emissions have the same distribution patterns as the dry matter variables. However, they differ in their values because each emission species has a different emission factor. Overall, the annual average CO_2 emission model data were 63% (Figure 9.a) and 67% (Figure 9.b) correlated with the GFED4s and GBEI data, respectively.

We also compared the modeled $PM_{2.5}$ emissions and their distribution patterns with the Copernicus Atmosphere Monitoring Service (CAMS) (Romanov et al., 2022) data in seven Russian territories during 2004-2021. The improved model data and CAMS data both exhibited an increasing trend (Figure 10.a and Figure 2 in Romanov et al. (2022)) and a correlation of 85.8% (Figure 10.b).

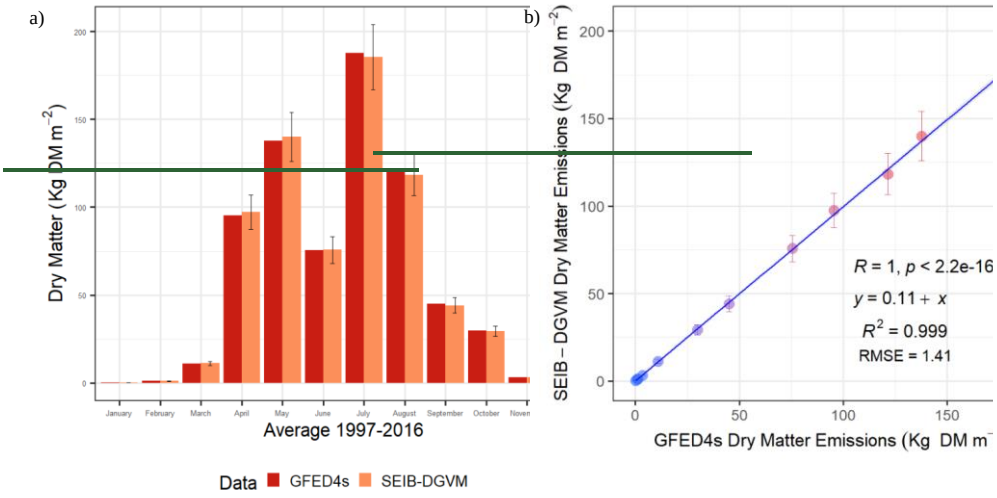

Figure 8. Monthly Average Dry Matter Emission data comparison of GFED4s and SEIB-DGVM SPITFIRE (1997-2016): a) Monthly average seasonality b) Monthly average comparison

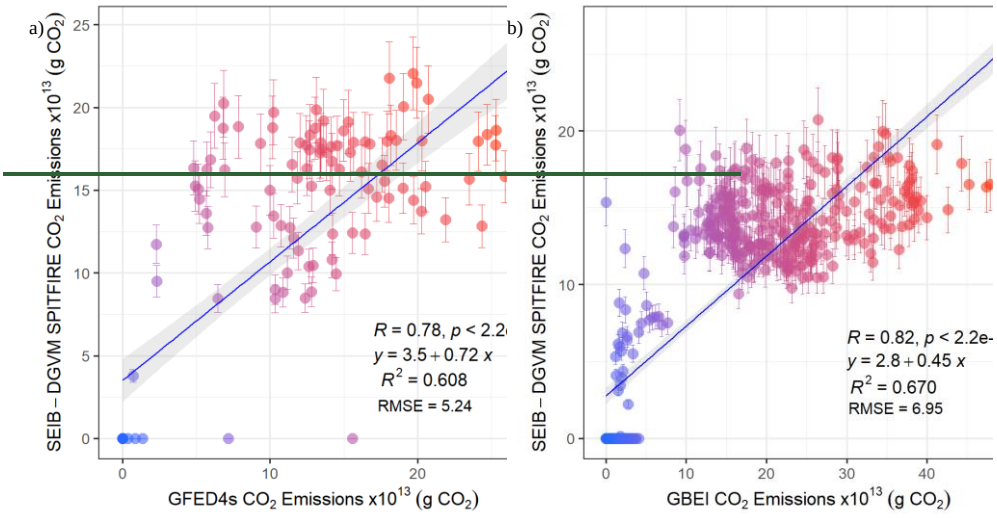

Figure 9. CO_2 emissions spatial average comparison of SEIB-DGVM-SPITFIRE module product under baseline climate product (CRU-TS.3.22) with: a) GFED4s data (1997-2016), b) with GBEI data (2001-2020)

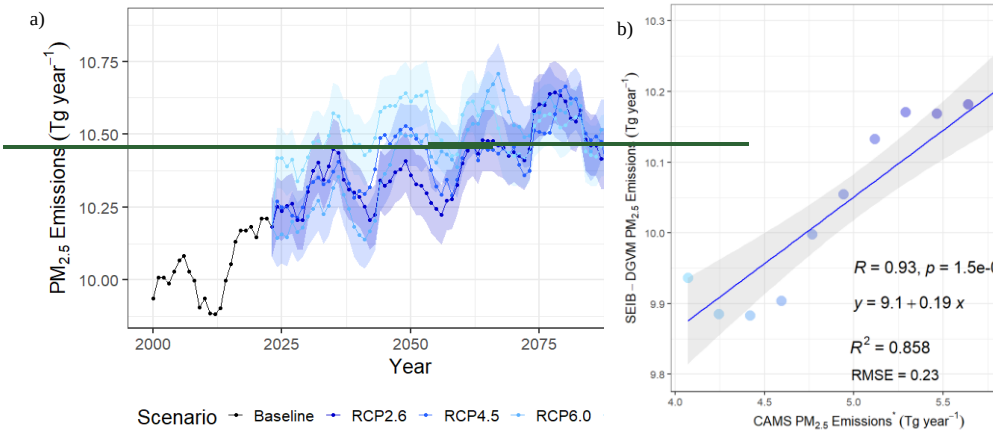

~~**Figure 10.** a) Projected $PM_{2.5}$ emissions under several climate scenarios (2003-2100), b) Comparison of $PM_{2.5}$ emissions from the SEIB-DGVM SPITFIRE model with *trendline data from the Copernicus Atmosphere Monitoring Service in Russia~~

3.8 Future projection of burned biomass emissions

Our model projects that from 2000 to 2100, some areas in Siberia will produce CO_2 emissions of 1.2 to 8,239.4 x10^{11} g CO_2 $year^{-1}$ (Figure 12). The distribution patterns of CO_2 and other emissions are similar because all emissions are calculated based on the same variable dry matter emissions. Over the twenty-year period, we projected an increasing trend in CO_2 emissions across the various RCP scenarios, which aligns with the projected increase in forest fires through 2100.

The average of 2000 to 2100 shows that CO_2 emissions are highest under the RCP8.5, RCP6.0, RCP4.5, and RCP2.6 scenarios with values of 801.49 ± 6.11, 796.79 ± 6.70, 794.21 ± 5.15, and 794.50 ± 5.29 respectively. Under the RCP8.5 climate scenario, it is projected that in 2021-2040, 2041-2060, 2061-2080, and 2081-2100, Siberia will produce CO_2 emissions of 797.15 ± 4.54, 804.6 ± 6.12, 803.11 ± 5.07, and 808.23 ± 8.6, respectively (Figure 13).

~~The spatial distribution pattern of emissions data in Siberia from 1996–2100 can be classified into two types based on the amount of emissions produced: high-emission and low-emission areas (Figure 11). Based on the comparison of CO_2 emissions in 2100 with those in 1996 (Figure 11), we found that the high-emission areas had a value of 1,525.852 ×10^8 g $year^{-1}$, while the low-emission areas had a negative value of −0.912 ×10^8 g $year^{-1}$.~~

~~Generally, the high-emission region (Figure 11) from 1996 to 2100 exhibited an increasing trend, but some areas exhibited negative values, indicating that the emissions in the following year were lower than those in the previous year. This was confirmed by the annual average CO_2 emission data from 2021–2040, which were lower than the corresponding values from 2000–2020 (Figure 12.a). Under the RCP6.0 scenario, there was an average decrease of −0.62 Tg $year^{-1}$ CO_2 from 2021–2040. However, under the RCP8.5 scenario, from 2000 to 2040, the average burned biomass emissions increased annually from ± 0.13 Tg $year^{-1}$ CO_2 to ± 0.25 Tg $year^{-1}$ CO_2 from 2061–2100 (Figure 12.a). Overall, the trend of CO_2 emissions in high-emission areas from 2000 to 2100 increased by 0.137 Tg $year^{-1}$.~~

~~In the low-emission regions, all of the RCP scenarios showed an increasing trend from 2000 to 2080, with an average increase of 2.49 × 10^{-3} Tg CO_2 $year^{-1}$. However, in 2081–2100, under the RCP8.5 scenario, the values were lower than those in the previous year, with a difference of 0.045 Tg. The average rate of emission reduction in 2081–2100 was −1.125 Tg CO_2 $year^{-1}$. Overall, in low-emission regions from 2000 to 2100, emissions increased by 0.154 Tg under the RCP8.5 scenario (1.54 × 10^{-3} Tg CO_2 $year^{-1}$).~~

The highest gaseous species emissions were CO_2, CO, $PM_{2.5}$, TPM, and TPC, and all of them exhibited similar increasing trends from 2023 to 2100 under all RCP scenarios. Under the RCP8.5 scenario, these emissions are expected to increase by ~~exhibited average annual increases of 2~~214.4 ± 79.4, 17.16 ± 6.35, 2.8 ± 1.03, 2.1 ± 0.78, and 1.47 ± 0.54 Gg species $year^{-1}$, respectively~~27.09, 18.18, 2.96, 2.24, and 1.55 Gg $year^{-1}$, respectively~~. The increasing trend of emissions production until 2100 is also in line with the FDI variable, which shows the same increasing trend (Figure S24.b~~Figure S22.b~~). Overall, by 2100, under the RCP8.5 scenario, the production of CO_2, CO, $PM_{2.5}$, TPM, and TPC emissions from forest biomass burning combustion are projected to reach 817.3 ± 79.4, 65.43 ± 6.35, 10.65 ± 1.03, 8.07 ± 0.78, and 5.59 ± 0.54 Tg, respectively. The

Formatted: Not Highlight

Formatted: Not Highlight

Formatted: Not Highlight

Formatted: Not Highlight

twenty-year averages of the CO_2, CO, $PM_{2.5}$, TPM, and TPC emission data under all the RCP scenarios are provided in Table 4, and the other twenty-eight emissions are provided in Table S6.~~Table S4.~~

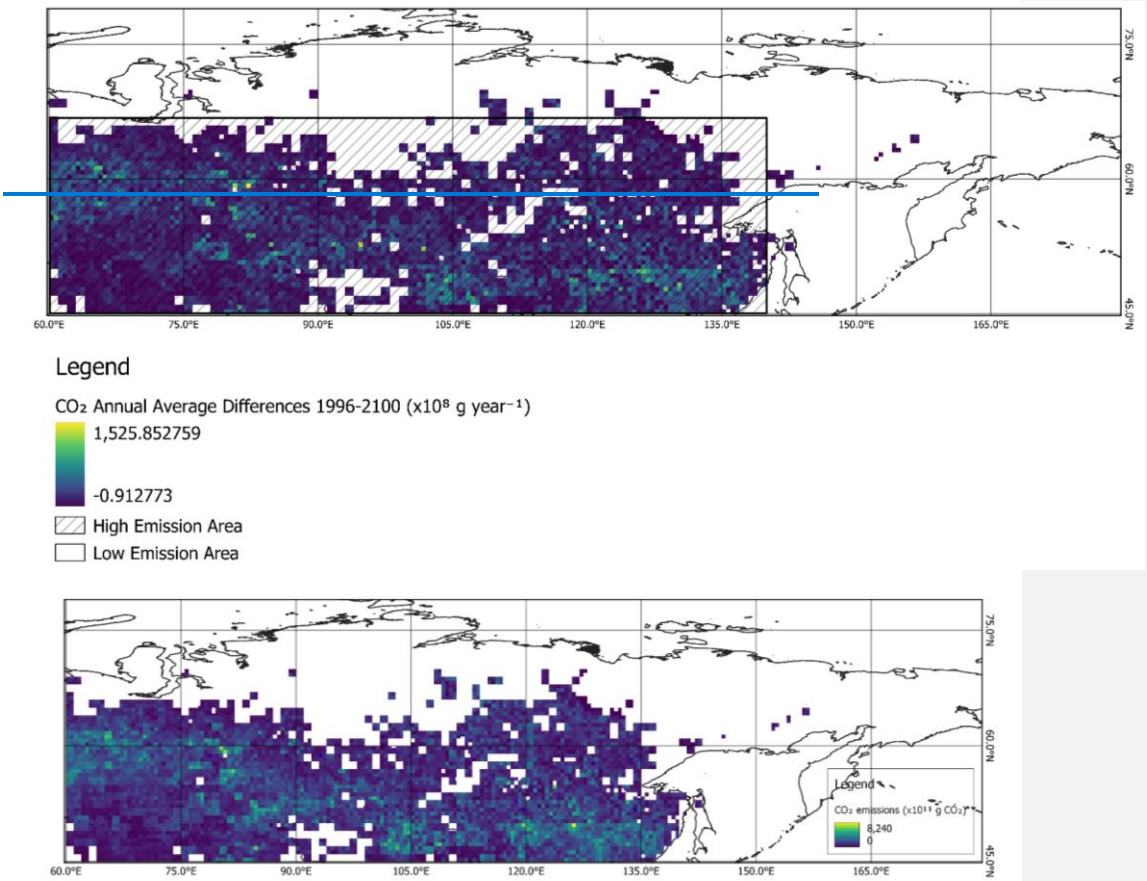

860 **Figure 1~~2~~1.** Spatial distribution of annual average projected CO_2 ~~Annual average differences map~~emissions (1996-2100) under RCP-8.5 scenario~~, and classification of areas based on the produced emissions~~

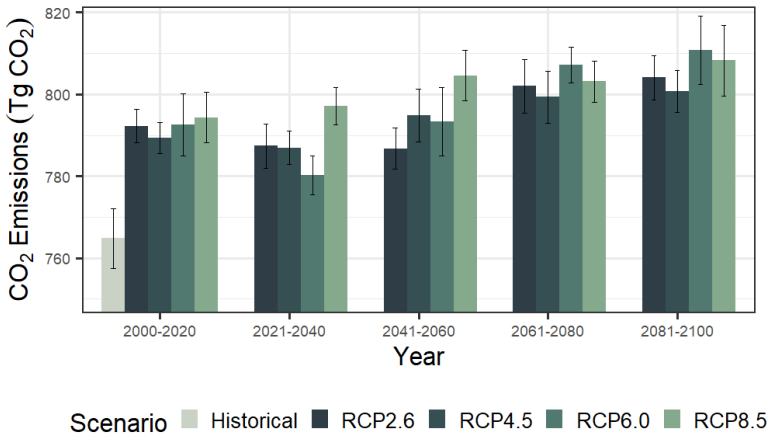

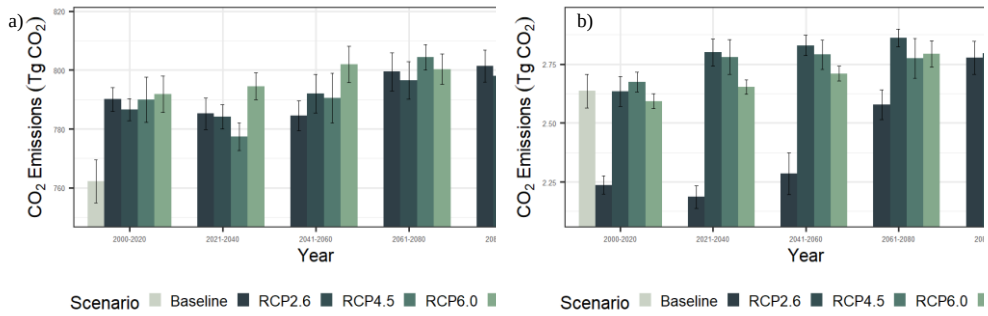

Figure 123. ~~Graph of 20-year average CO_2 emissions under different climate scenarios: a) high emission region, b) low emission region~~Temporal variation of projected CO_2 emissions from 2000 to 2100 under different RCPs scenarios.

Table 4. Twenty-year average (± 2 standard deviation) of projected emissions of CO_2, CO, $PM_{2.5}$, TPM, and TPC species from forest fires in Siberia (2023-2100). The emissions of the remaining 28 species are listed in Table S6 in the Supplement.

Formatted: Centered

Formatted: Centered

Formatted: Subscript

Formatted: Not Highlight

Emissions	Year	2000-2020	2021-2040	2041-2060	2061-2080	2081-2100
Tg CO_2 $year^{-1}$	~~Baseline~~Historical	768.7 ± 7.4	n.a	n.a	n.a	n.a
	RCP8.5	798.3 ± 6.1	801.4 ± 4.6	808.8 ± 6.1	807.1 ± 5.2	812.3 ± 8.5
	RCP6.0	796.4 ± 7.5	784.1 ± 4.5	797.4 ± 8.4	811.3 ± 4.5	815.2 ± 8.3
	RCP4.5	792.9 ± 3.7	790.7 ± 4.1	798.6 ± 6.5	803.2 ± 6.0	804.7 ± 5.09
	RCP2.6	795.8 ± 4.1	791.1 ± 5.4	790.4 ± 4.6	805.7 ± 6.4	807.8 ± 5.4
Tg CO $year^{-1}$	Historical~~Baseline~~	61.53 ± 0.592	n.a	n.a	n.a	n.a
	RCP8.5~~RCP85~~	63.91 ± 0.490	64.18 ± 0.368	64.75 ± 0.496	64.61 ± 0.41	65.03 ± 0.686
	RCP6.0~~RCP60~~	63.75 ± 0.605	62.77 ± 0.366	63.84 ± 0.677	64.94 ± 0.36	65.26 ± 0.671
	RCP4.5~~RCP45~~	63.47 ± 0.304	63.30 ± 0.335	63.93 ± 0.523	64.30 ± 0.48	64.42 ± 0.408
	RCP2.6~~RCP26~~	63.7 ± 0.328	63.33 ± 0.432	63.27 ± 0.371	64.50 ± 0.51	64.66 ± 0.438
Tg $PM_{2.5}$ $year^{-1}$	Historical~~Baseline~~	10.02 ± 0.096	n.a	n.a	n.a	n.a
	RCP8.5~~RCP85~~	10.41 ± 0.079	10.45 ± 0.060.1	10.54 ± 0.08	10.52 ± 0.068	10.59 ± 0.0111
	RCP6.0~~RCP60~~	10.38 ± 0.098	10.22 ± 0.059.7	10.39 ± 0.011	10.58 ± 0.059	10.63 ± 0.0109
	RCP4.5~~RCP45~~	10.34 ± 0.049	10.31 ± 0.054.7	10.41 ± 0.085	10.47 ± 0.079	10.49 ± 0.066

Formatted Table

Emissions	Year	2000-2020	2021-2040	2041-2060	2061-2080	2081-2100
	RCP2.6~~RCP26~~	10.37 ± 0.053	10.31 ± 0.070.5	10.30 ± 0.06	10.50 ± 0.084	10.53 ± 0.071
Tg TPM year^{-1}	Historical~~Baseline~~	7.59 ± 0.073	n.a	n.a	n.a	n.a
	RCP8.5~~RCP85~~	7.88 ± 0.060	7.91 ± 0.045.5	7.98 ± 0.061	7.97 ± 0.051	8.02 ± 0.084
	RCP6.0~~RCP60~~	7.86 ± 0.074	7.74 ± 0.045.3	7.87 ± 0.083	8.01 ± 0.044	8.05 ± 0.082
	RCP4.5~~RCP45~~	7.83 ± 0.037	7.81 ± 0.041.4	7.88 ± 0.064	7.93 ± 0.06	7.94 ± 0.050
	RCP2.6~~RCP26~~	7.86 ± 0.040	7.81 ± 0.053.4	7.80 ± 0.045	7.95 ± 0.063	7.97 ± 0.054
Tg TPC year^{-1}	Historical~~Baseline~~	5.26 ± 0.050	n.a	n.a	n.a	n.a
	RCP8.5~~RCP85~~	5.46 ± 0.041	5.48 ± 0.031.5	5.53 ± 0.042	5.52 ± 0.035	5.55 ± 0.058
	RCP6.0~~RCP60~~	5.44 ± 0.051	5.36 ± 0.031.4	5.45 ± 0.057	5.55 ± 0.031	5.57 ± 0.057
	RCP4.5~~RCP45~~	5.42 ± 0.026	5.41 ± 0.028.7	5.46 ± 0.044	5.49 ± 0.041	5.50 ± 0.034
	RCP2.6~~RCP26~~	5.44 ± 0.028	5.41 ± 0.037.0	5.40 ± 0.031	5.51 ± 0.044	5.52 ± 0.037

Formatted Table

4 Discussion

4.1 Feasibility of fire simulation

According to the default module, the fires spread throughout almost all of Siberia (S4.a-d, 4.a-d) because the module considered only the amount and moisture content of the litter. Thus, if the fuel load met the threshold requirement in any random grid, a fire appeared and could spread to other areas. Furthermore, the spatial distribution and trend of burned biomass under all of the RCP scenarios in the default fire module were not consistent with the burned fraction data. Areas with high burned fraction values should also have high burned biomass, and vice versa.

However, in the improved module, the fires ignited only in areas that were covered in the lightning ignition and population ignition datasets based on the calculation of each ignition factor. This is confirmed by the comparison of the fire variable with the ignition factor variables, the comparison of the burned fraction variable with the lightning flash strikes variable shows a strong correlation of 0.68 (R^2=0.45), and the comparison of the burned fraction variable with the population density variable shows a correlation of 0.24 (R^2=0.06) (Figure S7).~~The lighting flash rate affected fire ignition in Siberia by 46%, and the population density affected ignition by 6%.~~ These relatively low correlation values are due to the fact that the presence of an ignition factor does not guarantee that a fire will start; the area needs to have sufficient dry litter to feed the fire. Apart from these variables in the improved model, other factors also influence fire occurrence and spread in real life, such as slope and solar aspect (Rothermell, 1972), but their inclusion at this point was not possible due to the limitations of the model. In addition, when comparing the fire and AGB distributions, the SEIB-DGVM SPITFIRE showed greater agreement than did the default fire module.

However, differences remained between the spatial distribution patterns of the simulated fires and the GFED4s data in eastern Siberia. We believe that the main reason for the lack of simulated fires in eastern Siberia was the scarcity of available fuel and biomass for the ignition and spread of fires. We found that the AGB in these areas (130-142°E and 65-80°N; Figure S23~~Figure S21~~) was very low, averaging 65.59 g C m^{-2}. This value was far below the model minimum fuel load threshold requirement of 200 g C m^{-2} (Sato et al., 2007) for fire ignition or spread. All three benchmark datasets, the ESA Biomass CCI (aboveground biomass), GFED4 (burned area), and GFED4s (burned fraction), indicate that fire is present in this area, with ESA Biomass CCI showing an AGB of 2,309.67 g DM m^{-2}. It is challenging to produce a model product that precisely predicts observations, as the simulations are highly dependent on the input data and dynamics, while the benchmark datasets were obtained from satellite image estimations that are able to capture natural conditions and events in real time. Even predictions based on satellite observations can differ significantly from field-based observations. For example, the International Forest Fire News (IFFN) Russian Federation reported that 2003 had extremely severe fires in Siberia based both on ground and aerial observation. However, the burnt area was determined to be 2,654,000 ha based on field observations and 17,406,900 ha based on satellite-derived observations (NOAA AVHRR) (IFFN, 2003; Siegert and Huang, 2005). The difference between ground observation data and satellite-derived data is due to differences in the data collection time and continuity. Ground-based observations are

Formatted: Not Highlight

carried out only for a short time due to technical difficulties, while observations based on satellite data are carried out without any significant difficulties (IFFN, 2003). In this case, the SEIB-DGVM SPITFIRE model reported a burned area of 8,030,361 ha, an estimation centered between the observational and satellite data.

Overall, based on the fire variable outputs (burned fraction and burned area) from the improved model generated and validated with benchmark data, we project that Siberia will have an increasing trend until 2100 (Figure S4.d, Figure S6.b, and Figure 8.d). Yasunari et al., (2024) in a comprehensive assessment of the impacts of the Siberian wildfire using MIROC5 stated that there is high probability of increased Siberian wildfires in the future, and this estimate implies that worse air quality due to wildfires is predicted in the future, with frequent exceedances of air quality environmental standards (ES).

Kasischke and Bruhwiler (2003) stated that the level of uncertainty in the burned area parameter for estimating fire emissions in the Russian boreal forest is ± 30% for satellite imagery, while the uncertainty of the parameter is -300% according to official government statistics, resulting in fires being largely underestimated. This difference in uncertainty was caused by the diverse parameters/equations used for estimation, the varying levels of detail of the analysis, and other factors, such as forest type, location, fuel load, fire type, and aboveground biomass density. Differences are also extrapolated when estimations for large areas are based on individual fires (Kasischke and Bruhwiler, 2003; Kukavskaya et al., 2013). Therefore, uncertainties will inevitably persist in model- or simulation-based research when comparing model- or simulation-based data with direct observations.

4.2 Forest resilience under fire and climate change

Terrestrial NPP is an essential element of the carbon cycle and global climate dynamics, as it directly affects the CO_2 content of the atmosphere, resulting in delayed climatic changes (Running, 2022). If NPP decreases, the land's ability to absorb CO_2 will decrease, causing atmospheric CO_2 to increase faster and thereby contributing ~~and eventually causing~~ climate change (Running, 2022). Under the RCP8.5 scenario, NPP will decrease by 319.3 g C m^{-2} $year^{-1}$ due to wildfires until 2100. Satellite observations one year after boreal forest fires in Alaska and Canada recorded a 60–260 g C m^{-2} loss of NPP (Hicke et al., 2003). In the coniferous forests of the western United States, postfire NPP loss was also recorded and ranged from 67 to 312 g C m^{-2} $year^{-1}$ (Sparks et al., 2018). These data indicate that the NPP simulation results of the SEIB-DGVM SPITFIRE model are also consistent with some observational data in different areas.

NPP and NBP, both are significant elements of the global C cycle and are used as indicators of ecosystem function and are linked to biodiversity, biogeochemical cycling, ecosystem resilience, and other aspects of ecosystem services (Canadell et al., 2007; Richmond et al., 2007; Ito, 2011). However specifically, the mitigation ability of ecosystems is determined by net biome productivity (NBP) (Chapin et al., 2006; Fisher et al., 2014), dan climate-driven large anomalies in NBP could impact the structure, composition, and function of terrestrial ecosystems (Frank et al., 2015). The twenty-year average NBP from 2000-2100 shows a carbon sink in Siberia with a decreasing trend (Fig. rev 4). Overall from 2000 to 2100, RCP8.5 produces the lowest value, then RCP6.0, RCP2.6 and RCP4.5 with values of 136.39 ± 83.4, 79.05 ± 78.08, 82.46 ± 77.76, 94.51 ± 79.67, and 83.24 ± 78.66 Tg C $year^{-1}$, respectively (Table S4). The historical annual mean value of NBP in Siberia for 2000-2021 of

Formatted: Not Highlight
Formatted: Not Highlight
Formatted: Not Highlight
Formatted: Not Highlight
Formatted: Not Highlight
Formatted: Not Highlight
Formatted: Not Highlight
Formatted: Not Highlight

136.39 ± 83.4 Tg C year-1 is also similar to the CLM4CN simulations (annual average 1981-2006) in Eurasia and Boreal and Arctic of 204 and 284 Tg C year-1, respectively (Kantzas et al., 2013).

Under all of the climate scenario from 2021-2100 shows a declining trend (Figure S34), the standard deviation values greater than the NBP value itself (Table S4), which indicates that within the 20-year range there are areas that have negative values or indicate that the land becomes a carbon source (NBP<0) dominated by disturbance processes, such as wildfire (Figure S35). This trend is also supported by the fire fraction data which continues to increase until 2100 (Figure S4.d). There is an interesting pattern in the NBP data in 2021-2040 which shows a drastic decrease compared to the average data of the previous years, this is because the model simulates Heterotrophic respiration (HTR) with high values from 2000 to 2040 (Figure S36). The twenty-year average HR data is highest in 2000-2020, then 2021-2040, 2081-2100, 2061-2080 and 2041-2060 with values of 2532.49 ± 81.37, 2529.92 ± 96.78, 2518.42 ± 78.48, 2520.40 ± 78.81, and 2529.43 ± 98.95 Tg C $year^{-1}$, respectively (Table S5). Increased of heterotrophic respiration, tree mortality and increased disturbance (drought and fire) contribute significantly to negative carbon fluxes from the ecosystem due to increased temperature and atmospheric CO_2 (Sharma et al., 2023). Overall, SEIB-DGVM SPITFIRE simulates that until the end of the 21st century, there will continue to be a weakening of the land carbon sink in Siberia, this is also reinforced by the CESM2 model simulation which states the same globally. Negative NBP extremes become more frequent and saturated by the end of the 21st century, terrestrial ecosystems may lose their potential to absorb anthropogenic carbon and mitigate the effects of climate change (Sharma et al., 2023).

~~Overall, b~~Boreal forest vegetation is naturally influenced by a variety of periodic disturbances, such as wildfires (Kasischke et al., 1995), insect outbreaks, and windthrow. Wildfires and insect outbreaks are not necessarily independent, there is a likelihood of wildfires often increasing or decreasing after insect outbreaks (Meigs et al., 2015, 2016). However, wildfires are among the main disturbances that drive forest dynamics, shape forest composition and structure, and affect biomass and productivity (Burns and Honkala, 1990; Greene and Johnson, 1999). ~~, but wildfires are among the main disturbances that drive forest dynamics, shape forest composition and structure, and affect biomass and productivity (Burns and Honkala, 1990; Greene and Johnson, 1999). c~~Circumpolar northern boreal forests and tundra are likely to continue to warm more than most other terrestrial biomes according to available data from models and observations (Chapin et al., 2005; Foley, 2005; Meehl et al., 2007; Trenberth et al., 2007; Lee et al., 2021). ~~Chapin et al., 2005; Foley, 2005; Meehl et al., 2007; Trenberth et al., 2007).~~ Based on the observations and changes in regional attributes from 1950 to the present, it is projected that during 2071-2100, the WSB (West Siberia), ESB (East Siberia), and RFE (Russian Far East) will experience an increase in extreme temperatures with high confidence of more than 7 °C for all seasons under the RCP8.5 scenario. Projected warming is most evident on the large continental Siberian Plateau, which has boreal and subboreal climates and biomes (i.e., taiga forests and tundra), during the winter season (Ozturk et al., 2017; IPCC, 2021). Such changes in climatic extreme scenarios and seasonality are also likely to have multiple effects, including extended but drier growing seasons, the occurrence of more intense convective storms leading to more lightning-caused fires (Hessilt et al., 2021; Kharuk et al., 2022), and decreased forest productivity (Orangeville et al., 2018); additionally, longer, warmer, and drier summers may cause an increase in fire frequency and size in some areas of boreal forests (Krawchuk et al., 2009; Flannigan et al., 2016; Wotton et al., 2017). This finding is in line with our results,

Formatted: Not Highlight
Formatted: Not Highlight
Formatted: Not Highlight
Formatted: Not Highlight
Formatted: Not Highlight
Formatted: Not Highlight
Formatted: Not Highlight
Formatted: Not Highlight

which show that the assessment of forest ecology variables indicates tree mortality due to fire and succession as well as postfire vegetation (Figure S25.c~~Figure S23.b~~) and affects NPP dynamics in Siberia (Figure S25.a~~Figure S23.a~~).

Under the RCP4.5 scenario, the SEIB-DGVM estimated the average tree density to be 2,205 tree ha^{-1} between 1997 and 2023 in Siberia. The tree density is greater in northeastern Siberia (1,197 tree ha^{-1}) than in southern Siberia (Miesner et al., 2022). Our simulation resulted in higher tree densities than did the observations in northeastern Siberia, as we covered a larger area of forest at 60°-180°E and 45°-80°N. The number of trees is affected by the frequency of fires at a certain location. Additionally, the number of trees destroyed by wildfires depended upon the climate scenario used in the simulations but naturally increased with fire frequency and size. In all the RCP scenarios, the number of destroyed trees was greater than that in the base scenario, and the number of destroyed trees increased annually, indicating that changes in climatic factors affected the surviving tree density. The projected increase in the number of trees destroyed annually is consistent with the modeled fire product data, which exhibit an increasing trend until 2100. The difference in tree mortality data between climate scenarios is because each climate scenario has a different projected temperature increase. By 2100, the air temperature will increase by range 0.3-1.7 (1.0) °C under the RCP2.6 scenario, 1.1-2.6 (1.8) °C under the RCP4.5 scenario, 1.4-3.1 (2.2) °C under the RCP6.0, and 2.6-4.8 (3.7) °C under the RCP8.5 scenarios (IPCC 2021). ~~By 2100, the air temperature will increase by 1.5 °C under the RCP2.6 scenario, less than 2.0 °C under the RCP4.5 scenario, and possibly more than 2.0 °C under the RCP6.0 and RCP8.5 scenarios (IPCC 2021).~~

Formatted: Not Highlight

The DBH ranges of the trees in the fire-on and fire-off simulations were comparable to those in northeastern Siberia, where the DBH ranged up to 71,6 cm, the tree height up to 28,5 m, and the crown area averaged 4,77 m^2 (Miesner et al., 2022). As the average DBH variable was similar in the fire-on and fire-off simulations, trees with large DBHs are resistant to fire. This was also confirmed based on observational research in Yenisei Siberia, where trees with a DBH greater than 18.1 cm were the most resistant to further postfire succession (Bryukhanov et al., 2018).

Specifically, based on the division of regions, we found an interesting pattern, that in Siberia the central region has the highest value of allometry variables (tree height, tree DBH and crown area), then the west region and lowest is the east region (Figure S37, Figure S38, and Figure S39). In addition, we also found that the allometry variables in the central and west regions are projected to have a decreasing trend from 2000 to 2100, while the east region has an increasing trend (Figure S37, Figure S38, and Figure S39). Furthermore, the relationship between the three variables shows a positive linear relationship in the central and west regions, while in the east region it is naturally randomly distributed (Figure 11). We suggest that this is happens because the Siberian central region has the highest wildfire frequency followed by the west region, then the east region. The major Siberian Forest types are formed by larch (*Larix sibirica*, *L. gmelinii*, *and L. cajanderi*) and majority distributed in western and central Siberia (Figure 1, and Figure 1: (Kharuk et al., 2021)). Furthermore, larch is classified as pyrophytic species, that have adapted or evolved under conditions of periodic forest fires, they have adapted and gaining a competitive edge over non-fire adapted species in regenerating and growing in burned areas (Kharuk et al., 2021). The abundance of species and high frequency of wildfires in the Siberian central and western regions led to excellent larch succession and regeneration as evidenced by the high tree allometry variables and on the other hand the projected continuity of wildfires led to a downward

Formatted: Font: Italic, Complex Script Font: Italic

trend. On the other hand, in the east region, very little wildfire is simulated, which is partly due to the low aboveground biomass available in some areas of the region: Figure S23), which leads to low variable allometry, however due to the low frequency of wildfires, variable allometry is projected to have an increasing trend until 2100 in the Siberian east region. The unique relationship between allometry variables that are randomly distributed naturally (Figure 11.c) in the east region is also because the area is simulated to have a low wildfire frequency. The forest in the Siberian east region appears to grow and spread naturally without having high impact from the wildfire. While the majority tree species in Siberia: larch, regenerates extremely well on post-fire-mineralized soil, however on contrast, they regenerate very slowly over a ground floor covered in lichen and moss (where the soil's surface is tough for sapling roots to reach) (Kharuk et al., 2016).

Formatted: Font: (Default) Times New Roman, Complex Script Font: Times New Roman, 12 pt

4.3 Spatial distribution and temporal variation in biomass burning emissions under climate change scenarios

The spatiotemporal dynamics of the biomass burning emissions under all RCP scenarios had similar patterns and trends, but they had slightly different variations in dynamics because climate affects the frequency and distribution of fires. A comparison of the annual average values of projected CO_2 emissions in 2100 with those in 1996 reveals an interesting pattern, with some areas having lower emissions than in the previous year. A decrease in fire emissions in subsequent years could be caused by the fact that there is less biomass available for burning since some of the biomass has been burnt during previous years. Also, it could indicate the occurrence of postfire vegetation succession in these areas (Figure 12). ~~A lower emission value in the following year indicates the occurrence of postfire vegetation succession in these areas (Figure 11).~~ The difference in emission values between climate scenarios in the same year shows that temperature has an impact on vegetation succession and emission production from wildfires (Gutierrez et al., 2021; Stocker et al., 2021). The simulation results confirmed that on the spatial distribution map of high-emissions areas, there was a reduction in future emissions due to vegetation succession. However, in the low-emission areas, the total emission extraction data also revealed lower emissions than those in the previous year under the different climate scenarios, which, based on the overall simulation of Siberia, experienced a continuous increase in forest fires until 2100. Thus, the model is able to simulate and integrate fire disturbance, forest dynamics or vegetation succession, and burned biomass emissions well.

Formatted: Not Highlight

By 2100, in Siberia, our simulation predicted that forest fires will produce CO_2, CO, $PM_{2.5}$, TPM, and TPC emissions, amounting to 822.7 ± 21.4, 65.8 ± 1.7, 10.7 ± 0.27, 8.12 ± 0.2, and 5.63 ± 0.14 Tg, respectively (Table 4~~), Table S4, and Figure S28)~~. Spatially, the projections depict heterogeneous patterns of burned biomass emissions, with regions of high emissions intensity concentrated in areas of larch forest (Larix spp.), consistent with Figure 1 and our simulation results, where the fire and emission variables show high values in central to southern Siberia (Figure S4.b, Figure 8.b, and Figure S6.b). This is reinforced by field-based estimation data, that fires in this region result in high tree mortality 76%, Siberian larch forests experience greater aboveground carbon loss after fire than do North American forests, both in absolute and relative levels (Webb et al., 2024). We also visualized all the 33 graphs depicting projected burned biomass emissions, offering valuable insights into the future dynamics of the burned biomass emissions in Siberia. Across these graphs, we observe distinct temporal

Formatted: Not Highlight

patterns, revealing trends in burned biomass emissions over time. Under the RCP8.5 to RCP2.6 scenarios, overall emissions by 2100 are projected to increase by 2.6 %, 1.9 %, 1.05 % and 1.04 % compared to 2000 emissions (Figure S40), and the twenty-year dynamics are summarized in Table 4 and Table S6. In addition, different climate scenarios predicted different emissions depending on the radiative forcing values used (from the highest to the lowest): The RCP8.5, RCP6.0, RCP4.0, and RCP2.6 scenarios had average increases of 0.026% year^{-1}, 0.019% year^{-1}, 0.0105% year^{-1}, and 0.0104% year^{-1}, respectively, from 2000 to 2100. Our projection results are consistent with those of Riahi et al. (2011), in which the simulation result under the RCP8.5 scenario (with a radiative forcing of 8.5 W m^{-2}) produced the highest greenhouse gas emissions compared to those under the other RCP scenarios. Under the RCP4.5 scenario, radiative forcing stabilized until 2100 (Thomson et al., 2011), which is also consistent with our results, as emissions under the RCP4.5 scenario were more stable than those under the other RCP scenarios. Therefore, its indicated that the trend in fire emissions is consistent with the different scenario-dependent trends in radiative forcings. Overall, based on the RCPs climate scenario data used (MirocAR5), the emission scenario projected an increase in global mean surface temperature in the range of 1.0-3.7 (0.3~4.8) ºC (IPCC, 2014), and currently ranges between 1.5 and 6.0 ºC by 2100 compared to 1850-1900 mean value (Lee et al., 2021). ~~Therefore, it can be concluded that the SEIB-DGVM SPITFIRE model is able to project future burned biomass emissions accurately under different climate scenarios.~~

~~On average, climate change causes a 0.18 °C increase in global temperature per decade (Lindsey and Dahlman, 2023), with a projected increase of 2.0 °C by 2100 (Miranda et al., 2023).~~ One of the impacts of rising global temperatures is the increased occurrence and severity of forest fires, which lead to a greater prevalence of wildfire (Schoennagel et al., 2017; Haider et al., 2019). The global land area burned by wildfires is expected to increase by 35% if the global temperature increases by 2 °C and precipitation patterns change (Pörtner et al., 2022). Extremely high temperatures increase the frequency of severe droughts and proliferate wildfires in several regions, such as southern Europe, northern Eurasia, the USA, and Australia (IPCC, 2021). These frequent and severe wildfires will inevitably lead to an increase in the atmospheric concentration of biomass burning products (Marlon et al., 2008; Amiro et al., 2009; Tian et al., 2023).

Forests in Siberia are very important to monitor and assess continuously because they have a significant impact on regional (short-term) and global (long-term) air quality and human health due to the large amounts of carbon emissions, smoke aerosols, and trace gases in the atmosphere. In addition to the observed amount of emissions, OC/EC emissions exceeded 3 times, and emissions of inorganic ions (SO_4^{2-} and NH_4^+) were found to be 5 times greater than the annual average wildfire emissions from August 2010 to August 2011 (Popovicheva et al., 2014). Increased Siberian wildfire aerosols would significantly degrade air quality, particularly in the surrounding and downwind regions of Siberia (Yasunari et al., 2024).The emitted substances can be transported over long distances and affect air quality in other regions, including North America and Northeast China (Teakles et al., 2017; Johnson et al., 2021; Sun et al., 2023).

Estimating future fire emissions and their impact on air quality is challenging due to model limitations and uncertainties in estimation methods, potential mixing of emissions in the atmosphere, climate radiative forcing factors, and emission transport (Winiger et al., 2017; Schacht et al., 2019). The SEIB-DGVM SPITFIRE was not able to reproduce the events in the validation

Formatted: Not Highlight

Formatted: Not Highlight

Formatted: Not Highlight

Formatted: Not Highlight

Formatted: Not Highlight

data for the same year or month but simulated similar dynamic patterns and values. This difference occurs because the benchmark data obtained from satellite image data closely follow natural conditions, while the model accumulates uncertainties due to its long simulation period. The emission estimation method used in the model refers to the dry matter variable and the emission factor from Andreae and Merlet (2001) and Andreae (2019), where the emission factors are obtained from laboratory and small field experiments. Each species has specific characteristics that require different assessment methods, and the combustion characteristics can be very different from those of large-scale open biomass burning and wildfires. Kasischke and Bruhwiler (2003) reported that the level of uncertainty in the emission factor parameters for estimating emissions from fires in Russian boreal forests was ±20-50%, which agrees with the ±50% uncertainty level for major emissions presented by Andreae and Merlet (2001). However, in the SEIB-DGVM SPITFIRE, we also used the latest emission factor from Andreae (2019), which was developed for oxygenated volatile organic compounds and for HCN; this approach improved all assessment compound emissions significantly with more accurate measurements and has been widely used by various dynamic global vegetation models to estimate biomass burning emissions globally. Overall, the comparison between different climate RCP scenarios provides further insight into uncertainties and variability in the projections, offering valuable information for understanding the potential impacts of future burned biomass emissions on air quality, climate dynamics, and ecosystem health. Through this analysis, our study contributes to a better understanding of the drivers and implications of burned biomass emissions, informing policy decisions and management strategies aimed at mitigating their environmental and societal impacts.

Formatted: Not Highlight

4.4 Model uncertainty

Formatted: Not Highlight

Our study is a process of combining and improving the SEIB-DGVM model with the SPITFIRE fire module, each of which has different characteristics and some default variables, parameters, and inputs. The implementation of any complex model improvement inherently introduces uncertainty, stemming from various sources such as parameterization choices, model structure, new model input and the representation of complex biophysical processes. Specifically, in the context of the fire module enhancement, uncertainties may arise from the characterization of ignition sources, fire behavior, fuel dynamics, and fire spread mechanisms. These uncertainties can significantly influence the accuracy and reliability of model projections, particularly in simulating the spatial and temporal patterns of fire occurrence, intensity, and impacts on vegetation dynamics and carbon cycling.

Kasischke and Bruhwiler (2003), mentioned that in some cases, the data needed to generate input parameters for those equations are very well defined, whereas in others, they are based on a very limited set of the observations data. Thus, the input data selection and the parameter setting for those equations calculation is the source of the uncertainty, provided emission range (Table 5 in Kasischke and Bruhwiler, 2003). In more detail Kasischke and Bruhwiler (2003) stated that uncertainty can be classified into two groups. First, environmental characteristics (direct or indirect observations) including location, fire type, and aboveground/ground-layer biomass. Second, uncertainties from parameters that can be measured in individual biomass

combustion processes, while the application on a large scale, time differences and climatic influences are very challenging, and the combustion process consists of several stages that emit different emissions for each stage.

To mitigate model uncertainty, we have employed rigorous model verification, calibration, and evaluation procedures, comparing model outputs with several benchmark datasets (Table 3). The verification helps to ensure the new inputs (ignition factors) can be read, processed, and output properly. The process of calibrating all major variables with benchmark datasets is carried out sequentially and with several iterations, ensuring that the output of individual variables matches the benchmark dataset that is the target of validation. This validation process helps assess the model's ability to reproduce historical fire patterns and dynamics accurately.

However, this does not close the uncertainty in the model we have developed, we still have limitations where the emission variable distribution pattern of emissions is strongly influenced by the pattern of the resulting fire, because the emission variable is calculated with the same dry matter emissions. This spatial distribution also affected other vegetation variables, due to the relationship calculation between fire and vegetation variables. This is a potential further study to adjust the factors that affect the distribution of fire to be similar to the benchmark data. In addition, natural factors that affect the dynamics of significant fire disturbances at specific times are still not well simulated by our model. Inversely, our model also has the advantage of being able to simulate numerically averaged data in the long term very accurately, based on the results of numerical comparisons with benchmark data, the model is able to simulate with a value of 99%.

5 Conclusions and recommendations

We introduced the SPITFIRE fire module into the SEIB-DGVM and achieved a better representation of fire dynamics in Siberia between 1996 and 2100 by creating monthly outputs and producing several new outputs related to fires at a 0.5° spatial resolution, such as vegetation and burned biomass emission variables. Our modifications have led to a more realistic depiction of fire frequency, intensity, and extent, aligning the model outputs more closely with benchmark datasets. The major variables related to fire (vegetation, CO_2 and $PM_{2.5}$ emissions, burned area, burned fraction, aboveground biomass, and dry matter) all reached an agreement of 60% or greater with the observations. Additionally, the improved model accurately simulated forest structure, increasing the agreement between the simulated and observed dataset patterns and further emphasizing the reliability of our model and its emission projections. Under the RCP8.5 scenario, we estimated that the CO_2, CO, $PM_{2.5}$, total particulate matter (TPM), and total particulate carbon (TPC) emissions in Siberia will continue to increase annually until 2100 by an average of 214.4 ± 79.4, 17.16 ± 6.35, 2.8 ± 1.03, 2.1 ± 0.78, and 1.47 ± 0.54 ~~214.4, 17.16, 2.8, 2.1, and 1.47~~ Gg species year^{-1}, respectively. Moreover, forest fires in Siberia in 2100 are projected to emit all five of these compounds under the RCP8.5 scenario, amounting to 817.3 ± 79.4, 65.43 ± 6.35, 10.65 ± 1.03, 8.07 ± 0.78, and 5.59 ± 0.54 ~~817.37, 65.43, 10.65, 8.07, and 5.59~~ Tg, respectively.

Although our research has made significant steps, there are several limitations that require further research. Future studies should minimize the uncertainty of the simulations and achieve better fits with benchmark datasets on fire, vegetation, and emission products. Specific parameter settings need to also be developed to emphasize regional and seasonal differences. Continued improvement in the fire module and consideration of feedback loops will be crucial to continuously enhancing the accuracy of our models. Our work contributes to a more comprehensive understanding of the intricate interactions between fire dynamics, ecosystems, and climate, creating a new path for informed decision-making and broadening the field of biogeochemistry, global elemental cycles, and the importance of accurate vegetation dynamic modeling.

Appendix A

A.1 Input and outputs of the SEIB-DGVM SPITFIRE

A.1.1. Input

1) Location: Latitude and altitude.
2) Soil (fixed in time): Soil moisture at the saturation point, field capacity, matrix potential, wilting point, and albedo.
3) Climatic data (daily): Air temperature, soil temperature, fraction of cloud cover, precipitation, humidity, and wind velocity.
4) Atmospheric carbon dioxide (CO_2) concentrations
5) Fire ignition factors: population density (GPWv4) and lightning flash rate (LIS/OTD HRFC)

A.1.2. Output

1) Carbon dynamics (daily–yearly): Terrestrial carbon pool (woody biomass, grass biomass, litter, and soil organic matter), CO_2 absorption and emission rates.
2) Water dynamics (daily): Soil moisture content (in three layers), interception rate, evaporation rate, transpiration rate, interception rate, and runoff rate.
3) Radiation (daily): Albedo from the terrestrial surface.
4) Properties of vegetation (daily–yearly): Vegetation type, dominant plant functional type, leaf area index, tree density, size distribution of trees, age distribution of trees, woody biomass for each tree, and grass biomass per unit area.
5) Disturbances (monthly–yearly): fire fraction, burned area, burned biomass, FDI, complete SPITFIRE variables, and 33 types of burned biomass emissions.

A.2 Processes in the SEIB-DGVM SPITFIRE and the approaches used to represent each process

Process	Approach	References
Disturbance	Fire as an empirical function of fuel (litter and aboveground biomass), fuel moisture, and ignition factor (human- and lightning-caused)	(Thonicke et al., 2001, 2010)
Biogeochemical	Trace gas emissions as an empirical function of the total amount of biomass burning and emission factor of each trace gas species	(Andreae and Merlet, 2001)

A.3 Variables, parameters, and constants in the model's equations

Abbreviation	Description	Unit
M3	Probability of each PFTs survival after fire (varying 0.0–1.0)	-
$pool\ w$	The soil water content of each soil layer	mm/day
$Depth$	Depth of each soil layer	meter
Wfi	Field capacity	$m^3\ m^{-3}$
Ab	Area burnt	ha/time unit
A	Grid cell area	ha
ρ_b	Fuel bulk density	$kg\ m^{-3}$
FDI	Fire Danger Index (0.0–1.0)	-
L_B	Length to breadth ratio for woody and grass PFTs	-
$U_{forward}$	Forward wind speed	m/s
$E(N_{ig})$	Expected number of fire ignition event (sum of population and lightning ignitions)	km^2/time unit
$E(N_{ih})$	Expected number of human-caused fire ignition	km^2/time unit
$E(N_{il})$	Expected number of lightning-caused fire ignition	km^2/time unit
Ip	Ignition parameter: Define the power of lightning caused ignition (0.0–1.0)	-
ω_o	Relative moisture content	-
NI	Nesterov Index	$^oC^2$

Abbreviation	Description	Unit
NBP	Net Biome Production	g C year^{-1}
Tmax	Maximum temperature	^{o}C
Tmin	Minimum temperature	^{o}C
Tdew	Dew-point temperature	^{o}C
m_e	Moisture extinction	-
α_{av}	Drying parameters for 1-, 10- and 100-h fuel classes	^{o}C^{-2}
$ROS_{f,\ surface}$	Forward rate of spread of surface fire	m min^{-1}
$ROS_{b,\ surface}$	Backward rate of spread of a surface fire	m min^{-1}
I_R	Reaction intensity	kJ m^{-2} min^{-1}
ξ	Propagating flux ratio	-
ϕ_w	Wind factor	-
P_b	Probability of fire per unit time	Time unit^{-1}
ε	Effective heating number	-
Q_{ig}	Heat of preignition	kJ kg^{-1}
t_{fire}	Fire duration	min
$I_{surface}$	Surface fire intensity	kW m^{-1}
SH	Scorch Height	m
F	PFT-parameter in crown scorch equation	-
CK	Fraction of crown scorch	-
T_H	Tree height	m
CL	Crown length of woody PFT	m
P_m	Probability of postfire mortality	-
P_m(CK)	Probability of mortality as a result of crown scorching	-
$P_m(\tau)$	Probability of mortality by cambial damage	-
p	Parameter for woody PFTs used in P_m(CK) equation	-
τ_l	Residence time of the fire	min
τ_c	Critical time for cambial damage	min
BT	Bark thickness	cm
par1, par2	Parameters for woody PFTs used in bark thickness calculation	-
DBH	Diameter at breast height	m

Formatted: Font: 10 pt

Formatted: Font: 10 pt

Formatted: Not Superscript/ Subscript

Formatted: Superscript

Formatted: Font: 10 pt, Not Superscript/ Subscript

Formatted Table

Abbreviation	Description	Unit
$E_{i,j}$	Fire emissions of trace gas and aerosol species i and the PFT j	g species m^{-2} s^{-1}
$EF_{i,j}$	PFT-specific emission factor	g species (kg dry matter (DM))$^{-1}$
CE_j	Combusted biomass of *PFT* $_j$ due to the fire	g C m^{-2}
C	Unit conversion factor from carbon to dry matter	g C (kg DM)$^{-1}$
D_T	Distance traveled	m
$U_{forward}$	Forward wind speed	m min^{-1}

Additional equations and variables of the implemented SPITFIRE module are referred to with adjustments to Thonicke et al. (2010) Table A1 and Appendix A-B, respectively.

Code and data availability

The spatially explicit individual-based dynamic global vegetation model (SEIB-DGVM) SPITFIRE code and data generated from this study (fire, vegetation, and 33 emission variables in Siberia) are available at https://doi.org/10.5281/zenodo.8299732

Supplement

The supplement related to this article is available online at: https://egusphere.copernicus.org/preprints/2024/egusphere-2024-105/egusphere-2024-105-supplement.pdf

~~The supplement related to this article is available online at:~~

Author contributions

TK conceptualized of the project and experimental design with help from ND and HS. HN, LV, and TM contributed model cording and writing. developed the model code, and RN performed the model simulations and analyzed model output with validation data from TS and RH. RN prepared the paper with contributions from all co-authors.

Formatted: Normal

Competing interest

Disclaimer

Acknowledgments

The authors extend their gratitude to Tomohiro Hajima and Junko Mori from the Japan Agency for Marine-Earth Science and Technology (JAMSTEC) for providing the climate datasets for this study.

Financial support

This research was supported by the Japan Society for the Promotion of Science (JSPS) KAKENHI Grant-in-Aid for Scientific Research (B) 20H04317.

Review statement

References

Abaimov, A.P., Lesinski, J.A., Martinsson, O. and Milyutin, L.I. (1998) 'Variability and ecology of Siberian larch species', (43).

Abaimov, A.P. and Sofronov, M.A. (1996) 'The Main Trends of Post-Fire Succession in Near-Tundra Forests of Central Siberia', (Shumilova 1962), pp. 372–386. Available at: https://doi.org/10.1007/978-94-015-8737-2_33.

Akagi, S.K., Yokelson, R.J., Wiedinmyer, C., Alvarado, M.J., Reid, J.S., Karl, T., Crounse, J.D. and Wennberg, P.O. (2011) 'Emission factors for open and domestic biomass burning for use in atmospheric models', *Atmospheric Chemistry and Physics*, 11(9), pp. 4039–4072. Available at: https://doi.org/10.5194/acp-11-4039-2011.

Albini, F.A. (1976) 'Rocky Mountain Research Station', *USDA For. Serv., Intermt. For.Range Exp. Stn., Ogden, UT. Gen. Tech. Rep.*, pp. 1–22. Available at: https://www.fs.usda.gov/rm/pubs_series/int/gtr/int_gtr030.pdf.

Amiro, B.D., Cantin, A., Flannigan, M.D. and De Groot, W.J. (2009) 'Future emissions from Canadian boreal forest fires', *Canadian Journal of Forest Research*, 39(2), pp. 383–395. Available at: https://doi.org/10.1139/X08-154.

Andreae, M. (2019) 'Emission of trace gases and aerosols from biomass burning. Global Biogeochemical', *Atomospheric Chemistry and Physics*, 15 (4)(April), pp. 955–966. Available at: https://www.atmos-chem-phys-discuss.net/acp-2019-303/acp-2019-303.pdf.

Andreae, M.O. and Merlet, P. (2001) 'Emission of trace gases and aerosols from biomass burning', 15(4), pp. 955–966.

Arakida, H., Kotsuki, S., Otsuka, S., Sawada, Y. and Miyoshi, T. (2021) 'Regional-scale data assimilation with the Spatially Explicit Individual-based Dynamic Global Vegetation Model (SEIB-DGVM) over Siberia', *Progress in Earth and Planetary Science*, 8(1). Available at: https://doi.org/10.1186/s40645-021-00443-6.

Aurell, J., Mitchell, B., Greenwell, D., Holder, A., Tabor, D., Kiros, F. and Gullett, B. (2019) 'Measuring emission factors from open fires and detonations', *AQM 2019 - Air Quality Measurement Methods and Technology Conference 2019* [Preprint].

Bergeron, Y., Gauthier, S., Flannigan, M. and Kafka, V. (2004) 'Fire regimes at the transition between mixedwood and coniferous boreal forest in northwestern Quebec', *Ecology*, 85(7), pp. 1916–1932. Available at: https://doi.org/10.1890/02-0716.

Bonan, G.B. (2008) 'Forests and climate change: Forcings, feedbacks, and the climate benefits of forests', *Science*, 320(5882), pp. 1444–1449. Available at: https://doi.org/10.1126/science.1155121.

Bond, T.C., Doherty, S.J., Fahey, D.W., Forster, P.M., Berntsen, T., Deangelo, B.J., Flanner, M.G., Ghan, S., Kärcher, B., Koch, D., Kinne, S., Kondo, Y., Quinn, P.K., Sarofim, M.C., Schultz, M.G., Schulz, M., Venkataraman, C., Zhang, H., Zhang, S., Bellouin, N., Guttikunda, S.K., Hopke, P.K., Jacobson, M.Z., Kaiser, J.W., Klimont, Z., Lohmann, U., Schwarz, J.P., Shindell, D., Storelvmo, T., Warren, S.G. and Zender, C.S. (2013) 'Bounding the role of black carbon in the climate system: A scientific assessment', *Journal of Geophysical Research Atmospheres*, 118(11), pp. 5380–5552. Available at: https://doi.org/10.1002/jgrd.50171.

Bowman, D.M.J.S., Balch, J.K., Artaxo, P., Bond, W.J., Carlson, J.M., Cochrane, M.A., D'Antonio, C.M., DeFries, R.S., Doyle, J.C., Harrison, S.P., Johnston, F.H., Keeley, J.E., Krawchuk, M.A., Kull, C.A., Marston, J.B., Moritz, M.A., Prentice, I.C., Roos, C.I., Scott, A.C., Swetnam, T.W., Van Der Werf, G.R. and Pyne, S.J. (2009) 'Fire in the earth system', *Science*, 324(5926), pp. 481–484. Available at: https://doi.org/10.1126/science.1163886.

Bryukhanov, A. V., Panov, A. V., Ponomarev, E.I. and Sidenko, N. V. (2018) 'Wildfire Impact on the Main Tree Species of the Near-Yenisei Siberia', *Izvestiya - Atmospheric and Ocean Physics*, 54(11), pp. 1525–1533. Available at: https://doi.org/10.1134/S0001433818110026.

Burns, R.M. and Honkala, B.H. (1990) 'Silvics of North America: Volume 2. Hardwoods', *Agriculture Handbook 654*, 2, p. 877. Available at: http://www.na.fs.fed.us/spfo/pubs/silvics_manual/table_of_contents.htm.

Canadell, J. G., Le Quéré, C., Raupach, M. R., Field, C. B., Buitenhuis, E. T., Ciais, P., Conway, T. J., Gillett, N. P., Houghton, R. A., and Marland, G.: Contributions to accelerating atmospheric CO2 growth from economic activity, carbon intensity, and efficiency of natural sinks, Proc. Natl. Acad. Sci. U. S. A., 104, 18866–18870, https://doi.org/10.1073/pnas.0702737104, 2007.

Carnicer, J., Alegria, A., Giannakopoulos, C., Di Giuseppe, F., Karali, A., Koutsias, N., Lionello, P., Parrington, M. and Vitolo, C. (2022) 'Global warming is shifting the relationships between fire weather and realized fire-induced CO2 emissions in Europe', Scientific Reports, 12(1), pp. 8–13. Available at: https://doi.org/10.1038/s41598-022-14480-8.

Cascio, W.E. (2018) 'Wildland fire smoke and human health', *Science of the Total Environment*, 624, pp. 586–595. Available at: https://doi.org/10.1016/j.scitotenv.2017.12.086.

Cecil and Daniel, J. (2001) 'LIS/OTD 0.5 Degree High Resolution Full Climatology (HRFC) V2.3.2015'. NASA Global

Hydrometeorology Resource Center DAAC, Huntsville, Alabama, U.S.A. Available at: https://doi.org/http://dx.doi.org/10.5067/LIS/LIS-OTD/DATA302.

Chapin, F.S., Sturm, M., Serreze, M.C., McFadden, J.P., Key, J.R., Lloyd, A.H., McGuire, A.D., Rupp, T.S., Lynch, A.H., Schimel, J.P., Beringer, J., Chapman, W.L., Epstein, H.E., Euskirchen, E.S., Hinzman, L.D., Jia, G., Ping, C.L., Tape, K.D., Thompson, C.D.C., Walker, D.A. and Welker, J.M. (2005) 'Role of Land-Surface Changes in Arctic Summer Warming', *Science Reports*, p. 657. Available at: https://doi.org/10.1126/science.1117368.

Chapin, F. S., Woodwell, G. M., Randerson, J. T., Rastetter, E. B., Lovett, G. M., Baldocchi, D. D., Clark, D. A., Harmon, M. E., Schimel, D. S., Valentini, R., Wirth, C., Aber, J. D., Cole, J. J., Goulden, M. L., Harden, J. W., Heimann, M., Howarth, R. W., Matson, P. A., McGuire, A. D., Melillo, J. M., Mooney, H. A., Neff, J. C., Houghton, R. A., Pace, M. L., Ryan, M. G., Running, S. W., Sala, O. E., Schlesinger, W. H., and Schulze, E. D.: Reconciling carbon-cycle concepts, terminology, and methods, Ecosystems, 9, 1041–1050, https://doi.org/10.1007/s10021-005-0105-7, 2006.

Christian, T.J., Kleiss, B., Yokelson, R.J., Holzinger, R., Crutzen, P.J., Hao, W.M., Saharjo, B.H. and Ward, D.E. (2003) 'Comprehensive laboratory measurements of biomass-burning emissions: 1. Emissions from Indonesian, African, and other fuels', *Journal of Geophysical Research: Atmospheres*, 108(23). Available at: https://doi.org/10.1029/2003jd003704.

CIESIN (2018) 'Gridded Population of the World, Version 4.11 (GPWv4): Population Count, Revision 11', *Revision 11. Palisades, NY: NASA Socioeconomic Data and Applications Center (SEDAC)* [Preprint]. Palisades, NY: NASA Socioeconomic Data and Applications Center (SEDAC). Available at: https://doi.org/https://doi.org/10.7927/H4JW8BX5.

~~Doyle, J.C., Harrison, S.P., Johnston, F.H., Keeley, J.E., Krawchuk, M.A., Kull, C.A., Marston, J.B., Moritz, M.A., Prentice, I.C., Roos, C.I., Scott, A.C., Swetnam, T.W., Van Der Werf, G.R. and Pyne, S.J. (2009) 'Fire in the earth system', *Science*, 324(5926), pp. 481–484. Available at: https://doi.org/10.1126/science.1163886.~~

~~Bryukhanov, A. V., Panov, A. V., Ponomarev, E.I. and Sidenko, N. V. (2018) 'Wildfire Impact on the Main Tree Species of the Near-Yenisei Siberia', *Izvestiya - Atmospheric and Ocean Physics*, 54(11), pp. 1525–1533. Available at: https://doi.org/10.1134/S0001433818110026.~~

~~Burns, R.M. and Honkala, B.H. (1990) 'Silvics of North America: Volume 2. Hardwoods', *Agriculture Handbook 654*, 2, p. 877. Available at: http://www.na.fs.fed.us/spfo/pubs/silvics_manual/table_of_contents.htm.~~

~~Carnicer, J., Alegria, A., Giannakopoulos, C., Di Giuseppe, F., Karali, A., Koutsias, N., Lionello, P., Parrington, M. and Vitolo, C. (2022) 'Global warming is shifting the relationships between fire weather and realized fire-induced CO2 emissions in Europe', Scientific Reports, 12(1), pp. 8–13. Available at: https://doi.org/10.1038/s41598-022-14480-8.~~

~~Cascio, W.E. (2018) 'Wildland fire smoke and human health', *Science of the Total Environment*, 624, pp. 586–595. Available at: https://doi.org/10.1016/j.scitotenv.2017.12.086.~~

~~Cecil and Daniel, J. (2001) 'LIS/OTD 0.5 Degree High Resolution Full Climatology (HRFC) V2.3.2015'. NASA Global Hydrometeorology Resource Center DAAC, Huntsville, Alabama, U.S.A. Available at: https://doi.org/http://dx.doi.org/10.5067/LIS/LIS-OTD/DATA302.~~

~~Chapin, F.S., Sturm, M., Serreze, M.C., McFadden, J.P., Key, J.R., Lloyd, A.H., McGuire, A.D., Rupp, T.S., Lynch, A.H.,~~

Schimel, J.P., Beringer, J., Chapman, W.L., Epstein, H.E., Euskirchen, E.S., Hinzman, L.D., Jia, G., Ping, C.L., Tape, K.D., Thompson, C.D.C., Walker, D.A. and Welker, J.M. (2005) 'Role of Land Surface Changes in Arctic Summer Warming', *Science Reports*, p. 657. Available at: https://doi.org/10.1126/science.1117368.

Christian, T.J., Kleiss, B., Yokelson, R.J., Holzinger, R., Crutzen, P.J., Hao, W.M., Saharjo, B.H. and Ward, D.E. (2003) 'Comprehensive laboratory measurements of biomass-burning emissions: 1. Emissions from Indonesian, African, and other fuels', *Journal of Geophysical Research: Atmospheres*, 108(23). Available at: https://doi.org/10.1029/2003jd003704.

CIESIN (2018) 'Gridded Population of the World, Version 4.11 (GPWv4): Population Count, Revision 11', *Revision 11. Palisades, NY: NASA Socioeconomic Data and Applications Center (SEDAC)* [Preprint]. Palisades, NY: NASA Socioeconomic Data and Applications Center (SEDAC). Available at: https://doi.org/https://doi.org/10.7927/H4JW8BX5.

Clark, J.S. and Richard, P.J.H. (1996) 'The Role of Paleofire in Boreal and Other Cool-Coniferous Forests', pp. 65–89. Available at: https://doi.org/10.1007/978-94-015-8737-2_5.

Cleve, K.V. and Viereck, L.A. (1981) 'Forest Succession in Relation to Nutrient Cycling in the Boreal Forest of Alaska', pp. 185–211. Available at: https://doi.org/10.1007/978-1-4612-5950-3_13.

Clark, J.S. and Richard, P.J.H. (1996) 'The Role of Paleofire in Boreal and Other Cool-Coniferous Forests', pp. 65–89. Available at: https://doi.org/10.1007/978-94-015-8737-2_5.

Cleve, K.V. and Viereck, L.A. (1981) 'Forest Succession in Relation to Nutrient Cycling in the Boreal Forest of Alaska', pp. 185–211. Available at: https://doi.org/10.1007/978-1-4612-5950-3_13.

Cochrane, M.A. (2003) 'Fire science for rainforests', *Nature*, 421(6926), pp. 913–919. Available at: https://doi.org/10.1038/nature01437.

Collins, M., Knutti, R., Arblaster, J., Dufresne, J.L., Fichefet, T., Friedlingstein, P., Gao, X., Gutowski, W.J., Johns, T., Krinner, G., Shongwe, M., Tebaldi, C., Weaver, A.J. and Wehner, M. (2013) 'Long-term climate change: Projections, commitments and irreversibility', *Climate Change 2013 the Physical Science Basis: Working Group I Contribution to the Fifth Assessment Report of the Intergovernmental Panel on Climate Change*, 9781107057, pp. 1029–1136. Available at: https://doi.org/10.1017/CBO9781107415324.024.

Cramer, W., Bondeau, A., Woodward, F.I., Prentice, I.C., Betts, R.A., Brovkin, V., Cox, P.M., Fisher, V., Foley, J.A., Friend, A.D., Kucharik, C., Lomas, M.R., Ramankutty, N., Sitch, S., Smith, B., White, A. and Young-Molling, C. (2001) 'Global response of terrestrial ecosystem structure and function to CO2 and climate change: Results from six dynamic global vegetation models', *Global Change Biology*, 7(4), pp. 357–373. Available at: https://doi.org/10.1046/j.1365-2486.2001.00383.x.

Crutzen, P.J. and Goldammer, J.G. (1993) 'Fire in the Environment The Ecological, Atmospheric, and Climatic Importance of Vegetation Fires', *High Throughput Screening*, pp. 573–577. Available at: https://doi.org/10.1201/9781482269802-30.

Dickinson, M.B. and Johnson, E.A. (2001) 'Fire Effects on Trees', in *Forest Fires*, pp. 477–525. Available at: https://doi.org/10.1016/b978-012386660-8/50016-7.

Chylek, P., C. Folland, J. D. Klett, M. Wang, N. Hengartner, G. Lesins, et al. Annual Mean Arctic Amplification 1970-2020: Observed and Simulated by CMIP6 Climate Models Geophysical Research Letters 2022 Vol. 49 Issue 13 DOI:

10.1029/2022gl099371.

Dixon, A.R.K., Brown, S., Houghton, R.A., Solomon, A.M. and Trexler, M.C. (1994) 'Carbon Pools and Flux of Global Forest Ecosystems Published by : American Association for the Advancement of Science Stable URL : http://www.jstor.org/stable/2882371', *Advancement Of Science*, 263(5144), pp. 185–190.

Fisher, J. B., Huntzinger, D. N., Schwalm, C. R., and Sitch, S.: Modeling the terrestrial biosphere, Annu. Rev. Environ. Resour., 39, 91–123, https://doi.org/10.1146/annurev-environ-012913-093456, 2014.

Flannigan, M., Stocks, B., Turetsky, M. and Wotton, M. (2009) 'Impacts of climate change on fire activity and fire management in the circumboreal forest', *Global Change Biology*, 15(3), pp. 549–560. Available at: https://doi.org/10.1111/j.1365-2486.2008.01660.x.

Flannigan, M.D., Wotton, B.M., Marshall, G.A., Groot, W.J. de, Johnston, J., Jurko, N. and Cantin, A.S. (2016) 'Fuel moisture sensitivity to temperature and precipitation: climate change implications', *Climatic Change*, pp. 59–71. Available at: https://doi.org/10.1007/s10584-015-1521-0.

Foley, J.A. (2005) 'Tipping Points in the Tundra', 310(October), pp. 627–628.

Cochrane, M.A. (2003) 'Fire science for rainforests', *Nature*, 421(6926), pp. 913–919. Available at: https://doi.org/10.1038/nature01437.

Collins, M., Knutti, R., Arblaster, J., Dufresne, J.L., Fichefet, T., Friedlingstein, P., Gao, X., Gutowski, W.J., Johns, T., Krinner, G., Shongwe, M., Tebaldi, C., Weaver, A.J. and Wehner, M. (2013) 'Long-term climate change: Projections, commitments and irreversibility', *Climate Change 2013 the Physical Science Basis: Working Group I Contribution to the Fifth Assessment Report of the Intergovernmental Panel on Climate Change*, 9781107057, pp. 1029–1136. Available at: https://doi.org/10.1017/CBO9781107415324.024.

Cramer, W., Bondeau, A., Woodward, F.I., Prentice, I.C., Betts, R.A., Brovkin, V., Cox, P.M., Fisher, V., Foley, J.A., Friend, A.D., Kucharik, C., Lomas, M.R., Ramankutty, N., Sitch, S., Smith, B., White, A. and Young-Molling, C. (2001) 'Global response of terrestrial ecosystem structure and function to CO2 and climate change: Results from six dynamic global vegetation models', *Global Change Biology*, 7(4), pp. 357–373. Available at: https://doi.org/10.1046/j.1365-2486.2001.00383.x.

Crutzen, P.J. and Goldammer, J.G. (1993) 'Fire in the Environment The Ecological, Atmospheric, and Climatic Importance of Vegetation Fires', *High Throughput Screening*, pp. 573–577. Available at: https://doi.org/10.1201/9781482269802-30.

Dickinson, M.B. and Johnson, E.A. (2001) 'Fire Effects on Trees', in *Forest Fires*, pp. 477–525. Available at: https://doi.org/10.1016/b978-012386660-8/50016-7.

Dixon, A.R.K., Brown, S., Houghton, R.A., Solomon, A.M. and Trexler, M.C. (1994) 'Carbon Pools and Flux of Global Forest Ecosystems Published by : American Association for the Advancement of Science Stable URL : http://www.jstor.org/stable/2882371', *Advancement Of Science*, 263(5144), pp. 185–190.

Flannigan, M., Stocks, B., Turetsky, M. and Wotton, M. (2009) 'Impacts of climate change on fire activity and fire management in the circumboreal forest', *Global Change Biology*, 15(3), pp. 549–560. Available at: https://doi.org/10.1111/j.1365-2486.2008.01660.x.

Flannigan, M.D., Wotton, B.M., Marshall, G.A., Groot, W.J. de, Johnston, J., Jurko, N. and Cantin, A.S. (2016) 'Fuel moisture sensitivity to temperature and precipitation: climate change implications', *Climatic Change*, pp. 59–71. Available at: https://doi.org/10.1007/s10584-015-1521-0.

Foley, J.A. (2005) 'Tipping Points in the Tundra', 310(October), pp. 627–628.

Forestry Canada Fire Danger Group (1992) 'Development of the Canadian Forest Fire Behavior Prediction System', *Information Report ST-X-3*, p. 66. Available at: https://cfs.nrcan.gc.ca/publications?id=10068%0Ahttps://www.frames.gov/documents/catalog/forestry_canada_fire_danger_group_1992.pdf.

Forster, P., V. Ramaswamy, P. Artaxo, T. Berntsen, R. Betts, D.W. Fahey, J. Haywood, J. Lean, D.C. Lowe, G. Myhre, J. Nganga, R. Prinn, G. Raga, M. Schulz and R. Van Dorland (2018) 'Changes in Atmospheric Constituents and in Radiative Forcing', *Cancer Biology and Medicine*, 15(3), pp. 228–237. Available at: https://doi.org/10.20892/j.issn.2095-3941.2017.0150.

Forestry Canada Fire Danger Group (1992) 'Development of the Canadian Forest Fire Behavior Prediction System', *Information Report ST-X-3*, p. 66. Available at: https://cfs.nrcan.gc.ca/publications?id=10068%0Ahttps://www.frames.gov/documents/catalog/forestry_canada_fire_danger_group_1992.pdf.

Forster, P., V. Ramaswamy, P. Artaxo, T. Berntsen, R. Betts, D.W. Fahey, J. Haywood, J. Lean, D.C. Lowe, G. Myhre, J. Nganga, R. Prinn, G. Raga, M. Schulz and R. Van Dorland (2018) 'Changes in Atmospheric Constituents and in Radiative Forcing', *Cancer Biology and Medicine*, 15(3), pp. 228–237. Available at: https://doi.org/10.20892/j.issn.2095-3941.2017.0150.

Fosberg, M.A., Cramer, W., Brovkin, V., Fleming, R., Gardner, R., Gill, A.M., Goldammer, J.G., Keane, R., Koehler, P., Lenihan, J., Neilson, R., Sitch, S., Thornicke, K., Venevski, S., Weber, M.G. and Wittenberg, U. (1999) 'Strategy for a Fire Module in Dynamic Global Vegetation Models', *International Journal of Wildland Fire*, 9(1), pp. 79–84. Available at: https://doi.org/10.1071/wf99007.

Frank, D., Reichstein, M., Bahn, M., Thonicke, K., Frank, D., Mahecha, M. D., Smith, P., van der Velde, M., Vicca, S., Babst, F., Beer, C., Buchmann, N., Canadell, J. G., Ciais, P., Cramer, W., Ibrom, A., Miglietta, F., Poulter, B., Rammig, A., Seneviratne, S. I., Walz, A., Wattenbach, M., Zavala, M. A., and Zscheischler, J.: Effects of climate extremes on the terrestrial carbon cycle: Concepts, processes and potential future impacts, Glob. Chang. Biol., 21, 2861–2880, https://doi.org/10.1111/gcb.12916, 2015.

Freeborn, P.H., Wooster, M.J., Hao, W.M., Ryan, C.A., Nordgren, B.L., Baker, S.P. and Ichoku, C. (2008) 'Relationships between energy release, fuel mass loss, and trace gas an aerosol emissions during laboratory biomass fires', *Journal of Geophysical Research Atmospheres*, 113(1), pp. 1–17. Available at: https://doi.org/10.1029/2007JD008679.

Friedlingstein, P., O'Sullivan, M., Jones, M., Andrew, R., Hauck, J., Olsen, A., Peters, G., Peters, W., Pongratz, J., Sitch, S., Le Quéré, C., Canadell, J., Ciais, P., Jackson, R., Alin, S., Aragão, L., Arneth, A., Arora, V., Bates, N., Becker, M., Benoit-

Cattin, A., Bittig, H., Bopp, L., Bultan, S., Chandra, N., Chevallier, F., Chini, L., Evans, W., Florentie, L., Forster, P., Gasser, T., Gehlen, M., Gilfillan, D., Gkritzalis, T., Gregor, L., Gruber, N., Harris, I., Hartung, K., Haverd, V., Houghton, R., Ilyina, T., Jain, A., Joetzjer, E., Kadono, K., Kato, E., Kitidis, V., Korsbakken, J.I., Landschützer, P., Lefèvre, N., Lenton, A., Lienert, S., Liu, Z., Lombardozzi, D., Marland, G., Metzl, N., Munro, D., Nabel, J., Nakaoka, S.-I., Niwa, Y., O'Brien, K., Ono, T., Palmer, P., Pierrot, D., Poulter, B., Resplandy, L., Robertson, E., Rödenbeck, C., Schwinger, J., Séférian, R., Skjelvan, I., Smith, A., Sutton, A., Tanhua, T., Tans, P., Tian, H., Tilbrook, B., van der Werf, G., Vuichard, N., Walker, A., Wanninkhof, R., Watson, A., Willis, D., Wiltshire, A., Yuan, W., Yue, X. and Zaehle, S. (2020) 'Global Carbon Budget 2020', *Earth System Science Data Discussions*, (November), pp. 1–3. Available at: https://doi.org/10.5194/essd-2020-286.

Furyaev, V. V., Vaganov, E.A., Tchebakova, N.M. and Valendik, E.N. (2001) 'Effects of fire and climate on successions and structural changes in the Siberian boreal forest', *Eurasian Journal of Forest Research*, 2, pp. 1–15.

Galanter, M., Levy II, H., and Carmichael, G. R.: Impact of biomass burning of tropospheric CO, NOx, and O3, https://doi.org/https://doi.org/10.1029/1999JD901113, 2000.

Fosberg, M.A., Cramer, W., Brovkin, V., Fleming, R., Gardner, R., Gill, A.M., Goldammer, J.G., Keane, R., Koehler, P., Lenihan, J., Neilson, R., Sitch, S., Thornicke, K., Venevski, S., Weber, M.G. and Wittenberg, U. (1999) 'Strategy for a Fire Module in Dynamic Global Vegetation Models', *International Journal of Wildland Fire*, 9(1), pp. 79–84. Available at: https://doi.org/10.1071/wf99007.

Freeborn, P.H., Wooster, M.J., Hao, W.M., Ryan, C.A., Nordgren, B.L., Baker, S.P. and Ichoku, C. (2008) 'Relationships between energy release, fuel mass loss, and trace gas an aerosol emissions during laboratory biomass fires', *Journal of Geophysical Research Atmospheres*, 113(1), pp. 1–17. Available at: https://doi.org/10.1029/2007JD008679.

Friedlingstein, P., O'Sullivan, M., Jones, M., Andrew, R., Hauck, J., Olsen, A., Peters, G., Peters, W., Pongratz, J., Sitch, S., Le Quéré, C., Canadell, J., Ciais, P., Jackson, R., Alin, S., Aragão, L., Arneth, A., Arora, V., Bates, N., Becker, M., Benoit-Cattin, A., Bittig, H., Bopp, L., Bultan, S., Chandra, N., Chevallier, F., Chini, L., Evans, W., Florentie, L., Forster, P., Gasser, T., Gehlen, M., Gilfillan, D., Gkritzalis, T., Gregor, L., Gruber, N., Harris, I., Hartung, K., Haverd, V., Houghton, R., Ilyina, T., Jain, A., Joetzjer, E., Kadono, K., Kato, E., Kitidis, V., Korsbakken, J.I., Landschützer, P., Lefèvre, N., Lenton, A., Lienert, S., Liu, Z., Lombardozzi, D., Marland, G., Metzl, N., Munro, D., Nabel, J., Nakaoka, S.-I., Niwa, Y., O'Brien, K., Ono, T., Palmer, P., Pierrot, D., Poulter, B., Resplandy, L., Robertson, E., Rödenbeck, C., Schwinger, J., Séférian, R., Skjelvan, I., Smith, A., Sutton, A., Tanhua, T., Tans, P., Tian, H., Tilbrook, B., van der Werf, G., Vuichard, N., Walker, A., Wanninkhof, R., Watson, A., Willis, D., Wiltshire, A., Yuan, W., Yue, X. and Zaehle, S. (2020) 'Global Carbon Budget 2020', *Earth System Science Data Discussions*, (November), pp. 1–3. Available at: https://doi.org/10.5194/essd-2020-286.

Furyaev, V. V., Vaganov, E.A., Tchebakova, N.M. and Valendik, E.N. (2001) 'Effects of fire and climate on successions and structural changes in the Siberian boreal forest', *Eurasian Journal of Forest Research*, 2, pp. 1–15.

Giglio, L., Randerson, J.T. and Van Der Werf, G.R. (2013) 'Analysis of daily, monthly, and annual burned area using the fourth-generation global fire emissions database (GFED4)', *Journal of Geophysical Research: Biogeosciences*, 118(1), pp. 317–328. Available at: https://doi.org/10.1002/jgrg.20042.

~~Goldammer, J.G. and Furyaev, V. V (1996) 'Fire in ecosystems of boreal Eurasia', *Fire in ecosystems of boreal Eurasia*, pp. 1–2.~~

~~Gorbachev, V.N. and Popova, E.P. (1996) 'Fires and Soil Formation', pp. 331–336. Available at: https://doi.org/10.1007/978-94-015-8737-2_28.~~

~~Greene, D.F. and Johnson, E.A. (1999) 'Modelling recruitment of *Populus tremuloides*, *Pinus banksiana*, and *Picea mariana* following fire in the mixedwood boreal forest', *Canadian Journal of Forest Research*, 29(4), pp. 462–473. Available at: https://doi.org/10.1139/cjfr-29-4-462.~~

~~Groot, W.J. de, Cantin, A.S., Flannigan, M.D., Soja, A.J., Gowman, L.M. and Newbery, A. (2013) 'A comparison of Canadian and Russian boreal forest fire regimes', *Forest Ecology and Management*, 294, pp. 23–34. Available at: https://doi.org/10.1016/j.foreco.2012.07.033.~~

~~Groot, W.J. de, Goldammer, J.., Keenan, T., Brady, M.A., Lynham, T.J., Justice, C.O., Csiszar, I.A. and O'Loughlin, K. (2006) 'Developing a global early warning system for wildland fire', *International Conference on Forest Fire Research* [Preprint].~~

Gauthier, S., Bernier, P., Kuuluvainen, T., Shvidenko, A. Z., and Schepaschenko, D. G.: Boreal forest health and global change, Science (80-.)., 349, 819–822, https://doi.org/10.1126/science.aaa9092, 2015.

Giglio, L., Randerson, J.T. and Van Der Werf, G.R. (2013) 'Analysis of daily, monthly, and annual burned area using the fourth-generation global fire emissions database (GFED4)', *Journal of Geophysical Research: Biogeosciences*, 118(1), pp. 317–328. Available at: https://doi.org/10.1002/jgrg.20042.

Goldammer, J.G. and Furyaev, V. V (1996) 'Fire in ecosystems of boreal Eurasia', *Fire in ecosystems of boreal Eurasia*, pp. 1–2.

Gorbachev, V.N. and Popova, E.P. (1996) 'Fires and Soil Formation', pp. 331–336. Available at: https://doi.org/10.1007/978-94-015-8737-2_28.

Greene, D.F. and Johnson, E.A. (1999) 'Modelling recruitment of *Populus tremuloides*, *Pinus banksiana*, and *Picea mariana* following fire in the mixedwood boreal forest', *Canadian Journal of Forest Research*, 29(4), pp. 462–473. Available at: https://doi.org/10.1139/cjfr-29-4-462.

Groot, W.J. de, Cantin, A.S., Flannigan, M.D., Soja, A.J., Gowman, L.M. and Newbery, A. (2013) 'A comparison of Canadian and Russian boreal forest fire regimes', *Forest Ecology and Management*, 294, pp. 23–34. Available at: https://doi.org/10.1016/j.foreco.2012.07.033.

Groot, W.J. de, Goldammer, J.., Keenan, T., Brady, M.A., Lynham, T.J., Justice, C.O., Csiszar, I.A. and O'Loughlin, K. (2006) 'Developing a global early warning system for wildland fire', *International Conference on Forest Fire Research* [Preprint].

Haider, W., Knowler, D., Trenholm, R., Moore, J., Bradshaw, P. and Lertzman, K. (2019) 'Climate change, increasing forest fire incidence, and the value of visibility: Evidence from British Columbia, Canada', *Canadian Journal of Forest Research*, 49(10), pp. 1242–1255. Available at: https://doi.org/10.1139/cjfr-2018-0309.

Hantemirov, R. M., Corona, C., Guillet, S., Shiyatov, S. G., Stoffel, M., Osborn, T. J., Melvin, T. M., Gorlanova, L. A., Kukarskih, V. V., Surkov, A. Y., von Arx, G., and Fonti, P.: Current Siberian heating is unprecedented during the past seven

millennia, Nat. Commun., 13, 1–8, https://doi.org/10.1038/s41467-022-32629-x, 2022.

Hantson, S., Arneth, A., Harrison, S.P., Kelley, D.I., Colin Prentice, I., Rabin, S.S., Archibald, S., Mouillot, F., Arnold, S.R., Artaxo, P., Bachelet, D., Ciais, P., Forrest, M., Friedlingstein, P., Hickler, T., Kaplan, J.O., Kloster, S., Knorr, W., Lasslop, G., Li, F., Mangeon, S., Melton, J.R., Meyn, A., Sitch, S., Spessa, A., Van Der Werf, G.R., Voulgarakis, A. and Yue, C. (2016) 'The status and challenge of global fire modelling', *Biogeosciences*, 13(11), pp. 3359–3375. Available at: https://doi.org/10.5194/bg-13-3359-2016.

Hély, C., Bergeron, Y. and Flannigan, M.D. (2000) 'Effects of stand composition on fire hazard in mixed-wood Canadian boreal forest', *Journal of Vegetation Science*, 11(6), pp. 813–824. Available at: https://doi.org/10.2307/3236551.

Hély, C., Flannigan, M. and Bergeron, Y. (2003) 'Modeling tree mortality following wildfire in the southeastern Canadian mixed-wood boreal forest', *Forest Science*, 49(4), pp. 566–576.

Hessilt, T.D., Werf, G. Van Der, Abatzoglou, J.T. and Scholten, R.C. (2021) 'Future increases in lightning-ignited boreal fires from conjunct increases in dry fuels and lightning', *Proceedings of the 23rd EGU General Assembly* [Preprint].

Haider, W., Knowler, D., Trenholm, R., Moore, J., Bradshaw, P. and Lertzman, K. (2019) 'Climate change, increasing forest fire incidence, and the value of visibility: Evidence from British Columbia, Canada', *Canadian Journal of Forest Research*, 49(10), pp. 1242–1255. Available at: https://doi.org/10.1139/cjfr-2018-0309.

Hantson, S., Arneth, A., Harrison, S.P., Kelley, D.I., Colin Prentice, I., Rabin, S.S., Archibald, S., Mouillot, F., Arnold, S.R., Artaxo, P., Bachelet, D., Ciais, P., Forrest, M., Friedlingstein, P., Hickler, T., Kaplan, J.O., Kloster, S., Knorr, W., Lasslop, G., Li, F., Mangeon, S., Melton, J.R., Meyn, A., Sitch, S., Spessa, A., Van Der Werf, G.R., Voulgarakis, A. and Yue, C. (2016) 'The status and challenge of global fire modelling', *Biogeosciences*, 13(11), pp. 3359–3375. Available at: https://doi.org/10.5194/bg-13-3359-2016.

Hély, C., Bergeron, Y. and Flannigan, M.D. (2000) 'Effects of stand composition on fire hazard in mixed-wood Canadian boreal forest', *Journal of Vegetation Science*, 11(6), pp. 813–824. Available at: https://doi.org/10.2307/3236551.

Hély, C., Flannigan, M. and Bergeron, Y. (2003) 'Modeling tree mortality following wildfire in the southeastern Canadian mixed-wood boreal forest', *Forest Science*, 49(4), pp. 566–576.

Hessilt, T.D., Werf, G. Van Der, Abatzoglou, J.T. and Scholten, R.C. (2021) 'Future increases in lightning-ignited boreal fires from conjunct increases in dry fuels and lightning', *Proceedings of the 23rd EGU General Assembly* [Preprint].

Hicke, J.A., Asner, G.P., Kasischke, E.S., French, N.H.F., Randerson, J.T., Collatz, G.J., Stocks, B.J., Tucker, C.J., Los, S.O. and Field, C.B. (2003) 'Postfire response of North American boreal forest net primary productivity analyzed with satellite observations', *Global Change Biology*, 9(8), pp. 1145–1157. Available at: https://doi.org/10.1046/j.1365-2486.2003.00658.x.

Holm, S.M., Miller, M.D. and Balmes, J.R. (2021) 'Health effects of wildfire smoke in children and public health tools: a narrative review', *Journal of Exposure Science and Environmental Epidemiology*, 31(1), pp. 1–20. Available at: https://doi.org/10.1038/s41370-020-00267-4.

Ichoku, C., Giglio, L., Wooster, M.J. and Remer, L.A. (2008) 'Global characterization of biomass-burning patterns using satellite measurements of fire radiative energy', *Remote Sensing of Environment*, 112(6), pp. 2950–2962. Available at:

~~https://doi.org/10.1016/j.rse.2008.02.009.~~

~~IFFN (2003) *The Current Fire Situation in the Russian Federation : Implications for Enhancing International and Regional Cooperation in the UN Framework and the Global Programs on Fire Monitoring and Assessment*, *International Forest Fire News (IFFN)*.~~

~~IPCC (2007) *Intergovernmental Panel on Climate Change. Fourth Assessment Report. Geneva, Switzerland: Inter-governmental Panel on Climate Change. Cambridge; UK: Cambridge University Press; 2007. Available from: www. ipcc.ch.*, *Intergovernmental Panel on Climate Change*. Available at: https://doi.org/10.1038/446727a.~~

~~IPCC (2021) 'Climate Change 2021', *The Physical Science Basis. Contribution of Working Group 1 to Sixth Assessment Report of the Intergovernmental Panel on Climate Change*, p. In Press. Available at: https://www.ipcc.ch/report/ar6/wg1/.~~

Hicke, J.A., Asner, G.P., Kasischke, E.S., French, N.H.F., Randerson, J.T., Collatz, G.J., Stocks, B.J., Tucker, C.J., Los, S.O. and Field, C.B. (2003) 'Postfire response of North American boreal forest net primary productivity analyzed with satellite observations', *Global Change Biology*, 9(8), pp. 1145–1157. Available at: https://doi.org/10.1046/j.1365-2486.2003.00658.x.

Holm, S.M., Miller, M.D. and Balmes, J.R. (2021) 'Health effects of wildfire smoke in children and public health tools: a narrative review', *Journal of Exposure Science and Environmental Epidemiology*, 31(1), pp. 1–20. Available at: https://doi.org/10.1038/s41370-020-00267-4.

Ichoku, C., Giglio, L., Wooster, M.J. and Remer, L.A. (2008) 'Global characterization of biomass-burning patterns using satellite measurements of fire radiative energy', *Remote Sensing of Environment*, 112(6), pp. 2950–2962. Available at: https://doi.org/10.1016/j.rse.2008.02.009.

IFFN (2003) *The Current Fire Situation in the Russian Federation : Implications for Enhancing International and Regional Cooperation in the UN Framework and the Global Programs on Fire Monitoring and Assessment*, *International Forest Fire News (IFFN)*.

IPCC (2007) *Intergovernmental Panel on Climate Change. Fourth Assessment Report. Geneva, Switzerland: Inter-governmental Panel on Climate Change. Cambridge; UK: Cambridge University Press; 2007. Available from: www. ipcc.ch.*, *Intergovernmental Panel on Climate Change*. Available at: https://doi.org/10.1038/446727a.

IPCC, 2021: Climate Change 2021: The Physical Science Basis. Contribution of Working Group I to the Sixth Assessment Report of the Intergovernmental Panel on Climate Change [Masson-Delmotte, V., P. Zhai, A. Pirani, S.L. Connors, C. Péan, S. Berger, N. Caud, Y. Chen, L. Goldfarb, M.I. Gomis, M. Huang, K. Leitzell, E. Lonnoy, J.B.R. Matthews, T.K. Maycock, T. Waterfield, O. Yelekçi, R. Yu, and B. Zhou (eds.)]. Cambridge University Press, Cambridge, United Kingdom and New York, NY, USA, 2391 pp. doi:10.1017/9781009157896.

Ito, A. (2011) 'Mega fire emissions in Siberia: Potential supply of bioavailable iron from forests to the ocean', *Biogeosciences*, 8(6), pp. 1679–1697. Available at: https://doi.org/10.5194/bg-8-1679-2011.

Ito, A.: A historical meta-analysis of global terrestrial net primary productivity: Are estimates converging?, Glob. Chang. Biol., 17, 3161–3175, https://doi.org/10.1111/j.1365-2486.2011.02450.x, 2011.

Ivanov, V., Milyaev, I., Konstantinov, A. and Loiko, S. (2022) 'Land-Use Changes on Ob River Floodplain (Western Siberia,

Russia) in Context of Natural and Social Changes over Past 200 Years', *Land*, 11(12). Available at: https://doi.org/10.3390/land11122258.

Jacobson, T.A., Kler, J.S., Hernke, M.T., Braun, R.K., Meyer, K.C. and Funk, W.E. (2019) 'Direct human health risks of increased atmospheric carbon dioxide', *Nature Sustainability*, 2(8), pp. 691–701. Available at: https://doi.org/10.1038/s41893-019-0323-1.

Johnson, M.S., Strawbridge, K., Knowland, K.E., Keller, C. and Travis, M. (2021) 'Long-range transport of Siberian biomass burning emissions to North America during FIREX-AQ', *Atmospheric Environment*, 252(January). Available at: https://doi.org/10.1016/j.atmosenv.2021.118241.

Kaiser, J.W., Heil, A., Andreae, M.O., Benedetti, A., Chubarova, N., Jones, L., Morcrette, J.J., Razinger, M., Schultz, M.G., Ito, A. (2011) 'Mega fire emissions in Siberia: Potential supply of bioavailable iron from forests to the ocean', *Biogeosciences*, 8(6), pp. 1679–1697. Available at: https://doi.org/10.5194/bg-8-1679-2011.

Ivanov, V., Milyaev, I., Konstantinov, A. and Loiko, S. (2022) 'Land-Use Changes on Ob River Floodplain (Western Siberia, Russia) in Context of Natural and Social Changes over Past 200 Years', *Land*, 11(12). Available at: https://doi.org/10.3390/land11122258.

Jacobson, T.A., Kler, J.S., Hernke, M.T., Braun, R.K., Meyer, K.C. and Funk, W.E. (2019) 'Direct human health risks of increased atmospheric carbon dioxide', *Nature Sustainability*, 2(8), pp. 691–701. Available at: https://doi.org/10.1038/s41893-019-0323-1.

Johnson, M.S., Strawbridge, K., Knowland, K.E., Keller, C. and Travis, M. (2021) 'Long-range transport of Siberian biomass burning emissions to North America during FIREX-AQ', *Atmospheric Environment*, 252(January). Available at: https://doi.org/10.1016/j.atmosenv.2021.118241.

Kaiser, J.W., Heil, A., Andreae, M.O., Benedetti, A., Chubarova, N., Jones, L., Morcrette, J.J., Razinger, M., Schultz, M.G., Suttie, M. and Van Der Werf, G.R. (2012) 'Biomass burning emissions estimated with a global fire assimilation system based on observed fire radiative power', *Biogeosciences*, 9(1), pp. 527–554. Available at: https://doi.org/10.5194/bg-9-527-2012.

Kasischke, E.S. (2000) 'Boreal Ecosystems in the Global Carbon Cycle', (Houghton), pp. 19–30. Available at: https://doi.org/10.1007/978-0-387-21629-4_2.

Kasischke, E.S. and Bruhwiler, L.P. (2003) 'Emissions of carbon dioxide, carbon monoxide, and methane from boreal forest fires in 1998', *Journal of Geophysical Research: Atmospheres*, 108(1). Available at: https://doi.org/10.1029/2001jd000461.

Kasischke, E.S., Christensen, N.L. and Stocks, B.J. (1995) 'Fire, global warming, and the carbon balance of boreal forests', *Ecological Applications*, 5(2), pp. 437–451. Available at: https://doi.org/10.2307/1942034.

Kasischke, E.S. and Turetsky, M.R. (2006) 'Recent changes in the fire regime across the North American boreal region - Spatial and temporal patterns of burning across Canada and Alaska', *Geophysical Research Letters*, 33(9). Available at: https://doi.org/10.1029/2006GL025677.

Keane, R.E., Arno, S.F. and Brown, J.K. (1990) 'Simulating Cumulative Fire Effects in Ponderosa Pine / Douglas-Fir Forests Author (s): Robert E . Keane , Stephen F . Arno , James K . Brown Published by : Ecological Society of America Stable

URL : http://www.jstor.org/stable/1940259 . SIMULATING CUMUL', *America*, 71(1), pp. 189–203.
Kharuk, V.I., Dvinskaya, M.L., Im, S.T., Golyukov, A.S. and Smith, K.T. (2022) 'Wildfires in the Siberian Arctic', *Fire*, 5(4), pp. 1–16. Available at: https://doi.org/10.3390/fire5040106.
Kharuk, V.I., Ranson, K.J., Dvinskaya, M.L. and Im, S.T. (2011) 'Wildfires in northern Siberian larch dominated communities', *Environmental Research Letters*, 6(4). Available at: https://doi.org/10.1088/1748-9326/6/4/045208.
Kimball, B.A. and Idso, S.B. (1983) 'Increasing atmospheric CO2: effects on crop yield, water use and climate', *Agricultural Water Management*, 7(1–3), pp. 55–72. Available at: https://doi.org/10.1016/0378-3774(83)90075-6.
Suttie, M. and Van Der Werf, G.R. (2012) 'Biomass burning emissions estimated with a global fire assimilation system based on observed fire radiative power', *Biogeosciences*, 9(1), pp. 527–554. Available at: https://doi.org/10.5194/bg-9-527-2012.
Kasischke, E.S. (2000) 'Boreal Ecosystems in the Global Carbon Cycle', (Houghton), pp. 19–30. Available at: https://doi.org/10.1007/978-0-387-21629-4_2.
Kantzas, E., Lomas, M., and Quegan, S.: Fire at high latitudes: Data-model comparisons and their consequences, Global Biogeochem. Cycles, 27, 677–691, https://doi.org/10.1002/gbc.20059, 2013.
Kasischke, E.S. and Bruhwiler, L.P. (2003) 'Emissions of carbon dioxide, carbon monoxide, and methane from boreal forest fires in 1998', *Journal of Geophysical Research: Atmospheres*, 108(1). Available at: https://doi.org/10.1029/2001jd000461.
Kasischke, E.S., Christensen, N.L. and Stocks, B.J. (1995) 'Fire, global warming, and the carbon balance of boreal forests', *Ecological Applications*, 5(2), pp. 437–451. Available at: https://doi.org/10.2307/1942034.
Kasischke, E.S. and Turetsky, M.R. (2006) 'Recent changes in the fire regime across the North American boreal region - Spatial and temporal patterns of burning across Canada and Alaska', *Geophysical Research Letters*, 33(9). Available at: https://doi.org/10.1029/2006GL025677.
Keane, R.E., Arno, S.F. and Brown, J.K. (1990) 'Simulating Cumulative Fire Effects in Ponderosa Pine / Douglas-Fir Forests Author (s): Robert E . Keane , Stephen F . Arno , James K . Brown Published by : Ecological Society of America Stable URL : http://www.jstor.org/stable/1940259 . SIMULATING CUMUL', *America*, 71(1), pp. 189–203.
Kharuk, V.I., Ranson, K.J., Dvinskaya, M.L. and Im, S.T. (2011) 'Wildfires in northern Siberian larch dominated communities', *Environmental Research Letters*, 6(4). Available at: https://doi.org/10.1088/1748-9326/6/4/045208.
Kharuk, V. I., Mariya, L. D., Ilya, A. P., Sergei, T. I., and Kenneth, J. R.: Larch Forests of Middle Siberia: Long-Term Trends in Fire Return Intervals, Reg. Environ. Chang., 16, 2389–2397, https://doi.org/doi:10.1007/s10113-016-0964-9, 2016.
Kharuk, V. I., Ponomarev, E. I., Ivanova, G. A., Dvinskaya, M. L., Coogan, S. C. P., and Flannigan, M. D.: Wildfires in the Siberian taiga, Ambio, 50, 1953–1974, https://doi.org/10.1007/s13280-020-01490-x, 2021.
Kharuk, V.I., Dvinskaya, M.L., Im, S.T., Golyukov, A.S. and Smith, K.T. (2022) 'Wildfires in the Siberian Arctic', *Fire*, 5(4), pp. 1–16. Available at: https://doi.org/10.3390/fire5040106.
Kimball, B.A. and Idso, S.B. (1983) 'Increasing atmospheric CO2: effects on crop yield, water use and climate', *Agricultural Water Management*, 7(1–3), pp. 55–72. Available at: https://doi.org/10.1016/0378-3774(83)90075-6.
Krawchuk, M.A., Cumming, S.G. and Flannigan, M.D. (2009) 'Predicted changes in fire weather suggest increases in lightning

fire initiation and future area burned in the mixedwood boreal forest', *Climatic Change*, pp. 83–97. Available at: https://doi.org/10.1007/s10584-008-9460-7.

Krylov, A., McCarty, J.L., Potapov, P., Loboda, T., Tyukavina, A., Turubanova, S. and Hansen, M.C. (2014) 'Remote sensing estimates of stand-replacement fires in Russia, 2002-2011', *Environmental Research Letters*, 9(10). Available at: https://doi.org/10.1088/1748-9326/9/10/105007.

Kukavskaya, E.A., Soja, A.J., Petkov, A.P., Ponomarev, E.I., Ivanova, G.A. and Conard, S.G. (2013) 'Fire emissions estimates in siberia: Evaluation of uncertainties in area burned, land cover, and fuel consumption', *Canadian Journal of Forest Research*, 43(5), pp. 493–506. Available at: https://doi.org/10.1139/cjfr-2012-0367.

Landrum, L. and Holland, M. M.: Extremes become routine in an emerging new Arctic, Nat. Clim. Chang., 10, 1108–1115, https://doi.org/10.1038/s41558-020-0892-z, 2020.

Lee, J.-Y., J. Marotzke, G. Bala, L. Cao, S. Corti, J.P. Dunne, F. Engelbrecht, E. Fischer, J.C. Fyfe, C. Jones, A. Maycock, J.

~~Krawchuk, M.A., Cumming, S.G. and Flannigan, M.D. (2009) 'Predicted changes in fire weather suggest increases in lightning fire initiation and future area burned in the mixedwood boreal forest', *Climatic Change*, pp. 83–97. Available at: https://doi.org/10.1007/s10584-008-9460-7.~~

~~Krylov, A., McCarty, J.L., Potapov, P., Loboda, T., Tyukavina, A., Turubanova, S. and Hansen, M.C. (2014) 'Remote sensing estimates of stand-replacement fires in Russia, 2002-2011', *Environmental Research Letters*, 9(10). Available at: https://doi.org/10.1088/1748-9326/9/10/105007.~~

~~Kukavskaya, E.A., Soja, A.J., Petkov, A.P., Ponomarev, E.I., Ivanova, G.A. and Conard, S.G. (2013) 'Fire emissions estimates in siberia: Evaluation of uncertainties in area burned, land cover, and fuel consumption', *Canadian Journal of Forest Research*, 43(5), pp. 493–506. Available at: https://doi.org/10.1139/cjfr-2012-0367.~~

~~Li, F., Val Martin, M., Andreae, M.O., Arneth, A., Hantson, S., Kaiser, J.W., Lasslop, G., Yue, C., Bachelet, D., Forrest, M., Kluzek, E., Liu, X., Mangeon, S., Melton, J.R., Ward, D.S., Darmenov, A., Hickler, T., Ichoku, C., Magi, B.I., Sitch, S., Van Der Werf, G.R., Wiedinmyer, C. and Rabin, S.S. (2019) 'Historical (1700–2012) global multi-model estimates of the fire emissions from the Fire Modeling Intercomparison Project (FireMIP)', *Atmospheric Chemistry and Physics*, 19(19), pp. 12545–12567. Available at: https://doi.org/10.5194/acp-19-12545-2019.~~

~~Lin, N.H., Tsay, S.C., Maring, H.B., Yen, M.C., Sheu, G.R., Wang, S.H., Chi, K.H., Chuang, M.T., Ou-Yang, C.F., Fu, J.S., Reid, J.S., Lee, C. Te, Wang, L.C., Wang, J.L., Hsu, C.N., Sayer, A.M., Holben, B.N., Chu, Y.C., Nguyen, X.A., Sopajaree, K., Chen, S.J., Cheng, M.T., Tsuang, B.J., Tsai, C.J., Peng, C.M., Schnell, R.C., Conway, T., Chang, C.T., Lin, K.S., Tsai, Y.I., Lee, W.J., Chang, S.C., Liu, J.J., Chiang, W.L., Huang, S.J., Lin, T.H. and Liu, G.R. (2013) 'An overview of regional experiments on biomass burning aerosols and related pollutants in Southeast Asia: From BASE-ASIA and the Dongsha Experiment to 7-SEAS', *Atmospheric Environment*, 78, pp. 1–19. Available at: https://doi.org/10.1016/j.atmosenv.2013.04.066.~~

~~Lindsey, R. and Dahlman, L. (2023) *Climate Change: Global Temperature*, *Understanding Climate*. Available at: https://www.climate.gov/news-features/understanding-climate/ climate-change-global-temperature (Accessed: 26 November~~

2023).

Liousse, C., Guillaume, B., Grégoire, J.M., Mallet, M., Galy, C., Pont, V., Akpo, A., Bedou, M., Castéra, P., Dungall, L., Gardrat, E., Granier, C., Konaré, A., Malavelle, F., Mariscal, A., Mieville, A., Rosset, R., Serça, D., Solmon, F., Tummon, F., Assamoi, E., Yoboué, V. and Van Velthoven, P. (2010) 'Updated African biomass burning emission inventories in the framework of the AMMA-IDAF program, with an evaluation of combustion aerosols', *Atmospheric Chemistry and Physics*, 10(19), pp. 9631–9646. Available at: https://doi.org/10.5194/acp-10-9631-2010.

Liu, J.C., Pereira, G., Uhl, S.A., Bravo, M.A. and Bell, M.L. (2015) 'A systematic review of the physical health impacts from non-occupational exposure to wildfire smoke', *Environmental Research*, 136, pp. 120–132. Available at: https://doi.org/10.1016/j.envres.2014.10.015.

Mutemi, O. Ndiaye, S. Panickal, and T. Zhou, 2021: Future Global Climate: Scenario-Based Projections and Near Term Information. In Climate Change 2021: The Physical Science Basis. Contribution of Working Group I to the Sixth Assessment Report of the Intergovernmental Panel on Climate Change [Masson-Delmotte, V., P. Zhai, A. Pirani, S.L. Connors, C. Péan, S. Berger, N. Caud, Y. Chen, L. Goldfarb, M.I. Gomis, M. Huang, K. Leitzell, E. Lonnoy, J.B.R. Matthews, T.K. Maycock, T. Waterfield, O. Yelekçi, R. Yu, and B. Zhou (eds.)]. Cambridge University Press, Cambridge, United Kingdom and New York, NY, USA, pp. 553–672, doi:10.1017/9781009157896.006.

Li, F., Val Martin, M., Andreae, M.O., Arneth, A., Hantson, S., Kaiser, J.W., Lasslop, G., Yue, C., Bachelet, D., Forrest, M., Kluzek, E., Liu, X., Mangeon, S., Melton, J.R., Ward, D.S., Darmenov, A., Hickler, T., Ichoku, C., Magi, B.I., Sitch, S., Van Der Werf, G.R., Wiedinmyer, C. and Rabin, S.S. (2019) 'Historical (1700-2012) global multi-model estimates of the fire emissions from the Fire Modeling Intercomparison Project (FireMIP)', *Atmospheric Chemistry and Physics*, 19(19), pp. 12545–12567. Available at: https://doi.org/10.5194/acp-19-12545-2019.

Lin, N.H., Tsay, S.C., Maring, H.B., Yen, M.C., Sheu, G.R., Wang, S.H., Chi, K.H., Chuang, M.T., Ou-Yang, C.F., Fu, J.S., Reid, J.S., Lee, C. Te, Wang, L.C., Wang, J.L., Hsu, C.N., Sayer, A.M., Holben, B.N., Chu, Y.C., Nguyen, X.A., Sopajaree, K., Chen, S.J., Cheng, M.T., Tsuang, B.J., Tsai, C.J., Peng, C.M., Schnell, R.C., Conway, T., Chang, C.T., Lin, K.S., Tsai, Y.I., Lee, W.J., Chang, S.C., Liu, J.J., Chiang, W.L., Huang, S.J., Lin, T.H. and Liu, G.R. (2013) 'An overview of regional experiments on biomass burning aerosols and related pollutants in Southeast Asia: From BASE-ASIA and the Dongsha Experiment to 7-SEAS', *Atmospheric Environment*, 78, pp. 1–19. Available at: https://doi.org/10.1016/j.atmosenv.2013.04.066.

Lindsey, R. and Dahlman, L. (2023) *Climate Change: Global Temperature*, *Understanding Climate*. Available at: https://www.climate.gov/news-features/understanding-climate/ climate-change-global-temperature (Accessed: 26 November 2023).

Liousse, C., Guillaume, B., Grégoire, J.M., Mallet, M., Galy, C., Pont, V., Akpo, A., Bedou, M., Castéra, P., Dungall, L., Gardrat, E., Granier, C., Konaré, A., Malavelle, F., Mariscal, A., Mieville, A., Rosset, R., Serça, D., Solmon, F., Tummon, F., Assamoi, E., Yoboué, V. and Van Velthoven, P. (2010) 'Updated African biomass burning emission inventories in the framework of the AMMA-IDAF program, with an evaluation of combustion aerosols', *Atmospheric Chemistry and Physics*,

10(19), pp. 9631–9646. Available at: https://doi.org/10.5194/acp-10-9631-2010.

Liu, J.C., Pereira, G., Uhl, S.A., Bravo, M.A. and Bell, M.L. (2015) 'A systematic review of the physical health impacts from non-occupational exposure to wildfire smoke', *Environmental Research*, 136, pp. 120–132. Available at: https://doi.org/10.1016/j.envres.2014.10.015.

Lobert, J.M., Scharffe, D.H., Hao, W.M., Kuhlbusch, T.A., Seuwen, R., Warneck, P. and Crutzen, P.J. (1991) 'Experimental Evaluation of Biomass Burning Emissions: Nitrogen and Carbon Containing Compounds', *Global Biomass Burning: Atmospheric, Climatic, and Biospheric Implications*, (MIT Press), pp. 289–304. Available at: https://doi.org/10.7551/mitpress/3286.003.0041.

Marlon, J.R., Bartlein, P.J., Carcaillet, C., Gavin, D.G., Harrison, S.P., Higuera, P.E., Joos, F., Power, M.J. and Prentice, I.C.

~~Lobert, J.M., Scharffe, D.H., Hao, W.M., Kuhlbusch, T.A., Seuwen, R., Warneck, P. and Crutzen, P.J. (1991) 'Experimental Evaluation of Biomass Burning Emissions: Nitrogen and Carbon Containing Compounds', *Global Biomass Burning: Atmospheric, Climatic, and Biospheric Implications*, (MIT Press), pp. 289–304. Available at: https://doi.org/10.7551/mitpress/3286.003.0041.~~

~~Marlon, J.R., Bartlein, P.J., Carcaillet, C., Gavin, D.G., Harrison, S.P., Higuera, P.E., Joos, F., Power, M.J. and Prentice, I.C. (2008) 'Climate and human influences on global biomass burning over the past two millennia', *Nature Geoscience*, 1(10), pp. 697–702. Available at: https://doi.org/10.1038/ngeo313.~~

~~Martenies, S.E. and Batterman, S.A. (2018) 'Effectiveness of Using Enhanced Filters in Schools and Homes to Reduce Indoor Exposures to PM 2.5 from Outdoor Sources and Subsequent Health Benefits for Children with Asthma', *Environmental Science and Technology*, 52(18), pp. 10767–10776. Available at: https://doi.org/10.1021/acs.est.8b02053.~~

~~Meehl, G.A., T.F., S., W.D., C., P., F., A.T., G., J.M., G., A., K., R., K., J.M., M., A., N., S.C.B., R., I.G., W., A.J., W. and Zhao, Z.-C. (2007) 'Global Climate Projections', *Global Climate Projections. In: Climate Change 2007: The Physical Science Basis* [Preprint], (Contribution of Working Group I to the Fourth Assessment Report of the Intergovernmental Panel on Climate Change [Solomon, S., D. Qin, M. Manning, Z. Chen, M. Marquis, K.B. Averyt, M. Tignor and H.L. Miller (eds.)]. Cambridge University Press, Cambridge,).~~

~~Melillo, J.M., A. David, M., David, W.K., Berrien M. I., Charles J. V. and Annette L. S. (1993) 'Global climate change and terrestrial net primary production', *Nature*, 8(2), p. 312. Available at: https://doi.org/10.2307/2800863.~~

~~Miesner, T., Herzschuh, U., Pestryakova, L.A., Wieczorek, M., Zakharov, E.S., Kolmogorov, A.I., Davydova, P. V. and Kruse, S. (2022) 'Forest structure and individual tree inventories of northeastern Siberia along climatic gradients', *Earth System Science Data*, 14(12), pp. 5695–5716. Available at: https://doi.org/10.5194/essd-14-5695-2022.~~

~~Miller, C. and Urban, D.L. (1999) 'Interactions between forest heterogeneity and surface fire regimes in the southern Sierra Nevada', *Canadian Journal of Forest Research*, 29(2), pp. 202–212. Available at: https://doi.org/10.1139/x98-188.~~

~~Miranda, N.D., Lizana, J., Sparrow, S.N., Zachau-Walker, M., Watson, P.A.G., Wallom, D.C.H., Khosla, R. and McCulloch, M. (2023) 'Change in cooling degree days with global mean temperature increasing from 1.5 °C to 2.0 °C', *Nature Sustainability*, 6(November). Available at: https://doi.org/10.1038/s41893-023-01155-z.~~

(2008) ‘Climate and human influences on global biomass burning over the past two millennia’, *Nature Geoscience*, 1(10), pp. 697–702. Available at: https://doi.org/10.1038/ngeo313.

Martenies, S.E. and Batterman, S.A. (2018) ‘Effectiveness of Using Enhanced Filters in Schools and Homes to Reduce Indoor Exposures to PM 2.5 from Outdoor Sources and Subsequent Health Benefits for Children with Asthma’, *Environmental Science and Technology*, 52(18), pp. 10767–10776. Available at: https://doi.org/10.1021/acs.est.8b02053.

Meehl, G.A., T.F., S., W.D., C., P., F., A.T., G., J.M., G., A., K., R., K., J.M., M., A., N., S.C.B., R., I.G., W., A.J., W. and Zhao, Z.-C. (2007) ‘Global Climate Projections’, *Global Climate Projections. In: Climate Change 2007: The Physical Science Basis* [Preprint], (Contribution of Working Group I to the Fourth Assessment Report of the Intergovernmental Panel on Climate Change [Solomon, S., D. Qin, M. Manning, Z. Chen, M. Marquis, K.B. Averyt, M. Tignor and H.L. Miller (eds.)]. Cambridge University Press, Cambridge,).

Meigs, G.W., Campbell, J.L., Zald, H.S.J., Bailey, J.D., Shaw, D.C., Kennedy, R.E., 2015. Does wildfire likelihood increase following insect outbreaks in conifer forests? Ecosphere 6, 1–24. https://doi.org/10.1890/ES15-00037.1

Meigs, G.W., Zald, H.S.J., Campbell, J.L., Keeton, W.S., Kennedy, R.E., 2016. Do insect outbreaks reduce the severity of subsequent forest fires? Environ. Res. Lett. 11. https://doi.org/10.1088/1748-9326/11/4/045008

Melillo, J.M., A. David, M., David, W.K., Berrien M. I., Charles J. V. and Annette L. S. (1993) ‘Global climate change and terrestrial net primary production’, *Nature*, 8(2), p. 312. Available at: https://doi.org/10.2307/2800863.

Miesner, T., Herzschuh, U., Pestryakova, L.A., Wieczorek, M., Zakharov, E.S., Kolmogorov, A.I., Davydova, P. V. and Kruse, S. (2022) ‘Forest structure and individual tree inventories of northeastern Siberia along climatic gradients’, *Earth System Science Data*, 14(12), pp. 5695–5716. Available at: https://doi.org/10.5194/essd-14-5695-2022.

Miller, C. and Urban, D.L. (1999) ‘Interactions between forest heterogeneity and surface fire regimes in the southern Sierra Nevada’, *Canadian Journal of Forest Research*, 29(2), pp. 202–212. Available at: https://doi.org/10.1139/x98-188.

Miranda, N.D., Lizana, J., Sparrow, S.N., Zachau-Walker, M., Watson, P.A.G., Wallom, D.C.H., Khosla, R. and McCulloch, M. (2023) ‘Change in cooling degree days with global mean temperature increasing from 1.5 °C to 2.0 °C’, *Nature Sustainability*, 6(November). Available at: https://doi.org/10.1038/s41893-023-01155-z.

Mouillot, F., Schultz, M.G., Yue, C., Cadule, P., Tansey, K., Ciais, P. and Chuvieco, E. (2014) ‘Ten years of global burned area products from spaceborne remote sensing-A review: Analysis of user needs and recommendations for future developments’, *International Journal of Applied Earth Observation and Geoinformation*, 26(1), pp. 64–79. Available at: https://doi.org/10.1016/j.jag.2013.05.014.

Natali, S. M., Watts, J. D., Rogers, B. M., Potter, S., Ludwig, S. M., Selbmann, A. K., Sullivan, P. F., Abbott, B. W., Arndt, K. A., Birch, L., Björkman, M. P., Bloom, A. A., Celis, G., Christensen, T. R., Christiansen, C. T., Commane, R., Cooper, E. J., Crill, P., Czimczik, C., Davydov, S., Du, J., Egan, J. E., Elberling, B., Euskirchen, E. S., Friborg, T., Genet, H., Göckede, M., Goodrich, J. P., Grogan, P., Helbig, M., Jafarov, E. E., Jastrow, J. D., Kalhori, A. A. M., Kim, Y., Kimball, J. S., Kutzbach, L., Lara, M. J., Larsen, K. S., Lee, B. Y., Liu, Z., Loranty, M. M., Lund, M., Lupascu, M., Madani, N., Malhotra, A., Matamala, R., McFarland, J., McGuire, A. D., Michelsen, A., Minions, C., Oechel, W. C., Olefeldt, D., Parmentier, F. J. W., Pirk, N.,

Mouillot, F., Schultz, M.G., Yue, C., Cadule, P., Tansey, K., Ciais, P. and Chuvieco, E. (2014) 'Ten years of global burned area products from spaceborne remote sensing—A review: Analysis of user needs and recommendations for future developments', *International Journal of Applied Earth Observation and Geoinformation*, 26(1), pp. 64–79. Available at: https://doi.org/10.1016/j.jag.2013.05.014.

NASA (2012) *Wildfires in Siberia*. Available at: https://www.nasa.gov/mission_pages/fires/main/world/20120913-siberia.html (Accessed: 24 May 2023).

Neto, T.G.S., Carvalho, J.A., Veras, C.A.G., Alvarado, E.C., Gielow, R., Lincoln, E.N., Christian, T.J., Yokelson, R.J. and Santos, J.C. (2009) 'Biomass consumption and CO2, CO and main hydrocarbon gas emissions in an Amazonian forest clearing fire', *Atmospheric Environment*, 43(2), pp. 438–446. Available at: https://doi.org/10.1016/j.atmosenv.2008.07.063.

Nguyen, H.M. and Wooster, M.J. (2020) 'Advances in the estimation of high Spatio-temporal resolution pan-African top-down biomass burning emissions made using geostationary fire radiative power (FRP) and MAIAC aerosol optical depth (AOD) data', *Remote Sensing of Environment*, 248(July), p. 111971. Available at: https://doi.org/10.1016/j.rse.2020.111971.

Ninomiya, H., Kato, T., Végh, L. and Wu, L. (2023) 'Modeling of non-structural carbohydrate dynamics by the spatially explicitly individual-based dynamic global vegetation model SEIB–DGVM (SEIB-DGVM-NSC ver1.0)', (October), pp. 1–33. Available at: https://doi.org/10.5194/egusphere-2022-835.

Orangeville, L.D., Houle, D., Duchesne, L., Phillips, R.P., Bergeron, Y. and Kneeshaw, D. (2018) 'Beneficial effects of climate warming on boreal tree growth may be transitory', *Nature Communications*, (2018), pp. 1–10. Available at: https://doi.org/10.1038/s41467-018-05705-4.

Ozturk, T., Turp, M.T., Türke, M. and Kurnaz, M.L. (2017) 'Projected changes in temperature and precipitation climatology of Central Asia CORDEX Region 8 by using RegCM4.3.5', 183, pp. 296–307. Available at: https://doi.org/10.1016/j.atmosres.2016.09.008.

Pan, X., Chin, M., Gautam, R., Bian, H., Kim, D., Colarco, P.R., Diehl, T.L., Takemura, T., Pozzoli, L., Tsigaridis, K., Bauer, S. and Bellouin, N. (2015) 'A multi-model evaluation of aerosols over South Asia: Common problems and possible causes', *Atmospheric Chemistry and Physics*, 15(10), pp. 5903–5928. Available at: https://doi.org/10.5194/acp-15-5903-2015.

Pan, X., Ichoku, C., Chin, M., Bian, H., Darmenov, A., Colarco, P., Ellison, L., Kucsera, T., Da Silva, A., Wang, J., Oda, T. and Cui, G. (2020) 'Six global biomass burning emission datasets: Intercomparison and application in one global aerosol model', *Atmospheric Chemistry and Physics*, 20(2), pp. 969–994. Available at: https://doi.org/10.5194/acp-20-969-2020.

Pastor, J. and Post, W.M. (1986) 'Influence of climate, soil moisture, and succession on forest carbon and nitrogen cycles', (1923), pp. 3–27.

Pellegrini, A.F.A., Harden, J., Georgiou, K., Hemes, K.S., Malhotra, A., Nolan, C.J. and Jackson, R.B. (2021) 'Fire effects on the persistence of soil organic matter and long-term carbon storage', *Nature Geoscience*, 15(January). Available at: https://doi.org/10.1038/s41561-021-00867-1.

Poulter, B., Quinton, W., Rezanezhad, F., Risk, D., Sachs, T., Schaefer, K., Schmidt, N. M., Schuur, E. A. G., Semenchuk, P. R., Shaver, G., Sonnentag, O., Starr, G., Treat, C. C., Waldrop, M. P., Wang, Y., Welker, J., Wille, C., Xu, X., Zhang, Z.,

Zhuang, Q., and Zona, D.: Large loss of CO2 in winter observed across the northern permafrost region, Nat. Clim. Chang., 9, 852–857, https://doi.org/10.1038/s41558-019-0592-8, 2019.

NASA (2012) *Wildfires in Siberia*. Available at: https://www.nasa.gov/mission_pages/fires/main/world/20120913-siberia.html (Accessed: 24 May 2023).

Neto, T.G.S., Carvalho, J.A., Veras, C.A.G., Alvarado, E.C., Gielow, R., Lincoln, E.N., Christian, T.J., Yokelson, R.J. and Santos, J.C. (2009) 'Biomass consumption and CO2, CO and main hydrocarbon gas emissions in an Amazonian forest clearing fire', *Atmospheric Environment*, 43(2), pp. 438–446. Available at: https://doi.org/10.1016/j.atmosenv.2008.07.063.

Nguyen, H.M. and Wooster, M.J. (2020) 'Advances in the estimation of high Spatio-temporal resolution pan-African top-down biomass burning emissions made using geostationary fire radiative power (FRP) and MAIAC aerosol optical depth (AOD) data', *Remote Sensing of Environment*, 248(July), p. 111971. Available at: https://doi.org/10.1016/j.rse.2020.111971.

Ninomiya, H., Kato, T., Végh, L. and Wu, L. (2023) 'Modeling of non-structural carbohydrate dynamics by the spatially explicitly individual-based dynamic global vegetation model SEIB- DGVM (SEIB-DGVM-NSC ver1.0)', (October), pp. 1–33. Available at: https://doi.org/10.5194/egusphere-2022-835.

Nitzbon, J., Westermann, S., Langer, M., Martin, L. C. P., Strauss, J., Laboor, S., and Boike, J.: Fast response of cold ice-rich permafrost in northeast Siberia to a warming climate, Nat. Commun., 11, 1–11, https://doi.org/10.1038/s41467-020-15725-8, 2020.

Orangeville, L.D., Houle, D., Duchesne, L., Phillips, R.P., Bergeron, Y. and Kneeshaw, D. (2018) 'Beneficial effects of climate warming on boreal tree growth may be transitory', *Nature Communications*, (2018), pp. 1–10. Available at: https://doi.org/10.1038/s41467-018-05705-4.

Ozturk, T., Turp, M.T., Türke, M. and Kurnaz, M.L. (2017) 'Projected changes in temperature and precipitation climatology of Central Asia CORDEX Region 8 by using RegCM4.3.5', 183, pp. 296–307. Available at: https://doi.org/10.1016/j.atmosres.2016.09.008.

Pan, X., Chin, M., Gautam, R., Bian, H., Kim, D., Colarco, P.R., Diehl, T.L., Takemura, T., Pozzoli, L., Tsigaridis, K., Bauer, S. and Bellouin, N. (2015) 'A multi-model evaluation of aerosols over South Asia: Common problems and possible causes', *Atmospheric Chemistry and Physics*, 15(10), pp. 5903–5928. Available at: https://doi.org/10.5194/acp-15-5903-2015.

Pan, X., Ichoku, C., Chin, M., Bian, H., Darmenov, A., Colarco, P., Ellison, L., Kucsera, T., Da Silva, A., Wang, J., Oda, T. and Cui, G. (2020) 'Six global biomass burning emission datasets: Intercomparison and application in one global aerosol model', *Atmospheric Chemistry and Physics*, 20(2), pp. 969–994. Available at: https://doi.org/10.5194/acp-20-969-2020.

Pastor, J. and Post, W.M. (1986) 'Influence of climate, soil moisture, and succession on forest carbon and nitrogen cycles', (1923), pp. 3–27.

Pellegrini, A.F.A., Harden, J., Georgiou, K., Hemes, K.S., Malhotra, A., Nolan, C.J. and Jackson, R.B. (2021) 'Fire effects on the persistence of soil organic matter and long-term carbon storage', *Nature Geoscience*, 15(January). Available at: https://doi.org/10.1038/s41561-021-00867-1.~~Pereira, G., Siqueira, R., Rosário, N.E., Longo, K.L., Freitas, S.R., Cardozo, F.S., Kaiser, J.W. and Wooster, M.J. (2016) 'Assessment of fire emission inventories during the South American Biomass Burning~~

Analysis (SAMBBA) experiment', *Atmospheric Chemistry and Physics*, 16(11), pp. 6961–6975. Available at: https://doi.org/10.5194/acp-16-6961-2016.

Peterson, D.L. and Ryan, K.C. (1986) 'Modeling postfire conifer mortality for long-range planning', *Environmental Management*, 10(6), pp. 797–808. Available at: https://doi.org/10.1007/BF01867732.

Petrenko, M., Kahn, R., Chin, M. and Limbacher, J. (2017) 'Refined Use of Satellite Aerosol Optical Depth Snapshots to Constrain Biomass Burning Emissions in the GOCART Model', *Journal of Geophysical Research: Atmospheres*, 122(20), pp. 10,983–11,004. Available at: https://doi.org/10.1002/2017JD026693.

Petrenko, M., Kahn, R., Chin, M., Soja, A., Kucsera, T. and Harshvardhan (2012) 'The use of satellite-measured aerosol optical depth to constrain biomass burning emissions source strength in the global model GOCART', *Journal of Geophysical Research Atmospheres*, 117(17). Available at: https://doi.org/10.1029/2012JD017870.

Pickett, S.T., Wu, J. and Cadenasso., M.L. (1999) 'Patch dynamics and the ecology of disturbed ground: a framework for synthesis.', *Ecosystems of Disturbed Ground*, pp. 707–722.

Ponomarev, E.I., Kharuk, V.I. and Ranson, K.J. (2016) 'Wildfires dynamics in Siberian larch forests', *Forests*, 7(6), pp. 1–9. Available at: https://doi.org/10.3390/f7060125.

Popovicheva, O., Kistler, M., Kireeva, E., Persiantseva, N., Timofeev, M., Kopeikin, V. and Kasper-Giebl, A. (2014) 'Physicochemical characterization of smoke aerosol during large-scale wildfires: Extreme event of August 2010 in Moscow', *Atmospheric Environment*, 96(August 2011), pp. 405–414. Available at: https://doi.org/10.1016/j.atmosenv.2014.03.026.

Pörtner, H. O., Roberts, D.C., Adams, H., Adelekan, I., Adler, C., Adrian, R., Aldunce, P., Ali, E., Begum, R.A., BednarFriedl, B., Kerr, R.B., Biesbroek, R., Birkmann, J., Bowen, K., Caretta, M.A., Carnicer, J., Castellanos, E., Cheong, T.S., Chow, W., Cissé, G., Clayton, S., Constable, A., Cooley, S.R., Costello, M.J., Craig, M., Cramer, W., Dawson, R., Dodman, D., Efitre, J., Garschagen, M., Gilmore, E.A., Glavovic, B.C., Gutzler, D., Haasnoot, M., Harper, S., Hasegawa, T., Hayward, B., Hicke, J.A., Hirabayashi, Y., Huang, C., Kalaba, K., Kiessling, W., Kitoh, A., Lasco, R., Lawrence, J., Lemos, M.F., Lempert, R., Lennard, C., Ley, D., Lissner, T., Liu, Q., Liwenga, E., Lluch-Cota, S., Löschke, S., Lucatello, S., Luo, Y., Mackey, B., Mintenbeck, K., Mirzabaev, A., Möller, V., Vale, M.M., Morecroft, M.D., Mortsch, L., Mukherji, A., Mustonen, T., Mycoo, M., Nalau, J., New, M., Okem, A., Ometto, J.P., O'Neill, B., Pandey, R., Parmesan, C., Pelling, M., Pinho, P.F., Pinnegar, J., Poloczanska, E.S., Prakash, A., Preston, B., Racault, M.-F., Reckien, D., Revi, A., Rose, S.K., Schipper, E.L.F., Schmidt, D.N., Schoeman, D., Shaw, R., Simpson, N.P., Singh, C., Solecki, W., Stringer, L., Totin, E., Trisos, C.H., Trisurat, Y., Aalst, M. van, Viner, D., M.Wairiu, R.Warren, P.Wester, D.Wrathall and Ibrahim, Z.Z. (2022) *Technical Summary of IPCC Sixth Assessment Report, Climate Change and Land: an IPCC special report on climate change, desertification, land degradation, sustainable land management, food security, and greenhouse gas fluxes in terrestrial ecosystems*.

Pyne, S.J., Andrews, P.L. and Laren, R.D. (1996) 'Introduction to Wildland Fire'. Canada: John Wiley & Sons, Inc.

Pereira, G., Siqueira, R., Rosário, N.E., Longo, K.L., Freitas, S.R., Cardozo, F.S., Kaiser, J.W. and Wooster, M.J. (2016) 'Assessment of fire emission inventories during the South American Biomass Burning Analysis (SAMBBA) experiment',

Atmospheric Chemistry and Physics, 16(11), pp. 6961–6975. Available at: https://doi.org/10.5194/acp-16-6961-2016.

Peterson, D.L. and Ryan, K.C. (1986) 'Modeling postfire conifer mortality for long-range planning', *Environmental Management*, 10(6), pp. 797–808. Available at: https://doi.org/10.1007/BF01867732.

Petrenko, M., Kahn, R., Chin, M. and Limbacher, J. (2017) 'Refined Use of Satellite Aerosol Optical Depth Snapshots to Constrain Biomass Burning Emissions in the GOCART Model', *Journal of Geophysical Research: Atmospheres*, 122(20), pp. 10,983-11,004. Available at: https://doi.org/10.1002/2017JD026693.

Petrenko, M., Kahn, R., Chin, M., Soja, A., Kucsera, T. and Harshvardhan (2012) 'The use of satellite-measured aerosol optical depth to constrain biomass burning emissions source strength in the global model GOCART', *Journal of Geophysical Research Atmospheres*, 117(17). Available at: https://doi.org/10.1029/2012JD017870.

Pickett, S.T., Wu, J. and Cadenasso., M.L. (1999) 'Patch dynamics and the ecology of disturbed ground: a framework for synthesis.', *Ecosystems of Disturbed Ground*, pp. 707–722.

Ponomarev, E.I., Kharuk, V.I. and Ranson, K.J. (2016) 'Wildfires dynamics in Siberian larch forests', *Forests*, 7(6), pp. 1–9. Available at: https://doi.org/10.3390/f7060125.

Popovicheva, O., Kistler, M., Kireeva, E., Persiantseva, N., Timofeev, M., Kopeikin, V. and Kasper-Giebl, A. (2014) 'Physicochemical characterization of smoke aerosol during large-scale wildfires: Extreme event of August 2010 in Moscow', *Atmospheric Environment*, 96(August 2011), pp. 405–414. Available at: https://doi.org/10.1016/j.atmosenv.2014.03.026.

Pörtner, H.-O., Roberts, D.C., Adams, H., Adelekan, I., Adler, C., Adrian, R., Aldunce, P., Ali, E., Begum, R.A., BednarFriedl, B., Kerr, R.B., Biesbroek, R., Birkmann, J., Bowen, K., Caretta, M.A., Carnicer, J., Castellanos, E., Cheong, T.S., Chow, W., Cissé, G., Clayton, S., Constable, A., Cooley, S.R., Costello, M.J., Craig, M., Cramer, W., Dawson, R., Dodman, D., Efitre, J., Garschagen, M., Gilmore, E.A., Glavovic, B.C., Gutzler, D., Haasnoot, M., Harper, S., Hasegawa, T., Hayward, B., Hicke, J.A., Hirabayashi, Y., Huang, C., Kalaba, K., Kiessling, W., Kitoh, A., Lasco, R., Lawrence, J., Lemos, M.F., Lempert, R., Lennard, C., Ley, D., Lissner, T., Liu, Q., Liwenga, E., Lluch-Cota, S., Löschke, S., Lucatello, S., Luo, Y., Mackey, B., Mintenbeck, K., Mirzabaev, A., Möller, V., Vale, M.M., Morecroft, M.D., Mortsch, L., Mukherji, A., Mustonen, T., Mycoo, M., Nalau, J., New, M., Okem, A., Ometto, J.P., O'Neill, B., Pandey, R., Parmesan, C., Pelling, M., Pinho, P.F., Pinnegar, J., Poloczanska, E.S., Prakash, A., Preston, B., Racault, M.-F., Reckien, D., Revi, A., Rose, S.K., Schipper, E.L.F., Schmidt, D.N., Schoeman, D., Shaw, R., Simpson, N.P., Singh, C., Solecki, W., Stringer, L., Totin, E., Trisos, C.H., Trisurat, Y., Aalst, M. van, Viner, D., M.Wairiu, R.Warren, P.Wester, D.Wrathall and Ibrahim, Z.Z. (2022) *Technical Summary of IPCC Sixth Assessment Report, Climate Change and Land: an IPCC special report on climate change, desertification, land degradation, sustainable land management, food security, and greenhouse gas fluxes in terrestrial ecosystems*.

Pyne, S.J., Andrews, P.L. and Laren, R.D. (1996) 'Introduction to Wildland Fire'. Canada: John Wiley & Sons, Inc.

Rabin, S.S., Melton, J.R., Lasslop, G., Bachelet, D., Forrest, M., Hantson, S., Kaplan, J.O., Li, F., Mangeon, S., Ward, D.S., ~~Rabin, S.S., Melton, J.R., Lasslop, G., Bachelet, D., Forrest, M., Hantson, S., Kaplan, J.O., Li, F., Mangeon, S., Ward, D.S., Yue, C., Arora, V.K., Hickler, T., Kloster, S., Knorr, W., Nieradzik, L., Spessa, A., Folberth, G.A., Sheehan, T., Voulgarakis, A., Kelley, D.I., Colin Prentice, I., Sitch, S., Harrison, S. and Arneth, A. (2017) 'The Fire Modeling Intercomparison Project~~

(FireMIP), phase 1: Experimental and analytical protocols with detailed model descriptions', *Geoscientific Model Development*, 10(3), pp. 1175–1197. Available at: https://doi.org/10.5194/gmd-10-1175-2017.

Randerson, J.T., Chen, Y., Van Der Werf, G.R., Rogers, B.M. and Morton, D.C. (2012) 'Global burned area and biomass burning emissions from small fires', *Journal of Geophysical Research G: Biogeosciences*, 117(4). Available at: https://doi.org/10.1029/2012JG002128.

Randerson, J.T., Liu, H., Flanner, M.G., Chambers, S.D., Jin, Y., Hess, P.G., Pfister, G., Mack, M.C., Treseder, K.K., Welp, L.R., Chapin, F.S., Harden, J.W., Goulden, M.L., Lyons, E., Neff, J.C., Schuur, E.A.G. and Zender, C.S. (2006) 'The impact of boreal forest fire on climate warming', *Science*, 314(5802), pp. 1130–1132. Available at: https://doi.org/10.1126/science.1132075.

Reddington, C.L., Spracklen, D. V., Artaxo, P., Ridley, D.A., Rizzo, L. V. and Arana, A. (2016) 'Analysis of particulate emissions from tropical biomass burning using a global aerosol model and long-term surface observations', *Atmospheric Chemistry and Physics*, 16(17), pp. 11083–11106. Available at: https://doi.org/10.5194/acp-16-11083-2016.

Reinhardt, E.D., Keane, R.E. and Brown, J.K. (1997) 'First order fire effects model: FOFEM 4.0, user's guide', *USDA Forest Service, Intermountain Research Station*, p. INT-GTR-344. Available at: https://www.fs.fed.us/rm/pubs_int/int_gtr344.pdf.

Riahi, K., Rao, S., Krey, V., Cho, C., Chirkov, V., Fischer, G., Kindermann, G., Nakicenovic, N. and Rafaj, P. (2011) 'RCP 8.5-A scenario of comparatively high greenhouse gas emissions', *Climatic Change*, 109(1), pp. 33–57. Available at: https://doi.org/10.1007/s10584-011-0149-y.

Ritchie, H., Roser, M. and Rosado, P. (2020) *CO2 and Greenhouse Gas Emissions*, *ourworldindata.org*. Available at: https://ourworldindata.org/ co2-and-greenhouse-gas-emissions (Accessed: 30 November 2023).

Romanov, A.A., Tamarovskaya, A.N., Gusev, B.A., Leonenko, E. V., Vasiliev, A.S. and Krikunov, E.E. (2022) 'Catastrophic PM2.5 emissions from Siberian forest fires: Impacting factors analysis', *Environmental Pollution*, 306(February). Available at: https://doi.org/10.1016/j.envpol.2022.119324.

Rothermell, R.C. (1972) 'A Mathematical Model for Predicting Fire Spread', *United States Departament of Agriculture. Forest Service Research Paper*, p. 46.

Running, S.W. (2022) 'GLOBAL ARIDIFICATION AND THE DECLINE OF NPP: A COMMENTARY on Projected increases in global terrestrial net primary productivity loss caused by drought under climate change by Dan Cao, Jiahua Zhang, Jiaqi Han, Tian Zhang, Shanshan Yang, Jingwen Wang, Foyez', *Earth's Future*, 10(11), pp. 1–3. Available at: https://doi.org/10.1029/2022EF003113.

Santoro, M. and Cartus, O. (2021) 'ESA Biomass Climate Change Initiative (Biomass_cci): Global datasets of forest above-ground biomass for the years 2010, 2017 and 2018, v3'. NERC EDS Centre for Environmental Data Analysis. Available at: https://doi.org/http://dx.doi.org/10.5285/5f331c418e9f4935b8eb1b836f8a91b8.

Yue, C., Arora, V.K., Hickler, T., Kloster, S., Knorr, W., Nieradzik, L., Spessa, A., Folberth, G.A., Sheehan, T., Voulgarakis, A., Kelley, D.I., Colin Prentice, I., Sitch, S., Harrison, S. and Arneth, A. (2017) 'The Fire Modeling Intercomparison Project (FireMIP), phase 1: Experimental and analytical protocols with detailed model descriptions', *Geoscientific Model*

Development, 10(3), pp. 1175–1197. Available at: https://doi.org/10.5194/gmd-10-1175-2017.

Randerson, J.T., Chen, Y., Van Der Werf, G.R., Rogers, B.M. and Morton, D.C. (2012) 'Global burned area and biomass burning emissions from small fires', *Journal of Geophysical Research G: Biogeosciences*, 117(4). Available at: https://doi.org/10.1029/2012JG002128.

Randerson, J.T., Liu, H., Flanner, M.G., Chambers, S.D., Jin, Y., Hess, P.G., Pfister, G., Mack, M.C., Treseder, K.K., Welp, L.R., Chapin, F.S., Harden, J.W., Goulden, M.L., Lyons, E., Neff, J.C., Schuur, E.A.G. and Zender, C.S. (2006) 'The impact of boreal forest fire on climate warming', *Science*, 314(5802), pp. 1130–1132. Available at: https://doi.org/10.1126/science.1132075.

Reddington, C.L., Spracklen, D. V., Artaxo, P., Ridley, D.A., Rizzo, L. V. and Arana, A. (2016) 'Analysis of particulate emissions from tropical biomass burning using a global aerosol model and long-term surface observations', *Atmospheric Chemistry and Physics*, 16(17), pp. 11083–11106. Available at: https://doi.org/10.5194/acp-16-11083-2016.

Reinhardt, E.D., Keane, R.E. and Brown, J.K. (1997) 'First order fire effects model: FOFEM 4.0, user's guide', *USDA Forest Service, Intermountain Research Station*, p. INT-GTR-344. Available at: https://www.fs.fed.us/rm/pubs_int/int_gtr344.pdf.

Riahi, K., Rao, S., Krey, V., Cho, C., Chirkov, V., Fischer, G., Kindermann, G., Nakicenovic, N. and Rafaj, P. (2011) 'RCP 8.5-A scenario of comparatively high greenhouse gas emissions', *Climatic Change*, 109(1), pp. 33–57. Available at: https://doi.org/10.1007/s10584-011-0149-y.

Ritchie, H., Roser, M. and Rosado, P. (2020) *CO2 and Greenhouse Gas Emissions*, *ourworldindata.org*. Available at: https://ourworldindata.org/ co2-and-greenhouse-gas-emissions (Accessed: 30 November 2023).

Romanov, A.A., Tamarovskaya, A.N., Gusev, B.A., Leonenko, E. V., Vasiliev, A.S. and Krikunov, E.E. (2022) 'Catastrophic PM2.5 emissions from Siberian forest fires: Impacting factors analysis', *Environmental Pollution*, 306(February). Available at: https://doi.org/10.1016/j.envpol.2022.119324.

Richmond, A., Kaufmann, R. K., and Myneni, R. B.: Valuing ecosystem services: A shadow price for net primary production, Ecol. Econ., 64, 454–462, ttps://doi.org/10.1016/j.ecolecon.2007.03.009, 2007.

Rothermell, R.C. (1972) 'A Mathematical Model for Predicting Fire Spread', *United States Departament of Agriculture. Forest Service Research Paper*, p. 46.

Running, S.W. (2022) 'GLOBAL ARIDIFICATION AND THE DECLINE OF NPP: A COMMENTARY on Projected increases in global terrestrial net primary productivity loss caused by drought under climate change by Dan Cao, Jiahua Zhang, Jiaqi Han, Tian Zhang, Shanshan Yang, Jingwen Wang, Foyez', *Earth's Future*, 10(11), pp. 1–3. Available at: https://doi.org/10.1029/2022EF003113.

Santoro, M. and Cartus, O. (2021) 'ESA Biomass Climate Change Initiative (Biomass_cci): Global datasets of forest above-ground biomass for the years 2010, 2017 and 2018, v3'. NERC EDS Centre for Environmental Data Analysis. Available at: https://doi.org/http://dx.doi.org/10.5285/5f331c418e9f4935b8eb1b836f8a91b8.

~~Santoro, M., Cartus, O., Carvalhais, N., Rozendaal, D.M.A., Avitabile, V., Araza, A., De Bruin, S., Herold, M., Quegan, S., Rodríguez-Veiga, P., Balzter, H., Carreiras, J., Schepaschenko, D., Korets, M., Shimada, M., Itoh, T., Moreno Martínez, Á.,~~

Cavlovic, J., Gatti, R.C., Da Conceição Bispo, P., Dewnath, N., Labrière, N., Liang, J., Lindsell, J., Mitchard, E.T.A., Morel, A., Pacheco Pascagaza, A.M., Ryan, C.M., Slik, F., Vaglio Laurin, G., Verbeeck, H., Wijaya, A. and Willcock, S. (2021) 'The global forest above-ground biomass pool for 2010 estimated from high-resolution satellite observations', *Earth System Science Data*, 13(8), pp. 3927–3950. Available at: https://doi.org/10.5194/essd-13-3927-2021.

Sato, H. (2009) 'Simulation of the vegetation structure and function in a Malaysian tropical rain forest using the individual-based dynamic vegetation model SEIB-DGVM', *Forest Ecology and Management*, 257(11), pp. 2277–2286. Available at: https://doi.org/10.1016/j.foreco.2009.03.002.

Sato, H. and Ise, T. (2012) 'Effect of plant dynamic processes on African vegetation responses to climate change: Analysis using the spatially explicit individual-based dynamic global vegetation model (SEIB-DGVM)', *Journal of Geophysical Research: Biogeosciences*, 117(3), pp. 1–18. Available at: https://doi.org/10.1029/2012JG002056.

Sato, H., Itoh, A. and Kohyama, T. (2007) 'SEIB–DGVM: A new Dynamic Global Vegetation Model using a spatially explicit individual-based approach', *Ecological Modelling*, 200(3–4), pp. 279–307. Available at: https://doi.org/10.1016/j.ecolmodel.2006.09.006.

Sato, H., Kobayashi, H. and Delbart, N. (2010) 'Simulation study of the vegetation structure and function in eastern Siberian larch forests using the individual-based vegetation model SEIB-DGVM', *Forest Ecology and Management*, 259(3), pp. 301–311. Available at: https://doi.org/10.1016/j.foreco.2009.10.019.

Sato, H., Kobayashi, H., Iwahana, G. and Ohta, T. (2016) 'Endurance of larch forest ecosystems in eastern Siberia under warming trends', *Ecology and Evolution*, 6(16), pp. 5690–5704. Available at: https://doi.org/10.1002/ece3.2285.

Sato, H. and Kobayashi, H. (2018) 'Topography Controls the Abundance of Siberian Larch Forest', *Journal of Geophysical Research: Biogeosciences*, 123(1), pp. 106–116. Available at: https://doi.org/10.1002/2017JG004096.

Sato, H., Kobayashi, H., Beer, C. and Fedorov, A. (2020) 'Simulating interactions between topography, permafrost, and vegetation in Siberian larch forest', *Environmental Research Letters*, 15(9). Available at: https://doi.org/10.1088/1748-9326/ab9be4.

Schacht, J., Heinold, B., Quaas, J., Backman, J., Cherian, R., Ehrlich, A., Herber, A., Ting Katty Huang, W., Kondo, Y., Massling, A., Sinha, P.R., Weinzierl, B., Zanatta, M. and Tegen, I. (2019) 'The importance of the representation of air pollution emissions for the modeled distribution and radiative effects of black carbon in the Arctic', *Atmospheric Chemistry and Physics*, 19(17), pp. 11159–11183. Available at: https://doi.org/10.5194/acp-19-11159-2019.

Schimel, D.S., House, J.I., Hibbard, K.A., Bousquet, P., Ciais, P., Peylin, P., Braswell, B.H., Apps, M.J., Baker, D., Bondeau, A., Canadell, J., Churkina, G., Cramer, W., Denning, A.S., Field, C.B., Friedlingstein, P., Goodale, C., Heimann, M., Houghton, R.A., Melillo, J.M., Moore, B., Murdiyarso, D., Noble, I., Pacala, S.W., Prentice, I.C., Raupach, M.R., Rayner, P.J., Scholes, R.J., Steffen, W.L. and Wirth, C. (2001) 'Recent patterns and mechanisms of carbon exchange by terrestrial ecosystems', *Nature*, 414(6860), pp. 169–172. Available at: https://doi.org/10.1038/35102500.

Santoro, M., Cartus, O., Carvalhais, N., Rozendaal, D.M.A., Avitabile, V., Araza, A., De Bruin, S., Herold, M., Quegan, S., Rodríguez-Veiga, P., Balzter, H., Carreiras, J., Schepaschenko, D., Korets, M., Shimada, M., Itoh, T., Moreno Martínez, Á.,

Cavlovic, J., Gatti, R.C., Da Conceição Bispo, P., Dewnath, N., Labrière, N., Liang, J., Lindsell, J., Mitchard, E.T.A., Morel, A., Pacheco Pascagaza, A.M., Ryan, C.M., Slik, F., Vaglio Laurin, G., Verbeeck, H., Wijaya, A. and Willcock, S. (2021) 'The global forest above-ground biomass pool for 2010 estimated from high-resolution satellite observations', *Earth System Science Data*, 13(8), pp. 3927–3950. Available at: https://doi.org/10.5194/essd-13-3927-2021.

Sato, H. (2009) 'Simulation of the vegetation structure and function in a Malaysian tropical rain forest using the individual-based dynamic vegetation model SEIB-DGVM', *Forest Ecology and Management*, 257(11), pp. 2277–2286. Available at: https://doi.org/10.1016/j.foreco.2009.03.002.

Sato, H. and Ise, T. (2012) 'Effect of plant dynamic processes on African vegetation responses to climate change: Analysis using the spatially explicit individual-based dynamic global vegetation model (SEIB-DGVM)', *Journal of Geophysical Research: Biogeosciences*, 117(3), pp. 1–18. Available at: https://doi.org/10.1029/2012JG002056.

Sato, H., Itoh, A. and Kohyama, T. (2007) 'SEIB-DGVM: A new Dynamic Global Vegetation Model using a spatially explicit individual-based approach', *Ecological Modelling*, 200(3–4), pp. 279–307. Available at: https://doi.org/10.1016/j.ecolmodel.2006.09.006.

Sato, H., Kobayashi, H. and Delbart, N. (2010) 'Simulation study of the vegetation structure and function in eastern Siberian larch forests using the individual-based vegetation model SEIB-DGVM', *Forest Ecology and Management*, 259(3), pp. 301–311. Available at: https://doi.org/10.1016/j.foreco.2009.10.019.

Sato, H., Kobayashi, H., Iwahana, G. and Ohta, T. (2016) 'Endurance of larch forest ecosystems in eastern Siberia under warming trends', *Ecology and Evolution*, 6(16), pp. 5690–5704. Available at: https://doi.org/10.1002/ece3.2285.

Sato, H. and Kobayashi, H. (2018) 'Topography Controls the Abundance of Siberian Larch Forest', *Journal of Geophysical Research: Biogeosciences*, 123(1), pp. 106–116. Available at: https://doi.org/10.1002/2017JG004096.

Sato, H., Kobayashi, H., Beer, C. and Fedorov, A. (2020) 'Simulating interactions between topography, permafrost, and vegetation in Siberian larch forest', *Environmental Research Letters*, 15(9). Available at: https://doi.org/10.1088/1748-9326/ab9be4.

Schacht, J., Heinold, B., Quaas, J., Backman, J., Cherian, R., Ehrlich, A., Herber, A., Ting Katty Huang, W., Kondo, Y., Massling, A., Sinha, P.R., Weinzierl, B., Zanatta, M. and Tegen, I. (2019) 'The importance of the representation of air pollution emissions for the modeled distribution and radiative effects of black carbon in the Arctic', *Atmospheric Chemistry and Physics*, 19(17), pp. 11159–11183. Available at: https://doi.org/10.5194/acp-19-11159-2019.

Schimel, D.S., House, J.I., Hibbard, K.A., Bousquet, P., Ciais, P., Peylin, P., Braswell, B.H., Apps, M.J., Baker, D., Bondeau, A., Canadell, J., Churkina, G., Cramer, W., Denning, A.S., Field, C.B., Friedlingstein, P., Goodale, C., Heimann, M., Houghton, R.A., Melillo, J.M., Moore, B., Murdiyarso, D., Noble, I., Pacala, S.W., Prentice, I.C., Raupach, M.R., Rayner, P.J., Scholes, R.J., Steffen, W.L. and Wirth, C. (2001) 'Recent patterns and mechanisms of carbon exchange by terrestrial

~~Schmoldt, D.L., Peterson, D.L., Keane, R.E., Lenihan, J.M., McKenzie, D., Weise, D.R. and Sandberg, D. V. (1999) 'Assessing the effects of fire disturbances on ecosystems: A scientific agenda for research and management', *General Technical Reports of the US Department of Agriculture, Forest Service*, (PNW-GTR-455), pp. 1–104.~~

Schoennagel, T., Balch, J.K., Brenkert-Smith, H., Dennison, P.E., Harvey, B.J., Krawchuk, M.A., Mietkiewicz, N., Morgan, P., Moritz, M.A., Rasker, R., Turner, M.G. and Whitlock, C. (2017) 'Adapt to more wildfire in western North American forests as climate changes', *Proceedings of the National Academy of Sciences of the United States of America*, 114(18), pp. 4582–4590. Available at: https://doi.org/10.1073/pnas.1617464114.

Schultz, M.G., Heil, A., Hoelzemann, J.J., Spessa, A., Thonicke, K., Goldammer, J.G., Held, A.C., Pereira, J.M.C. and van Het Bolscher, M. (2008) 'Global wildland fire emissions from 1960 to 2000', *Global Biogeochemical Cycles*, 22(2), pp. 1–17. Available at: https://doi.org/10.1029/2007GB003031.

Seiler, W. and Crutzen, P. (1980) 'Estimates of Gross and Net Fluxes of Carbon Between', *Climatic Change*, 2, pp. 207–247.

Shiraishi, T., Hirata, R. and Hirano, T. (2021) 'New inventories of global carbon dioxide emissions through biomass burning in 2001–2020', *Remote Sensing*, 13(10). Available at: https://doi.org/10.3390/rs13101914.

Shorohova, E., Kneeshaw, D., Kuuluvainen, T. and Gauthier, S. (2011) 'Variability and dynamics of old-growth forests in the circumboreal zone: Implications for conservation, restoration and management', *Silva Fennica*, 45(5), pp. 785–806. Available at: https://doi.org/10.14214/sf.72.

Shorohova, E., Kuuluvainen, T., Kangur, A. and Jõgiste, K. (2009) 'Natural stand structures, disturbance regimes and successional dynamics in the Eurasian boreal forests: A review with special reference to Russian studies', *Annals of Forest Science*, 66(2), pp. 201–201. Available at: https://doi.org/10.1051/forest/2008083.

Shvidenko, A. and Nilsson, S. (2003) 'A synthesis of the impact of Russian forests on the global carbon budget for 1961–1998', *Tellus B: Chemical and Physical Meteorology*, 55(2), p. 391. Available at: https://doi.org/10.3402/tellusb.v55i2.16722.

Siegert, F. and Huang, S. (2005) 'Large-Scale Forest Fires in Siberia Analysed by MODIS, MERIS and ASTER Multiresolution Satellite Imagery', *Prociding of the 2004 Envisat & ERS Symposium, Salzburg, Austria* [Preprint].

Soja, A.J., Tchebakova, N.M., French, N.H.F., Flannigan, M.D., Shugart, H.H., Stocks, B.J., Sukhinin, A.I., Parfenova, E.I., Chapin, F.S. and Stackhouse, P.W. (2007) 'Climate-induced boreal forest change: Predictions versus current observations', *Global and Planetary Change*, 56(3–4), pp. 274–296. Available at: https://doi.org/10.1016/j.gloplacha.2006.07.028.

Sparks, A.M., Kolden, C.A., Smith, A.M.S., Boschetti, L., Johnson, D.M. and Cochrane, M.A. (2018) 'Fire intensity impacts on post-fire temperate coniferous forest net primary productivity', *Biogeosciences*, 15(4), pp. 1173–1183. Available at: https://doi.org/10.5194/bg-15-1173-2018.

Sun, L., Yang, L., Wang, D. and Zhang, T. (2023) 'Influence of the Long-Range Transport of Siberian Biomass Burnings on Air Quality in Northeast China in June 2017', *Sensors*, 23(2), pp. 1–13. Available at: https://doi.org/10.3390/s23020682.

Tchebakova, N.M., Monserud, R.A. and Nazimova, D.I. (1994) 'A Siberian vegetation model based on climatic parameters', *Canadian Journal of Forest Research*, Volume 24,. Available at: https://doi.org/10.1139/x94-208.

ecosystems', *Nature*, 414(6860), pp. 169–172. Available at: https://doi.org/10.1038/35102500.

Schmoldt, D. L., Peterson, D. L., Keane, R. E., Lenihan, J. M., McKenzie, D., Weise, D. R., and Sandberg, D. V.: Assessing the effects of fire disturbances on ecosystems: A scientific agenda for research and management, Gen. Tech. Reports US Dep. Agric. For. Serv., 1–104, 1999.

Schoennagel, T., Balch, J.K., Brenkert-Smith, H., Dennison, P.E., Harvey, B.J., Krawchuk, M.A., Mietkiewicz, N., Morgan, P., Moritz, M.A., Rasker, R., Turner, M.G. and Whitlock, C. (2017) 'Adapt tomore wildfire in western North American forests as climate changes', *Proceedings of the National Academy of Sciences of the United States of America*, 114(18), pp. 4582–4590. Available at: https://doi.org/10.1073/pnas.1617464114.

Schultz, M.G., Heil, A., Hoelzemann, J.J., Spessa, A., Thonicke, K., Goldammer, J.G., Held, A.C., Pereira, J.M.C. and van Het Bolscher, M. (2008) 'Global wildland fire emissions from 1960 to 2000', *Global Biogeochemical Cycles*, 22(2), pp. 1–17. Available at: https://doi.org/10.1029/2007GB003031.

Schuur, E. A. G., McGuire, A. D., Schädel, C., Grosse, G., Harden, J. W., Hayes, D. J., Hugelius, G., Koven, C. D., Kuhry, P., Lawrence, D. M., Natali, S. M., Olefeldt, D., Romanovsky, V. E., Schaefer, K., Turetsky, M. R., Treat, C. C., and Vonk, J. E.: Climate change and the permafrost carbon feedback, Nature, 520, 171–179, https://doi.org/10.1038/nature14338, 2015.

Seiler, W. and Crutzen, P. (1980) 'Estimates of Gross and Net Fluxes of Carbon Between', *Climatic Change*, 2, pp. 207–247.

Shiraishi, T., Hirata, R. and Hirano, T. (2021) 'New inventories of global carbon dioxide emissions through biomass burning in 2001–2020', *Remote Sensing*, 13(10). Available at: https://doi.org/10.3390/rs13101914.

Sharma, B., Kumar, J., Ganguly, A. R., and Hoffman, F. M.: Carbon cycle extremes accelerate weakening of the land carbon sink in the late 21st century, Biogeosciences, 20, 1829–1841, https://doi.org/10.5194/bg-20-1829-2023, 2023.

Shorohova, E., Kneeshaw, D., Kuuluvainen, T. and Gauthier, S. (2011) 'Variability and dynamics of old- growth forests in the circumboreal zone: Implications for conservation, restoration and management', *Silva Fennica*, 45(5), pp. 785–806. Available at: https://doi.org/10.14214/sf.72.

Shorohova, E., Kuuluvainen, T., Kangur, A. and Jõgiste, K. (2009) 'Natural stand structures, disturbance regimes and successional dynamics in the Eurasian boreal forests: A review with special reference to Russian studies', *Annals of Forest Science*, 66(2), pp. 201–201. Available at: https://doi.org/10.1051/forest/2008083.

Shvidenko, A. and Nilsson, S. (2003) 'A synthesis of the impact of Russian forests on the global carbon budget for 1961–1998', *Tellus B: Chemical and Physical Meteorology*, 55(2), p. 391. Available at: https://doi.org/10.3402/tellusb.v55i2.16722.

Siegert, F. and Huang, S. (2005) 'Large-Scale Forest Fires in Siberia Analysed by MODIS, MERIS and ASTER Multiresolution Satellite Imagery', *Prociding of the 2004 Envisat & ERS Symposium, Salzburg, Austria* [Preprint].

Soja, A.J., Tchebakova, N.M., French, N.H.F., Flannigan, M.D., Shugart, H.H., Stocks, B.J., Sukhinin, A.I., Parfenova, E.I., Chapin, F.S. and Stackhouse, P.W. (2007) 'Climate-induced boreal forest change: Predictions versus current observations', *Global and Planetary Change*, 56(3–4), pp. 274–296. Available at: https://doi.org/10.1016/j.gloplacha.2006.07.028.

Sparks, A.M., Kolden, C.A., Smith, A.M.S., Boschetti, L., Johnson, D.M. and Cochrane, M.A. (2018) 'Fire intensity impacts on post-fire temperate coniferous forest net primary productivity', *Biogeosciences*, 15(4), pp. 1173–1183. Available at: https://doi.org/10.5194/bg-15-1173-2018.

~~Teakles, A.D., So, R., Ainslie, B., Nissen, R., Schiller, C., Vingarzan, R., McKendry, I., Marie Macdonald, A., Jaffe, A.D., Bertram, K.A., Strawbridge, B.K., Richard Leaitch, W., Hanna, S., Toom, D., Baik, J. and Huang, L. (2017) 'Impacts of the July 2012 Siberian fire plume on air quality in the Pacific Northwest', *Atmospheric Chemistry and Physics*, 17(4), pp. 2593–~~

2611. Available at: https://doi.org/10.5194/acp-17-2593-2017.

Thomson, A.M., Calvin, K. V., Smith, S.J., Kyle, G.P., Volke, A., Patel, P., Delgado-Arias, S., Bond-Lamberty, B., Wise, M.A., Clarke, L.E. and Edmonds, J.A. (2011) 'RCP4.5: A pathway for stabilization of radiative forcing by 2100', *Climatic Change*, 109(1), pp. 77–94. Available at: https://doi.org/10.1007/s10584-011-0151-4.

Thonicke, K., Spessa, A., Prentice, I.C., Harrison, S.P., Dong, L. and Carmona-Moreno, C. (2010) 'The influence of vegetation, fire spread and fire behaviour on biomass burning and trace gas emissions: Results from a process-based model', *Biogeosciences*, 7(6), pp. 1991–2011. Available at: https://doi.org/10.5194/bg-7-1991-2010.

Thonicke, K., Venevsky, S. and Sitch, S. (2001) 'The role of fire disturbance for global vegetation dynamics: coupling fire into a Dynamic Global Vegetation Model', *Global Ecology & Biogeography*, 10, pp. 661–677.

Tian, C., Yue, X., Zhu, J., Liao, H., Yang, Y., Chen, L., Zhou, X., Lei, Y., Zhou, H. and Cao, Y. (2023) 'Projections of fire emissions and the consequent impacts on air quality under 1.5 °C and 2 °C global warming', *Environmental Pollution*, 323(November 2022), p. 121311. Available at: https://doi.org/10.1016/j.envpol.2023.121311.

Trenberth, K.E., P.D., J., P., A., R., B., D., E., A. Klein, T., D., P., F., R., J.A., R., M., R., B., S. and P., Z. (2007) 'Observations: Surface and Atmospheric Climate', *Climate Change 2007: The Physical Science Basis* [Preprint], (Contribution of Working Group I to the Fourth Assessment Report of the Intergovernmental Panel on Climate Change [Solomon, S., D. Qin, M. Manning, Z. Chen, M. Marquis, K.B. Averyt, M. Tignor and H.L. Miller (eds.)]. Cambridge University Press, Cambridge,).

University of East Anglia Climatic Research Unit; Harris, I.C.; Jones, P.D. (2014) *CRU TS3.22: Climatic Research Unit (CRU) Time-Series (TS) Version 3.22 of High-Resolution Gridded Data of Month-by-month Variation in Climate (Jan. 1901–Dec. 2013)*. Available at: https://doi.org/https://dx.doi.org/10.5285/18BE23F8-D252-482D-8AF9-5D6A2D40990C.

Ward, D.E. and Hardy, C.C. (1991) 'Smoke emissions from wildland fires', *Environment International*, 17(2–3), pp. 117–134. Available at: https://doi.org/10.1016/0160-4120(91)90095-8.

Van Der Werf, G.R., Randerson, J.T., Giglio, L., Collatz, G.J., Kasibhatla, P.S. and Arellano, A.F. (2006) 'Interannual variability in global biomass burning emissions from 1997 to 2004', *Atmospheric Chemistry and Physics*, 6(11), pp. 3423–3441. Available at: https://doi.org/10.5194/acp-6-3423-2006.

Van Der Werf, G.R., Randerson, J.T., Giglio, L., Collatz, G.J., Mu, M., Kasibhatla, P.S., Morton, D.C., Defries, R.S., Jin, Y. and Van Leeuwen, T.T. (2010) 'Global fire emissions and the contribution of deforestation, savanna, forest, agricultural, and peat fires (1997–2009)', *Atmospheric Chemistry and Physics*, 10(23), pp. 11707–11735. Available at: https://doi.org/10.5194/acp-10-11707-2010.

Van Der Werf, G.R., Randerson, J.T., Giglio, L., Van Leeuwen, T.T., Chen, Y., Rogers, B.M., Mu, M., Van Marle, M.J.E., Morton, D.C., Collatz, G.J., Yokelson, R.J. and Kasibhatla, P.S. (2017) 'Global fire emissions estimates during 1997–2016', *Earth System Science Data*, 9(2), pp. 697–720. Available at: https://doi.org/10.5194/essd-9-697-2017.

Sun, L., Yang, L., Wang, D. and Zhang, T. (2023) 'Influence of the Long-Range Transport of Siberian Biomass Burnings on Air Quality in Northeast China in June 2017', *Sensors*, 23(2), pp. 1–13. Available at: https://doi.org/10.3390/s23020682.

Teakles, A.D., So, R., Ainslie, B., Nissen, R., Schiller, C., Vingarzan, R., McKendry, I., Marie Macdonald, A., Jaffe, A.D.,

Bertram, K.A., Strawbridge, B.K., Richard Leaitch, W., Hanna, S., Toom, D., Baik, J. and Huang, L. (2017) 'Impacts of the July 2012 Siberian fire plume on air quality in the Pacific Northwest', *Atmospheric Chemistry and Physics*, 17(4), pp. 2593–2611. Available at: https://doi.org/10.5194/acp-17-2593-2017.

Thomson, A.M., Calvin, K. V., Smith, S.J., Kyle, G.P., Volke, A., Patel, P., Delgado-Arias, S., Bond-Lamberty, B., Wise, M.A., Clarke, L.E. and Edmonds, J.A. (2011) 'RCP4.5: A pathway for stabilization of radiative forcing by 2100', *Climatic Change*, 109(1), pp. 77–94. Available at: https://doi.org/10.1007/s10584-011-0151-4.

Thonicke, K., Spessa, A., Prentice, I.C., Harrison, S.P., Dong, L. and Carmona-Moreno, C. (2010) 'The influence of vegetation, fire spread and fire behaviour on biomass burning and trace gas emissions: Results from a process-based model', *Biogeosciences*, 7(6), pp. 1991–2011. Available at: https://doi.org/10.5194/bg-7-1991-2010.

Thonicke, K., Venevsky, S. and Sitch, S. (2001) 'The role of fire disturbance for global vegetation dynamics: coupling fire into a Dynamic Global Vegetation Model', *Global Ecology & Biogeography*, 10, pp. 661–677.

Tian, C., Yue, X., Zhu, J., Liao, H., Yang, Y., Chen, L., Zhou, X., Lei, Y., Zhou, H. and Cao, Y. (2023) 'Projections of fire emissions and the consequent impacts on air quality under 1.5 °C and 2 °C global warming', *Environmental Pollution*, 323(November 2022), p. 121311. Available at: https://doi.org/10.1016/j.envpol.2023.121311.

Trenberth, K.E., P.D., J., P., A., R., B., D., E., A. Klein, T., D., P., F., R., J.A., R., M., R., B., S. and P., Z. (2007) 'Observations: Surface and Atmospheric Climate', *Climate Change 2007: The Physical Science Basis* [Preprint], (Contribution of Working Group I to the Fourth Assessment Report of the Intergovernmental Panel on Climate Change [Solomon, S., D. Qin, M. Manning, Z. Chen, M. Marquis, K.B. Averyt, M. Tignor and H.L. Miller (eds.)]. Cambridge University Press, Cambridge,).

University of East Anglia Climatic Research Unit; Harris, I.C.; Jones, P.D. (2014) *CRU TS3.22: Climatic Research Unit (CRU) Time-Series (TS) Version 3.22 of High Resolution Gridded Data of Month-by-month Variation in Climate (Jan. 1901- Dec. 2013)*. Available at: https://doi.org/https://dx.doi.org/10.5285/18BE23F8-D252-482D-8AF9-5D6A2D40990C.

Ward, D.E. and Hardy, C.C. (1991) 'Smoke emissions from wildland fires', *Environment International*, 17(2–3), pp. 117–134. Available at: https://doi.org/10.1016/0160-4120(91)90095-8.

Van Der Werf, G.R., Randerson, J.T., Giglio, L., Collatz, G.J., Kasibhatla, P.S. and Arellano, A.F. (2006) 'Interannual variability in global biomass burning emissions from 1997 to 2004', *Atmospheric Chemistry and Physics*, 6(11), pp. 3423–3441. Available at: https://doi.org/10.5194/acp-6-3423-2006.

Van Der Werf, G.R., Randerson, J.T., Giglio, L., Collatz, G.J., Mu, M., Kasibhatla, P.S., Morton, D.C., Defries, R.S., Jin, Y. and Van Leeuwen, T.T. (2010) 'Global fire emissions and the contribution of deforestation, savanna, forest, agricultural, and peat fires (1997-2009)', *Atmospheric Chemistry and Physics*, 10(23), pp. 11707–11735. Available at: https://doi.org/10.5194/acp-10-11707-2010.

Van Der Werf, G.R., Randerson, J.T., Giglio, L., Van Leeuwen, T.T., Chen, Y., Rogers, B.M., Mu, M., Van Marle, M.J.E., Morton, D.C., Collatz, G.J., Yokelson, R.J. and Kasibhatla, P.S. (2017) 'Global fire emissions estimates during 1997-2016', *Earth System Science Data*, 9(2), pp. 697–720. Available at: https://doi.org/10.5194/essd-9-697-2017.

Végh, L. and Kato, T. (2024) 'Modified SEIB-DGVM enables simulation of masting in a temperate forest', Ecological Modelling, 488(December 2023). Available at: https://doi.org/10.1016/j.ecolmodel.2023.110577.

Webb, E. E., Alexander, H. D., Paulson, A. K., Loranty, M. M., DeMarco, J., Talucci, A. C., Spektor, V., Zimov, N., and Lichstein, J. W.: Fire-Induced Carbon Loss and Tree Mortality in Siberian Larch Forests, Geophys. Res. Lett., 51, https://doi.org/10.1029/2023GL105216, 2024.

Westerling, A.L., Hidalgo, H.G., Cayan, D.R. and Swetnam, T.W. (2006) 'Warming and earlier spring increase Western U.S. forest wildfire activity', *Science*, 313(5789), pp. 940–943. Available at: https://doi.org/10.1126/science.1128834.

Whelan, R.J. (2009) 'The ecology of fire-developments since 1995 and outstanding questions', *Proceedings of the Royal Society of Queensland*, 115(August), pp. 59–68.

Williams, R.J., Gill, A.M. and Moore, P.H.R. (1998) 'Seasonal changes in fire behaviour in a tropical savanna in Northern Australia', *International Journal of Wildland Fire*, 8(4), pp. 227–239. Available at: https://doi.org/10.1071/WF9980227.

Wilson, R.A. (1982) 'A Reexamination of Fire Spread in Free-Burning Porous Fuel Beds', *United States Department of Agriculture, Forest Service* [Preprint].

Winiger, P., Andersson, A., Eckhardt, S., Stohl, A., Semiletov, I.P., Dudarev, O. V., Charkin, A., Shakhova, N., Klimont, Z., Heyes, C. and Gustafsson, Ö. (2017) 'Siberian Arctic black carbon sources constrained by model and observation', *Proceedings of the National Academy of Sciences of the United States of America*, 114(7), pp. E1054–E1061. Available at: https://doi.org/10.1073/pnas.1613401114.

Wotton, B.M., Flannigan, M.D. and Marshall, G.A. (2017) 'Potential climate change impacts on fire intensity and key wildfire suppression thresholds in Canada', *Environmental Research Letters*, 12, p. 13.

Wu, L., Kato, T., Sato, H., Hirano, T. and Yazaki, T. (2019) 'Sensitivity analysis of the typhoon disturbance effect on forest dynamics and carbon balance in the future in a cool-temperate forest in northern Japan by using SEIB-DGVM', *Forest Ecology and Management*, 451(August), p. 117529. Available at: https://doi.org/10.1016/j.foreco.2019.117529.

Yasunari, T. J., Narita, D., Takemura, T., Wakabayashi, S., and Takeshima, A.: Comprehensive Impact of Changing Siberian Wildfire Severities on Air Quality, Climate, and Economy: MIROC5 Global Climate Model's Sensitivity Assessments, Earth's Futur., 12, https://doi.org/10.1029/2023EF004129, 2024.

Zhang, F., Wang, J., Ichoku, C., Hyer, E.J., Yang, Z., Ge, C., Su, S., Zhang, X., Kondragunta, S., Kaiser, J.W., Wiedinmyer, C. and Da Silva, A. (2014) 'Sensitivity of mesoscale modeling of smoke direct radiative effect to the emission inventory: A case study in northern sub-Saharan African region', *Environmental Research Letters*, 9(7). Available at: https://doi.org/10.1088/1748-9326/9/7/075002.

Zheng, B., Ciais, P., Chevallier, F., Chuvieco, E., Chen, Y. and Yang, H. (2021) 'Increasing forest fire emissions despite the decline in global burned area', *Science Advances*, 7(39). Available at: https://doi.org/10.1126/sciadv.abh2646.~~Végh, L. and Kato, T. (2024) 'Modified SEIB-DGVM enables simulation of masting in a temperate forest', Ecological Modelling, 488(December 2023). Available at: https://doi.org/10.1016/j.ecolmodel.2023.110577.~~

Formatted: Font: (Default) +Headings (Times New Roman), Complex Script Font: +Headings (Times New Roman), 10 pt

Formatted: Automatically adjust right indent when grid is defined, Space After: 0 pt, Line spacing: 1.5 lines, Adjust space between Latin and Asian text, Adjust space between Asian text and numbers

Formatted: No widow/orphan control

Westerling, A.L., Hidalgo, H.G., Cayan, D.R. and Swetnam, T.W. (2006) 'Warming and earlier spring increase Western U.S. forest wildfire activity', *Science*, 313(5789), pp. 940–943. Available at: https://doi.org/10.1126/science.1128834.

Whelan, R.J. (2009) 'The ecology of fire–developments since 1995 and outstanding questions', *Proceedings of the Royal Society of Queensland*, 115(August), pp. 59–68.

Williams, R.J., Gill, A.M. and Moore, P.H.R. (1998) 'Seasonal changes in fire behaviour in a tropical savanna in Northern Australia', *International Journal of Wildland Fire*, 8(4), pp. 227–239. Available at: https://doi.org/10.1071/WF9980227.

Wilson, R.A. (1982) 'A Reexamination of Fire Spread in Free-Burning Porous Fuel Beds', *United States Department of Agriculture, Forest Service* [Preprint].

Winiger, P., Andersson, A., Eckhardt, S., Stohl, A., Semiletov, I.P., Dudarev, O. V., Charkin, A., Shakhova, N., Klimont, Z., Heyes, C. and Gustafsson, Ö. (2017) 'Siberian Arctic black carbon sources constrained by model and observation', *Proceedings of the National Academy of Sciences of the United States of America*, 114(7), pp. E1054–E1061. Available at: https://doi.org/10.1073/pnas.1613401114.

Wotton, B.M., Flannigan, M.D. and Marshall, G.A. (2017) 'Potential climate change impacts on fire intensity and key wildfire suppression thresholds in Canada', *Environmental Research Letters*, 12, p. 13.

Wu, L., Kato, T., Sato, H., Hirano, T. and Yazaki, T. (2019) 'Sensitivity analysis of the typhoon disturbance effect on forest dynamics and carbon balance in the future in a cool-temperate forest in northern Japan by using SEIB-DGVM', *Forest Ecology and Management*, 451(August), p. 117529. Available at: https://doi.org/10.1016/j.foreco.2019.117529.

Zhang, F., Wang, J., Ichoku, C., Hyer, E.J., Yang, Z., Ge, C., Su, S., Zhang, X., Kondragunta, S., Kaiser, J.W., Wiedinmyer, C. and Da Silva, A. (2014) 'Sensitivity of mesoscale modeling of smoke direct radiative effect to the emission inventory: A case study in northern sub-Saharan African region', *Environmental Research Letters*, 9(7). Available at: https://doi.org/10.1088/1748-9326/9/7/075002.

Zheng, B., Ciais, P., Chevallier, F., Chuvieco, E., Chen, Y. and Yang, H. (2021) 'Increasing forest fire emissions despite the decline in global burned area', *Science Advances*, 7(39). Available at: https://doi.org/10.1126/sciadv.abh2646.